UNIVERSIDADE FEDERAL DE MINAS GERAIS
Instituto de Geociências
Programa de Pós-Graduação em Geologia

Fernando Estevão Rodrigues Crincoli Pacheco

Proveniência Sedimentar e Relações entre o Grupo Macaúbas e o Complexo Jequitinhonha na Divisa Minas Gerais/Bahia

Nº 61

Belo Horizonte
01/08/2022

Fernando Estevão Rodrigues Crincoli Pacheco

Proveniência Sedimentar e Relações entre o Grupo Macaúbas e o Complexo Jequitinhonha na Divisa Minas Gerais/Bahia

Versão final

Tese apresentada ao Programa de Pós-Graduação em Geologia da Universidade Federal de Minas Gerais como requisito parcial para obtenção do título de Doutor em Geologia.

Orientador: Prof. Dr. Fabrício de Andrade Caxito

Coorientador: Prof. Dr. Antônio Carlos Pedrosa-Soares

Belo Horizonte
2022

P116p
2022

Pacheco, Fernando Estevão Rodrigues Crincoli.

Proveniência sedimentar e relações entre o Grupo Macaúbas e o Complexo Jequitinhonha na divisa Minas Gerais/Bahia [manuscrito] / Fernando Estevão Rodrigues Crincoli Pacheco . – 2022.

107 f., enc. il. (principalmente color.)

Orientador: Fabrício de Andrade Caxito.

Coorientador: Antônio Carlos Pedrosa-Soares.

Tese (doutorado) – Universidade Federal de Minas Gerais, Instituto de Geociências, 2022.

Área de concentração: Geologia Regional.

Bibliografia: f. 71-87.

Inclui anexo.

1. Grafita – Minas Gerais – Teses. 2. Grafita – Bahia – Teses. 3. Gnaisse – Minas Gerais – Teses. 4. Gnaisse – Bahia – Teses. 5. Isótopos – Teses. 6. Gondwana – Teses. I. Caxito, Fabrício de Andrade. II. Pedrosa-Soares, Antônio Carlos. III. Universidade Federal de Minas Gerais. Instituto de Geociências. IV. Título.

CDU: 551.3.051(813.8+815.1)

Ficha catalográfica elaborada por Elisabete Quatrini Vieira – CRB6 2210
Biblioteca “Vitória Pedersoli”, Instituto de Geociências da UFMG

UNIVERSIDADE FEDERAL DE MINAS GERAIS

PROGRAMA DE PÓS-GRADUAÇÃO EM GEOLOGIA DO IGC-UFMG

FOLHA DE APROVAÇÃO

Proveniência Sedimentar e Relações entre o Grupo Macaúbas e o Complexo Jequitinhonha na Divisa Minas Gerais/Bahia

FERNANDO ESTEVÃO RODRIGUES CRINCOLI PACHECO

Tese submetida à Banca Examinadora designada pelo Colegiado do Programa de Pós-Graduação em GEOLOGIA, como requisito para obtenção do grau de Doutor em GEOLOGIA, área de concentração GEOLOGIA REGIONAL, pelo Programa de Pós-graduação em Geologia do Instituto de Geociências da Universidade Federal de Minas Gerais.

Aprovada em 01 de agosto de 2022, pela banca constituída pelos membros:

Prof. Fabrício de Andrade Caxito - Orientador
UFMG

Prof. Alexandre Uhlein
UFMG

Prof. Tiago Amâncio Novo
UFMG

Profa. Simone Cerqueira Pereira Cruz
UFBA

Prof. Matheus Henrique Kuchenbecker do Amaral
UFVJM

Belo Horizonte, 01 de agosto de 2022.

AGRADECIMENTOS

Agradeço ao meu orientador, Prof. Dr. Fabrício de Andrade Caxito, e meu co-orientador, Prof. Dr. Antônio Carlos Pedrosa-Soares, pelo suporte intelectual e motivacional ao longo dessa pesquisa. Esse trabalho foi possível devido ao suporte da Universidade Federal de Minas Gerais (UFMG), do Programa de Pós-graduação em Geologia (PPGEOL), do Instituto de Geociências (IGC), do Departamento de Geologia, do CPMTC-IGC, da Fundação de Amparo à Pesquisa do Estado de Minas Gerais (FAPEMIG, processo PPM-00618-18), do Conselho Nacional de Desenvolvimento Científico e Tecnológico (CNPq, processo 408815/2021-3), do Instituto Serrapilheira (Serra-1912-31510) através do Project MOBILE: Mountains Belts and the Inception of Complex Life on Earth (geolifemobile.com). O presente trabalho foi realizado com apoio da Coordenação de Aperfeiçoamento de Pessoal de Nível Superior - Brasil (CAPES) - Código de Financiamento 001.

Agradeço às professoras Dra. Eliza Peixoto e Dra. Maria Eugênia Souza pelas revisões após qualificação e aos professores integrantes da banca de defesa de tese pelos comentários e sugestões. Agradeço aos amigos da "salinha da pós" que estiveram presentes em tantos momentos, em especial a Tobias Fonte Boa, Paula Serrano, Raíssa Santiago, Christopher Rezende, Ana Fonseca, Samuel Amaral e Luíza Carneiro. Agradeço a meus pais pelo apoio e amor e ao meu marido pelo apoio incondicional, confiança e motivação ao longo dessa jornada.

RESUMO

A bacia precursora do Sistema Orogênico Araçuaí – Congo Ocidental formou um largo golfo dentro do Paleocontinente São Francisco – Congo, onde sucessões sedimentares atribuídas ao Complexo Jequitinhonha e ao Grupo Macaúbas foram depositadas durante o Neoproterozoico. Essa bacia precursora compreende um aulacógeno de idade Toniana inferior e um rifte Criogeniano que evoluiu para margem passiva com espalhamento de litosfera oceânica até o início do Ediacarano. O Complexo Jequitinhonha é uma extensa unidade metassedimentar localizada na porção nordeste do Orógeno Araçuaí, constituído por paragnaisses ricos em alumínio (kinzingito), silimanita-grafita gnaisses e depósitos econômicos de grafita tipo *flake* associados, quartzitos e lentes de rochas calcissilicáticas, apresentando metamorfismo de facies anfibolito superior a granulito, que ocorreu em torno de 570-550 Ma. O Grupo Macaúbas é a unidade da bacia precursora mais bem preservada no Orógeno Araçuaí, apresenta uma sequência vulcanossedimentar dividida em três sucessões relacionadas com a presença de diamictitos glaciogênicos: i) uma sequência pré-glacial depositada em ambiente fluvial a marinho raso, onde os diamictitos estão ausentes; ii) uma sequência rica em diamictitos glaciogênicos; e iii) uma sequencia pós-glacial contend turbiditos finos e depósitos sedimentares exalativos intercalados com rochas máficas e ultramáficas interpretadas como remanescentes de litosfera oceânica neoproterozoica. Dados U-Pb (LA-MC-ICP-MS) de 110 zircões detríticos do paleossoma de um paragnaisse migmatítico do Complexo Jequitinhonha, juntamente com dados isotópicos Lu-Hf (LA-MC-ICP-MS) de 106 zircões detríticos sugerem as seguintes fontes de sedimentação: grãos Neoarqueanos a Orosirianos do embasamento do Paleocontinente São Francisco – Congo, grãos de idade Toniana inferior da província magmática anorogênica e grãos Criogenianos a Ediacaranos fornecidos pela Província Alcalina do Sul do Estado da Bahia e do Arco Magmático do Rio Doce. Dados U-Pb (LA-MC-ICP-MS) de 182 zircões detríticos da Formação Chapada Acauã Inferior e de 104 cristais de zircão de um clasto granítico do diamictito sugerem contribuição Arqueana e Paleoproterozóica do embasamento do Paleocontinente São Francisco – Congo e complexos metamórficos, Mesoproterozóica de rochas intrusivas e vulcânicas do Cráton do São Francisco e Toniana da Suíte Salto da Divisa. A sedimentação dos protólitos do Complexo Jequitinhonha ocorreu no Criogeniano a Ediacarano Inferior. A ausência de grãos do Criogeniano Superior na Formação Chapada Acauã Inferior deixa em aberto se a sua sedimentação está relacionada à glaciação Sturtiana, à Marinoana ou ambas.

Palavras-chave: grafita; gnaisse kinzingítico; isótopos de U-Pb e Lu-Hf; Orógeno Araçuaí e Congo Ocidental; Gondwana; proveniência sedimentar

ABSTRACT

The precursor basin of the Araçuaí – West Congo Orogenic System (AWCO) formed a large gulf within the São Francisco – Congo Paleocontinent (SFCP), where sedimentary successions ascribed to the Jequitinhonha Complex and Macaúbas Group were deposited in the Neoproterozoic. This precursor basin system comprises an aborted continental rift of Early Tonian age and a Cryogenian rift that evolved to ocean-floor spreading up to the Early Ediacaran. The Jequitinhonha Complex is an extensive metasedimentary unit located in the northeastern Araçuaí Orogen, consisting of Al-rich paragneiss (kinzigite), sillimanite-graphite gneiss and associated economic deposits of flake graphite, quartzite and lenses of calc-silicate rock, metamorphosed to upper amphibolite or granulite facies around 570–550 Ma. The Macaúbas Group is the best preserved unit of the precursor basin of the Araçuaí Orogen, has a volcano-sedimentary sequence divided into three successions in relation to the presence of glaciogenic diamictites: i) a diamictite-free preglacial succession deposited in fluvial to shallow marine systems; ii) successions rich in glaciogenic diamictites; and iii) a post-glacial succession containing fine-grained turbidites and sedimentary exhalative deposits interleaved with metamafic and meta-ultramafic rocks that are interpreted as remnants of a Neoproterozoic oceanic lithosphere. U-Pb (LA-MC-ICP-MS) data of 110 detrital zircon grains from the paleosome of a migmatitic paragneiss of Jequitinhonha Complex coupled with Lu-Hf in zircon (LA-MC-ICP-MS) data for 106 zircon grains suggest the following sources: Neoarchean to Orosirian grains were sourced from the SFCP basement, Early Tonian grains from the anorogenic magmatic province, and Cryogenian to Early Ediacaran grains were provided by the Southern Bahia Alkaline Province and Rio Doce magmatic arc. U-Pb (LA-MC-ICP-MS) data of 189 detrital zircon grains of the Lower Chapada Acauã Formation and of 104 zircon crystals from a granitic clast of the diamictite suggests a contribution from the Archean and Paleoproterozoic basement of the São Francisco – Congo paleocontinent and metamorphic complexes, from the Mesoproterozoic intrusive and volcanic rocks of São Francisco Craton, and from the Tonian Salto da Divisa Suite. The sedimentation of Jequitinhonha Complex protoliths developed from the Cryogenian to Early Ediacaran. The absence of late Cryogenian grains in lower Chapada Acauã Formation leaves open the question of whether this formation is related to the Sturtian, to the Marinoan, or both Snowball glaciations.

Keywords: graphite; kinzigite; U-Pb and Lu-Hf isotopes; Araçuaí – West Congo Orogen; Gondwana; Ediacaran carbon, sedimentary provenance

LISTA DE FIGURAS

SUMÁRIO

1. INTRODUÇÃO

O presente trabalho "Proveniência Sedimentar e Relações Entre o Grupo Macaúbas e o Complexo Jequitinhonha na Divisa Minas Gerais/Bahia" apresenta a pesquisa desenvolvida ao longo dos anos de 2017 a 2022 no projeto de doutorado e faz parte da tese de doutoramento.

O Grupo Macaúbas ainda não apresenta uma idade definitiva para as suas rochas depositadas em ambientes glaciais. As análises geocronológicas feitas em diamictitos apresentam a idade mais nova de zircão detrítico em torno de 900 Ma (Babinski et al., 2012). Sendo assim não é possível distinguir se essas rochas foram depositadas durante a glaciação Sturtiana (~740 Ma) ou Marinoana (~630 Ma) ou se diamictitos mais basais e mais superiores foram depositados em glaciações diferentes.

O Complexo Jequitinhonha apresenta idade máxima de 839 ± 17 Ma e representa um pacote sedimentar depositado em ambiente de margem passiva da bacia precursora do Orógeno Araçuaí, incluindo sequências distais e proximais (Gonçalves-Dias et al., 2011, 2016). A distribuição das sucessões proximais e distais do Complexo Jequitinhonha, com relação à margem cratônica, assemelha-se a transição dos depósitos areno-pelíticos da Formação Chapada Acauã superior aos depósitos pelíticos de mar profundo da Formação Ribeirão da Folha (Uhlein et al., 1998; Pedrosa-Soares et al. 2011; Gonçalves-Dias, 2012). O Complexo Jequitinhonha também possui depósitos econômicos importantes de grafita tipo flake disseminados em saprólitos do silimanita-grafita gnaisse, sendo uma das maiores regiões produtoras de grafita do mundo (Belém, 2018).

Na área de estudo, não temos uma relação definida entre o Grupo Macaúbas e o Complexo Jequitinhonha. O contato entre essas unidades é brusco, passando de um grau metamórfico baixo para alto, provavelmente por movimentações em zonas de cisalhamento e falhas posteriores. Desta forma, a geoquímica isotópica em zircão pode contribuir para um melhor entendimento desse problema.

A área de pesquisa não foi estudada em detalhe anteriormente e possui a característica única da proximidade com as únicas intrusões de idade Criogeniana de toda a região, cristalizadas entre os períodos de glaciação (735~675 Ma). Desta forma, a presença de

clastos dessas rochas no arcabouço dos diamictitos poderia indicar diferenças de idades entre os diversos diamictitos do Grupo Macaúbas, que não são encontrados nas outras regiões devido à distância desta área-fonte específica, podendo assim fornecer embasamento para correlacionar glaciações globais com o Grupo Macaúbas. Destaca-se também que a área não possui ainda um arcabouço estratigráfico e estrutural bem definido, que foi também objetivo de levantamento neste trabalho.

1.1. Localização e acesso

A área de estudo localiza-se nas regiões Norte do estado de Minas Gerais (MG) e sul do estado da Bahia (BA), entre as coordenadas geográficas 39ºW e 41ºW longitudinais e 15ºS e 17ºS latitudinais (Fig. 1.1). Sua distância de Belo Horizonte (MG) é de, aproximadamente, 890 km e o acesso se dá através das rodovias BR-135 até Curvelo, BR-259 e BR-367 até Itaobim e BR-116 até Vitória da Conquista. De Salvador (BA), a distância é de, aproximadamente, 540 km e o acesso se dá através das rodovias BR-324 até Feira de Santana e BR-116 até Vitória da Conquista.

1.2. Objetivos

Os estudos desenvolvidos têm como principal objetivo a reconstrução do ambiente sedimentar do Grupo Macaúbas e rochas correlatas na região noroeste do Orógeno Araçuaí, especificamente através de:

i. Caracterização da porção norte da bacia sedimentar da bacia Macaúbas, situada na borda sul do Cráton São Francisco;
ii. Determinação da proveniência sedimentar das rochas encontradas na região;
iii. Determinação das idades máximas de deposição das rochas do Grupo Macaúbas e do Complexo Jequitinhonha através de análises U-Pb de zircões detríticos;
iv. Caracterizar as relações cronoestratigráficas entre o Grupo Macaúbas e rochas correlatas (Complexo Jequitinhonha).

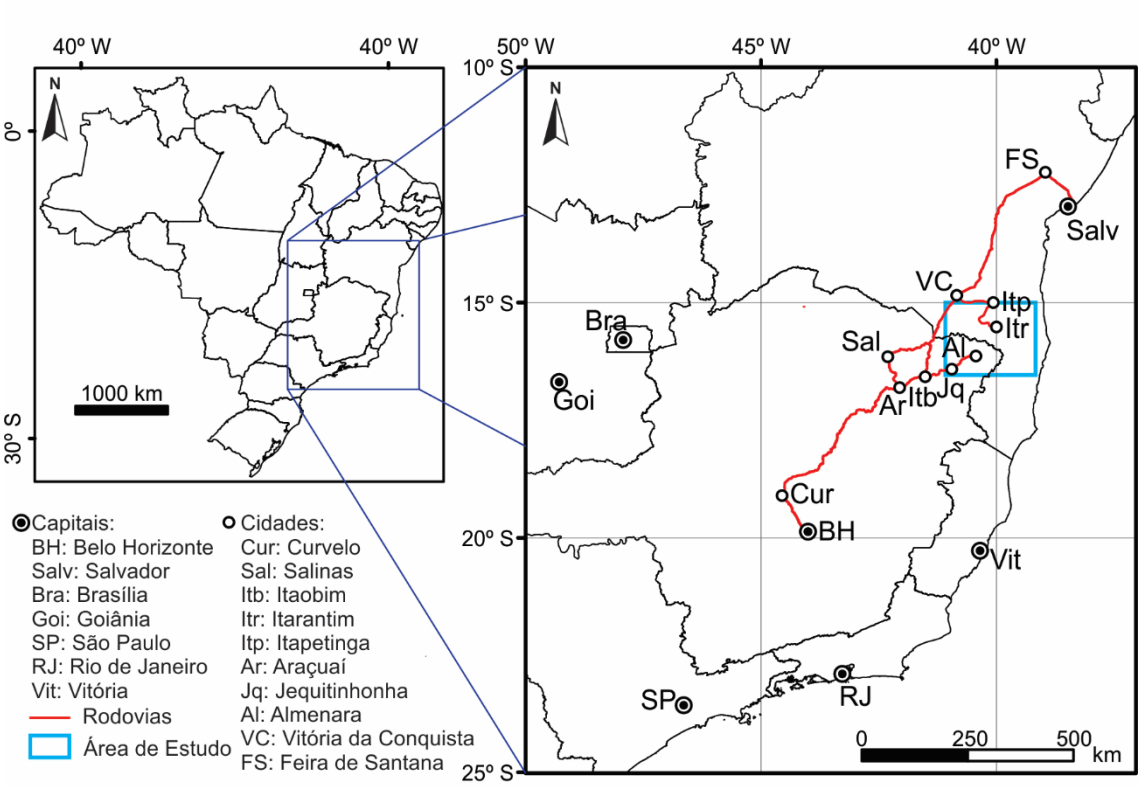

Figura 1.1 - Mapa de localização e acesso da área de estudo, com principais cidades e rodovias de acesso.

1.3. Metodologia

1.3.1. Revisão bibliográfica

A revisão bibliográfica foi feita de forma a abordar os seguintes tópicos: Orógeno Araçuaí e Congo Ocidental (I), Litoestratigrafia e Geocronologia do Grupo Macaúbas (II), Litoestratigrafia e geocronologia do Complexo Jequitinhonha (III), Geocronologia de possíveis fontes detríticas na região do Orógeno Araçuaí e Congo Ocidental (IV). A seguir são elencadas as principais fontes base para cada tópico, sendo apresentadas outras fontes ao longo dos capítulos 2, 3 e 4.

I. Para melhor compreensão do Orógeno Araçuaí e Congo Ocidental, foram utilizados trabalhos como Pedrosa-Soares et al. (1998, 2000, 2007, 2008, 2011a), Noce et al. (2007a, 2007b), Pedrosa-Soares & Alkmim (2011), Heilbron et al. (2010, 2017) entre outros citados ao longo do trabalho.

II. A Litoestratigrafia e Geocronologia do Grupo Macaúbas encontra-se detalhada em trabalhos como Pedrosa-Soares et al. (2011b), Babinski et al. (2012), Kuchenbecker et al. (2015).

III. Para a Litoestratigrafia e Geocronologia do Complexo Jequitinhonha, foram utilizadas como referências os trabalhos de Almeida & Litwinski (1984), Pedrosa-Soares & Wiedemann-Leonardos (2000), Belém (2006, 2018) e Gonçalves-Dias et al. (2011, 2016).

IV. Quanto a Geocronologia de possíveis fontes detríticas na região do Orógeno Araçuaí e Congo Ocidental, foram considerados trabalhos realizados em áreas como Arco Magmático do Rio Doce, Arco Magmático do Rio Negro, Província Alcalina do Sul do Estado da Bahia, magmatismos anorogênicos, enxames de diques encontrados tanto na porção brasileira quanto na porção africana, rochas de Complexos metamórficos como Mantiqueira, Juiz de Fora, Pocrane, Porteirinha, rochas do embasamento do Paleocontinente São Francisco-Congo. Essas referências podem ser conferidas nos capítulos 3 e 4.

1.3.2. Preparação de amostras para análises isotópicas

A preparação das amostras ocorreu no Laboratório de Separação Mineral de Alta Pureza – SEPURA – no Centro de Pesquisa Manoel Teixeira da Costa (CPMTC), na Universidade Federal de Minas Gerais (UFMG). Inicialmente as amostras foram submetidas ao processo de britagem e moagem e, a seguir, os concentrados de grãos/cristais de zircão foram obtidos através de separação magnética (Frantz), gravimétrica e catação na lupa binocular. Os grãos/cristais de zircão foram colocados em um disco de epoxy e polidos. As imagens de catodoluminescência da amostra do artigo I foram feitas no MultiLab (UERJ) através de um microscópio de varredura eletrônica (MEV, Quanta-250-FEI), enquanto as imagens das amostras do artigo II foram obtidas no Laboratório de Geoquímica Isotópica e Geocronologia (UFOP) também a partir de microscópio eletrônico de varredura (MEV, JEOL 6510). As descrições detalhadas das análises isotópicas U-Pb (LA-ICP-MS) e Lu-Hf (LA-ICP-MS) se encontram no corpo dos artigos, nos capítulos 3 e 4.

1.4. Estrutura da tese

Esse trabalho apresenta uma síntese da revisão bibliográfica referente ao Grupo Macaúbas e o Complexo Jequitinhonha, descrita no capítulo 2 e detalhada ao longo dos capítulos 3 e 4, onde também são apresentados os artigos desenvolvidos nessa tese. No capítulo 5 são apresentadas considerações finais e conclusões deste trabalho.

O primeiro artigo desenvolvido no projeto de doutorado, intitulado *"Detrital zircon U-Pb and Lu-Hf data for a kinzigitic gneiss (Jequitinhonha Complex, Araçuaí Orogen, SE Brazil) constrain the age of a huge storage of Ediacaran carbon"*, encontra-se publicado na revista *Journal of South American Earth Sciences*, na edição especial *"A tribute to Márcio M. Pimentel – A Leader in South American Geology and Isotope Geology"*. Esse artigo apresenta novas análises geocronológicas de zircões detríticos encontrados no gnaisse do Complexo Jequitinhonha, trazendo uma idade mais jovem para a sua formação, além de caracterizar as suas fontes com análises de isótopos de Lutécio e Háfnio.

O segundo artigo intitulado *"Detrital zircon U-Pb analysis constrains the depositional age and provenance of Cryogenian glacial successions of the Macaúbas Group in the northeastern Araçuaí Orogen, eastern Brazil*" foi submetido à revista *Journal of South American Earth Sciences*, na edição especial *"Geological evolution of the South American Platform"*. Esse artigo apresenta novas análises geocronológicas de matriz de diamictitos encontrados no Grupo Macaúbas na porção norte do Orógeno Araçuaí.

Como o segundo artigo encontra-se em fase de submissão, as informações apresentadas nessa tese podem estar desatualizadas. Recomenta-se citar os artigos a partir da sua publicação, principalmente o segundo por poder apresentar modificações após publicação.

2. CONTEXTO GEOLÓGICO

O Orógeno Araçuaí situa-se entre o limite leste do Cráton do São Francisco e o Oceano Atlântico, entre os paralelos 15º e 21º S (Fig. 2.1), e tem a Faixa Congo Ocidental como contraparte no sudoeste africano (Pedrosa-Soares et al. 2001, 2008), englobando um conjunto de componentes geotectônicos que caracterizam um orógeno colisional sucessor de um orógeno acrescionário de margem continental ativa. A assembleia litológica do Orógeno Araçuaí compreende (I) rochas do embasamento de idade Arqueano-Paleoproterozoico e unidades de idade Estateriano-Mesoproterozoico; (II) unidades metassedimentares e lascas ofiolíticas do Grupo Macaúbas e unidades correlatas, dos períodos Toniano e Criogeniano; (III) o Arco Magmático do Rio Doce e rochas metavulcânicas e sequências metassedimentares associadas, datados do Ediacarano; (VI) a bacia orogênica representada pela Formação Salinas; e (V) as rochas intrusivas colisionais a pós-colisionais (Fig. 2.2).

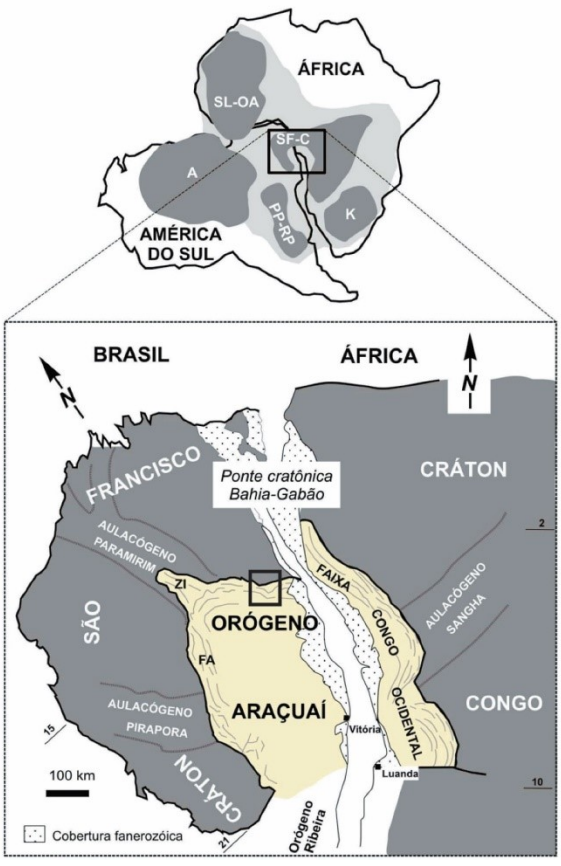

Figura 2.1 - Orógeno Araçuaí na região central do Paleocontinente Gondwana, (Pedrosa-Soares, et al. 2007). A região de interesse desta dissertação é indicada pelo retângulo preto.

O embasamento do Orógeno Araçuaí é representado por greenstone belts e complexos TTG associados, do Arqueano a Paleoproterozóico, unidades metassedimentares e intrusões do Sideriano, e arcos magmáticos e sequências volcano-sedimentares do Riaciano-Orosiriano relacionados à agutinação do paleocontinente Sao Francisco-Congo (Noce et al., 2007; Teixeira et al., 2000, 2017; Novo, 2013, Aguilar et al., 2017; Degler et al., 2018). Ao longo do Estateriano – Mesoproterozoico, ocorreu a deposição de rochas sedimentares relacionadas ao rifte-sag Espinhaço e rochas vulcânicas associadas, além da formação de granitos anorogênicos durante o Estateriano (Chemale Jr et al., 2012; Guadagnin et al., 2015; Costa et al., 2018; Magalhães et al., 2019).

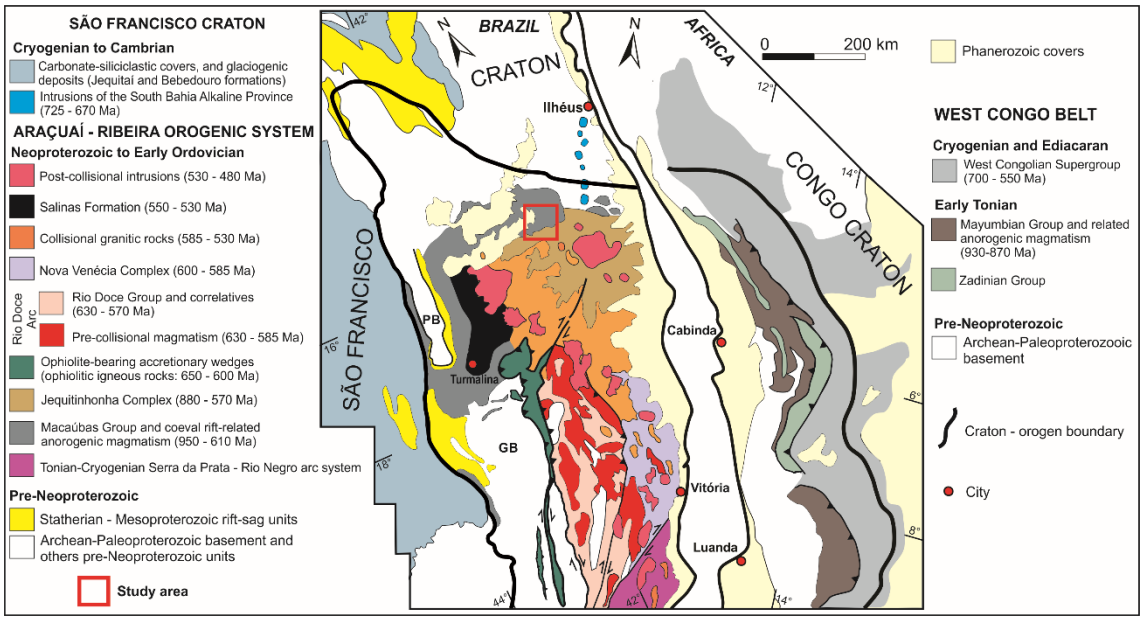

Figura 2.2 – Contexto geotectônico e mapa geológico do Orógeno Araçuaí – Congo Ocidental (modificado e atualizado de Alkmim et al., 2006, Pedrosa-Soares et al., 2008, 2011a, 2011b). GB = Bloco Guanhães, PB = Bloco Porteirinha. Espectros de idades U-Pb para unidades metassedimentares e metavulcanoclásticas baseadas em dados de rochas vulcanossedimentares singenéticas ou zircão detrítico mais jovem, indicando a idade máxima de sedimentação e idade U-Pb metamórfica mais antiga limitando a idade minima de sedimentação. Referências para idades em: Gradim et al. (2014), Pedrosa-Soares et al. (2016), Richter et al. (2016), Tedeschi et al. (2016), Degler et al. (2017), Peixoto et al. (2017), Araujo et al. (2019), e Castro et al. (2020).

O Grupo Macaúbas representa o registro da bacia homônima precursora do Orógeno Araçuaí, compreendendo um extenso empilhamento vulcano-sedimentar estimado de até 10 km (e.g. Pedrosa-Soares & Alkmim, 2011). A bacia Macaúbas compreende um sistema bacinal complexo e policíclico com o registro de, pelo menos, dois eventos neoproterozoicos de rifteamento continentais sobrepostos no espaço e no tempo (Pedrosa-Soares & Alkmim, 2011; Kuchenbecker et al., 2015). O primeiro ocorreu no Toniano Inferior (aproximadamente 940-870 Ma), formando um sistema de aulacógeno

(e.g., Tack et al., 2001; Costa & Danderfer, 2017; Castro et al., 2019; Bitencourt et al., 2019; Souza et al., 2019), e o segundo, ocorrendo no Toniano Superior ao Criogeniano Inferior (aproximadamente 735-675 Ma) que evoluiu para uma configuração de margem passiva continental com espalhamento de assoalho oceânico (e.g. Pedrosa-Soares et al., 1998, 2008, 2011a; Rosa et al., 2007; Straathof, 2011; Thiéblemont et al., 2009; Kuchenbecker et al., 2015; Amaral et al., 2020) (Fig. 2.3).

A sequência basal, de idade Toniano Inferior, compreende rochas metavulcanossedimentares, delimitadas por não conformidades no topo e base, e registra o evento de rifte abortado, constituída pelas formações Capelinha, Matã-Duas Barras, Planalto de Minas e Rio Peixe Bravo. Essa sequencia, depositada em ambiente fluvial a marinho raso, não apresenta diamictitos e foi nomeada como Grupo Macaúbas Inferior (ou sequencia pré-diamictitica – sequencia pré-glacial) (Martins et al., 2008; Pedrosa-Soares et al., 2011b; Babinski et al., 2012; Kuchenbecker et al., 2015; Castro et al., 2019; Souza et al., 2019).

A sequência superior, de idade Toniano Superior a Criogeniano Inferior, é representada por magmatismo orogênico nas margens do Cráton São Francisco-Congo (Texeira et al., 1997; Rosa et al., 2007; Thiéblemont et al., 2009a,b; Straathof, 2011), restringindo a idade do segundo evento relacionado ao rifteamento da Bacia Macaúbas. Esse rifte continental é responsável pela deposição de ao menos um evento glacial representado pelas unidades que apresentam diamictitos: Formação Serra do Catuni, Formação Nova Aurora e Formação Chapada Acauã Inferior (Pedrosa-Soares et al., 2011b; Babinski et al., 2012; Caxito et al., 2012, 2021b; Kuchenbecker et al., 2015; Castro et al., 2020).

O segundo evento de rifte evoluiu até a deposição complete da bacia Macaúbas, com o estabelecimento de uma margem passiva continental com expansão de crosta oceânica (Pedrosa-Soares et al., 1992; 1998; 2001; 2011b; Queiroga et al., 2007; Peixoto et al., 2015; Amaral et al., 2020). Essa unidade pós-glacial, correspondendo às unidades Formação Chapada Acauã Superior e Formação Ribeirão da Folha, apresenta turbiditos finos e depósitos sedimentares exalativos intercalados com rochas metamáficas e meta-ultramáficas. As rochas metamáficas e meta-ultramáficas são interpretadas como resto de litosfera oceânica Neoproterozóica (Pedrosa-Soares et al. 1998, Amaral et al., 2020), e estudos realizados em plagiogranitos apresentaram idade U-Pb (SHRIMP e LA-

ICPMS) em torno de 645 ± 10 Ma, referente à formação do assoalho oceânico (Queiroga et al., 2007; Amaral et al., 2020).

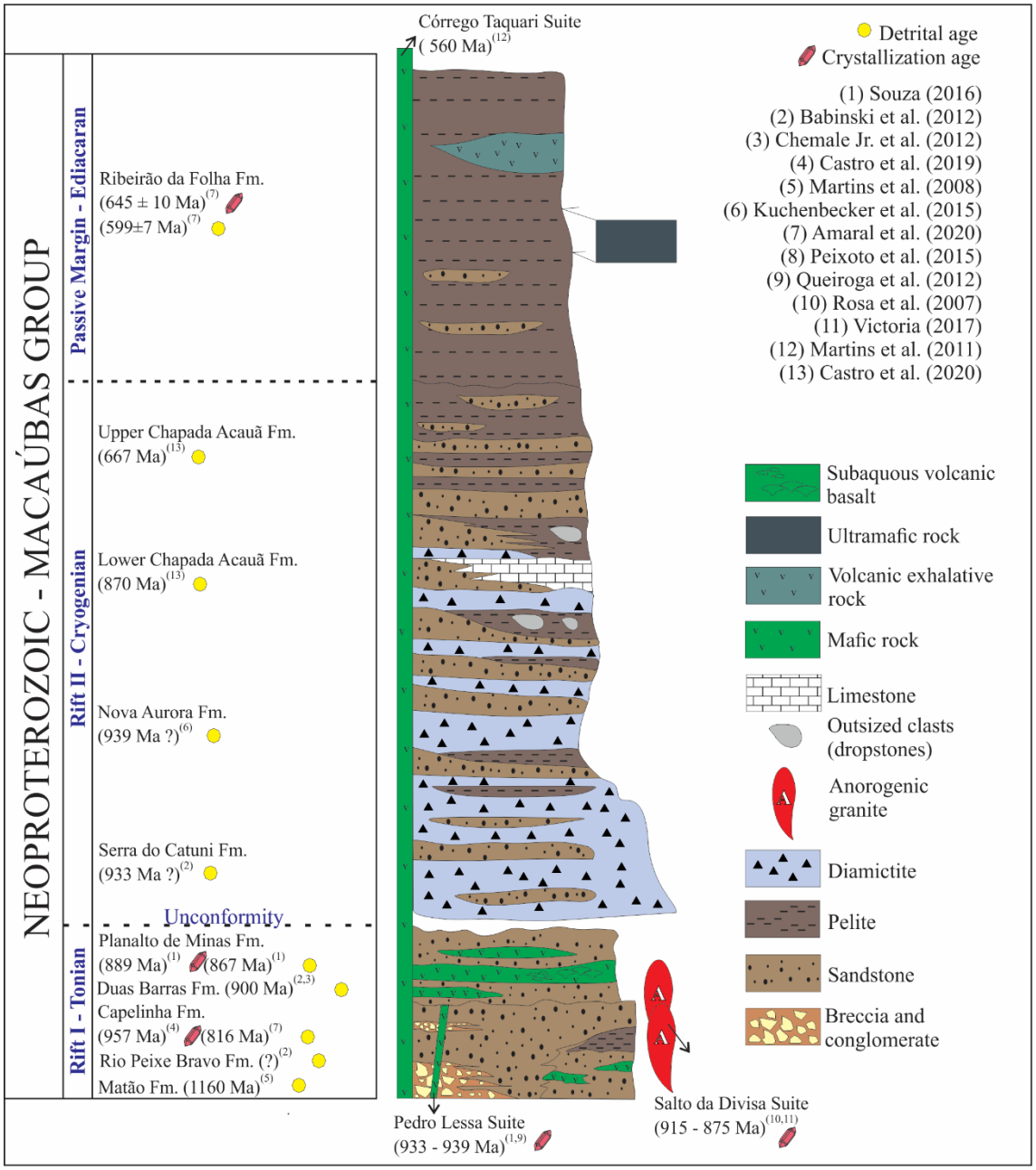

Figura 2.3 – Coluna estratigráfica e dados geocronológicos disponíveis para o Grupo Macaúbas (modificado Pedrosa-Soares & Alkmim, 2011, adaptado de Souza et al., 2019).

O fechamento da bacia oceânica foi responsável pela geração do Arco Magmático do Rio Doce (ca. 630–585 Ma) e bacias relacionadas ao arco (Nalini Jr. et al., 2000; Pedrosa-Soares et al., 2011a; Tedeschi et al., 2016; Novo et al., 2018). Paragnaisses peraluminosos com intercalações de rochas calcissilicáticas representam a deposição pré-colisional na bacia atrás do arco (Noce et al., 2004; Gradim et al., 2014; Richter et

al., 2016; Araujo et al., 2019), e nas bacias intra-arco e frente do arco (Degler et al., 2017).

A Formação Salinas consiste de uma sequência espessa de grauvacas turbidíticas e pelitos, contend lentes de conglomerados e rochas calcissilicáticas, recobrindo diferentes unidades do Grupo Macaúbas e definindo uma não conformidade regional (Lima et al., 2002; Peixoto et al., 2015; Deluca et al., 2019). Representa uma sedimentação orogênica cuja maior contribuição detrítica foi o Arco do Rio Doce (Lima et al., 2002; Santos et al., 2009; Costa et al., 2018; Deluca et al., 2019).

Durante o estágio collisional do Orógeno Araçuaí, ocorreu ampla anatexia nos complexos paragnaissicos, gerando um grande volume de granitos tipo-S (ca. 585 Ma – 540 Ma) (Pedrosa Soares et al. 2011a; Gradim et al., 2014; Melo et al., 2017), seguidos por inúmeras intrusões pós-colisionais de rochas graníticas ou rochas máficas do tipo-I e tipo-A (Pedrosa-Soares et al., 2011a; Gradim et al., 2014; Campos et al., 2016; Serrano et al., 2018; Araujo et al., 2019). Esses processos magmáticos da fase pós-colisional foram associados à extensão e descompressão da crosta e ao colapso gravitacional relacionado à delaminação do manto e ascensão de pluma mantélica (Serrano et al., 2018). Análises de monazitas em plutons graníticos relacionados ao colpaso orogênico indicam que esse processo pode ter durado até cerca de 490 Ma (Gonçalves et al., 2019).

2.1.Depósitos Sin-glaciais do Grupo Macaúbas

A Formação Serra do Catuni é a mais antiga unidade que contém diamictitos no Grupo Macaúbas, sendo um pacote muito extenso de diamictitos e, intercalados em menores quantidades, arenitos e pelitos. Blocos caóticos e clastos facetados/estirados representam feições glaciais nessa unidade (Pedrosa-Soares et al., 2011, Kuchenbecker et al., 2015).

A Formação Nova Aurora representa um segundo pacote de diamictitos, com intercalações e em menor quantidade de arenitos e poucos pelitos. A unidade basal apresenta diamictitos predominantemente enriquecidos em ferro e, em menor quantidade, diamictitos não ferruginosos. O tamanho de grão, composição de matriz e razão clasto/matriz tem uma variação considerável nesses diamictitos. A unidade

superior apresenta diamictitos estratificados, com camadas e lentes subordinadas de arenitos com granodecrescência ascendente e finas intercalações pelíticas (Pedrosa-Soares et al., 2011).

Por fim, a Formação Chapada Acauã Inferior encerra a sequência glacial e apresenta basicamente ciclos de diamictitos estratificados com granodecrescência ascendente, arenitos e ritmitos pelíticos (Pedrosa-Soares et al., 2011). A razão clasto/matriz apresenta grandes variações nas camadas de diamictito, com clastos de tamanho grânulo a bloco. As camadas e lentes de arenito apresentam granodecrescência ascendente e as camadas de ritmitos apresentam localmente clastos pingados, principalmente de tamanho cascalho e bloco (Kuchenbecker et al., 2015).

2.1.1. Área de estudo do Grupo Macaúbas

Na região de estudo próxima às cidades de Itambé, Encruzilhada e Macarani (BA), de acordo com Araújo (2000), Drumond (2000) e Souza et al. (2003), ocorrem exposições de rochas do Grupo Macaúbas e Complexo Jequitinhonha, além de granitos pós-colisionais (sudoeste) e embasamento cratônico (nordeste) (Fig. 2.4). De acordo com Souza et al. (2003), as rochas do Toniano pertencentes ao Grupo Macaúbas que afloram no estado da Bahia seriam paragnaisses e as rochas definidas pelo autor como pertencentes Grupo Macaúbas, de idade Criogeniana, seriam metadiamictitos e grauvacas xistificadas da Formação Chapada Acauã e micaxistos bandados, metagrauvacas e quartzitos. O alvo de estudo em campo foram os afloramentos referentes aos metadiamictitos e grauvacas xistificadas da Formação Chapada Acauã, conforme será abordado no item 4. Em campo, essas rochas encontram-se muito alteradas e, portanto, os afloramentos são escassos.

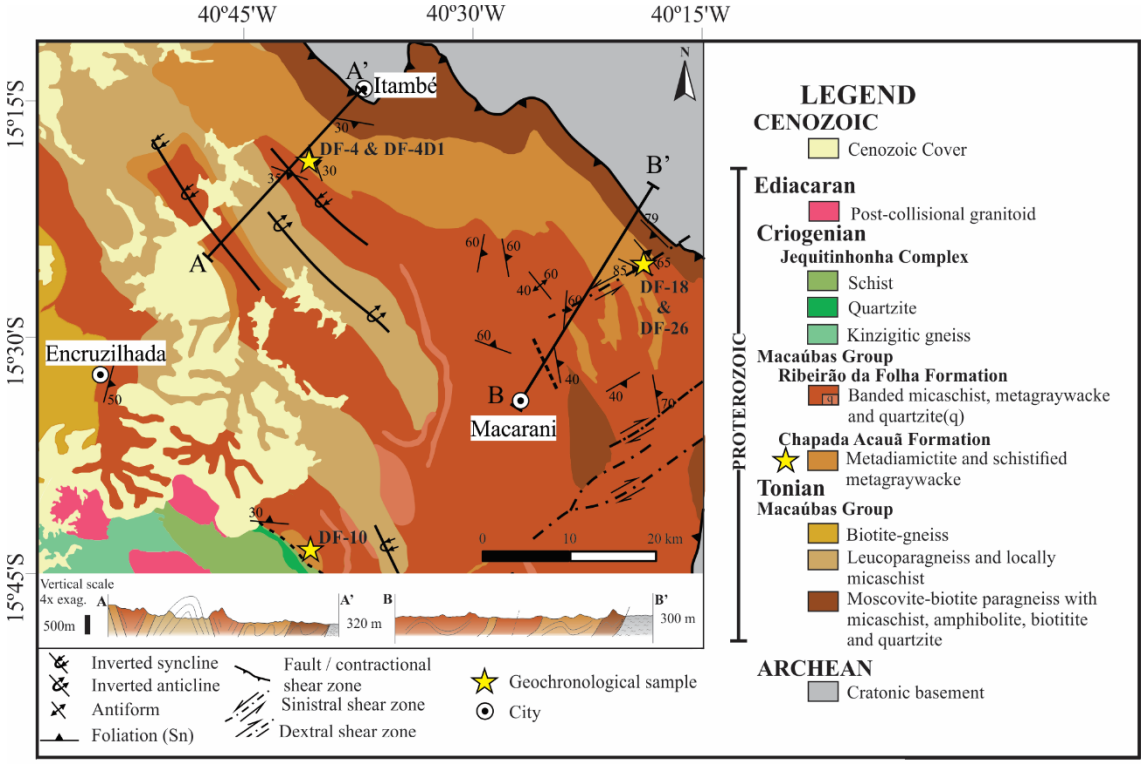

Figura 2.4 – Mapa geológico da área de estudo com a localização das amostras utilizadas para estudo grocronológico. Mapa geológico compilado de Araújo (2000), Drumond (2000) e Souza et al. (2003).

2.2.Complexo Jequitinhonha

O Complexo Jequitinhonha representa um das mais extensas unidades estratigráficas do Orógeno Araçuaí, ocorrendo no nordeste do estado de Minas Gerais e sudeste do estado da Bahia. O Complexo Jequitinhonha apresenta principalmente uma série de paragnaisses enriquecidos em e com quantidades variáveis de biotita, granada, cordierita e silimanita em relação a quartzo e feldspato, devido a variações nas frações de argila e nas frações de silte e areia. A composição dos gnaisses ricos em aluminossilicatos se assemelha a um gnaisse kinzigítico (Mehnert, 1971), sendo esse um silimanita-cordierita-granada-biotita gnaisse com traços de grafita e sulfetos. Esse pacote regional de paragnaisses apresenta intercalações de silimanita-grafita gnaisse (representando uma lama rica em carbono), ortoquartzitos a ± grafita ± mica-quartzitos (metarenitos), além de lentes menores de rocha paraderivada calcissilicática (margas) (Pedrosa-Soares & Wiedemann-Leonardos, 2000; Gonçalves Dias et al., 2011, 2016).

O Complexo Jequitinhonha também apresenta depósitos econômicos de grafita, chegando a aproximadamente um bilhão de toneladas de grafita (e.g., Faria, 1997; Reis, 1999; Guimarães, 2000; Daconti, 2004; Belém, 2006, 2018), e geralmente ocorrem

como saprolitos de silimanita-grafita gnaisse (ou xisto). Esse gnaisse rico em grafita é espacialmente associado a camadas de quartzito pobres ou sem grafita.

Os paragnaisses do Complexo Jequitinhonha formam os paleossomas dos migmatitos, que apresentam diferentes graus de fusão parcial, compostos por metatexitos e diatexitos metamorfisados em condições de fácis anfibolito alto a granulito (700-900 ºC, 5 a 7 kbar; Belém, 2006; Moraes et al., 2015). Análises de U-Pb em zircão detrítico do leucossoma dos paragnaisses e de outros corpos graníticos gerados através de fusão parcial dos paragnaisses mostram uma idade de metamorfismo collisional e migmatização entre 570-540 Ma, com episódio pós-colisional em aproximadamente 500 Ma (Gradim et al., 2014; Richter et al., 2016; Degler et al., 2017; Melo et al., 2017; Serrano et al., 2018). O Complexo Jequitinhonha é interpretado como margem distal passive Neoproterozócia da bacia precursora do Orógeno Araçuaí, com a sedimentação dos protólitos ocorrendo provavelmente durante o Criogeniano (Gonçalves-Dias et al., 2011, 2016).

2.2.1. Área de estudo do Complexo Jequitinhonha

Na região de estudo do Complexo Jequitinhonha (abordado no item 3), onde ocorrem afloramentos de gnaisses kinzigíticos, com lentes de quartzito e grafita gnaisse, também existem afloramentos de intrusões graníticas (e.g. Pluton Rubim) (Uhlein et al., 1998; Paes et al., 2010). Os granitos tipo G2 são intrusões graníticas sin-colisionais podendo ser granitos peraluminosos (com granada e cordierita e/ou silimanita) com granito a duas micas e granodiorito granatífero subordinados e que registram a deformação regional. Os granitos tipo G3 são leucogranitos com granada e/ou cordierita, empobrecidos em mica e sem registro de deformação regional (Pedrosa-Soares et al., 2007).

A granitogênese G5 é representada por plútons livres de foliação regional, do estágio pós-colisional. Esse plutonismo é cálcio-alcalino rico em potássio e ferro, com composição predominantemente granítica ou charnockítica, com porções enderbíticas e noríticas subordinadas, possuindo diversas evidências de mistura de magma (*migling* e *mixling*) (Pedrosa-Soares et al., 2007).

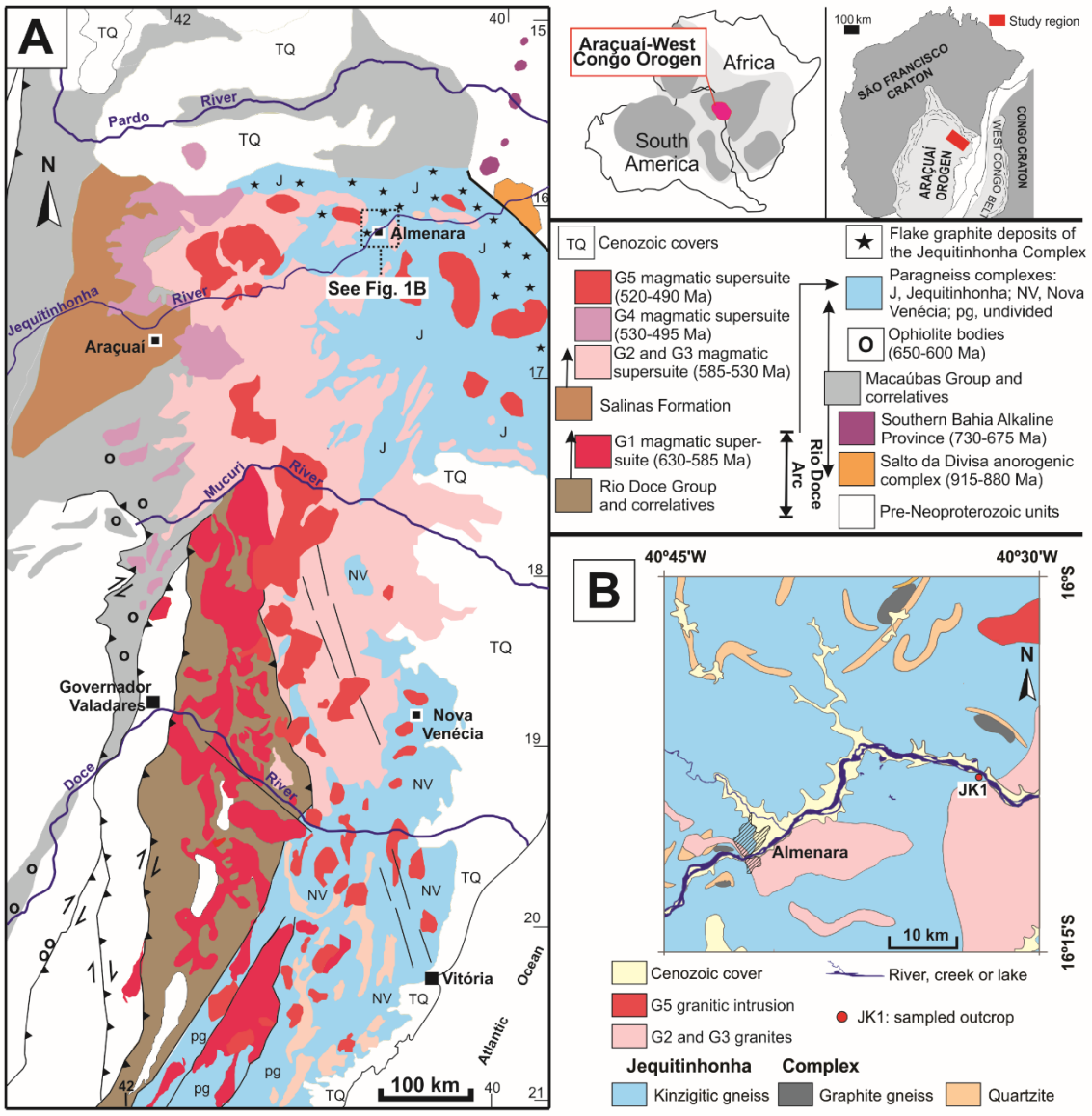

Figura 2.5 – A – Contexto tectônico e mapa geológico do Orógeno Araçuaí (modificado de Pedrosa-Soares et al., 2008). B – Mapa geológico da região de estudo, próximo à cidade de Almenara, onde afloram rochas do Complexo Jequitinhonha (modificado de Paes et al., 2010). Localização da amostra estudada (JK1) indicada como ponto vermelho (16◦7′57”S/40◦32′24”W/WGS84).

3. ARTIGO I - Detrital zircon U-Pb and Lu-Hf data for a kinzigitic gneiss (Jequitinhonha Complex, Araçuaí Orogen, SE Brazil) constrain the age of a huge storage of Ediacaran carbon

Fernando Estevão Rodrigues Crincoli Pacheco[1*]; Fabrício de Andrade Caxito[1#]; Antônio Carlos Pedrosa-Soares[1#]; Ivo Antônio Dussin[2#]; Tatiana Gonçalves-Dias[1]

[1]Programa de Pós-Graduação em Geologia, Universidade Federal de Minas Gerais, CPMTC-IGC-UFMG, Av. Antônio Carlos 6627, Pampulha, 31270-901 Belo Horizonte, MG, Brazil.

[2]Universidade Estadual do Rio de Janeiro, Faculdade de Geologia, R. São Francisco Xavier 524, Maracanã, 20550-900, Rio de Janeiro, RJ, Brazil.

*Corresponding author: ferodrigues@live.it

[#]Fellow of the Brazilian Research Council (CNPq)

Abstract

The precursor basin of the Araçuaí – West Congo Orogenic System (AWCO) formed a large gulf within the São Francisco – Congo Paleocontinent (SFCP), where sedimentary successions ascribed to the Jequitinhonha Complex and Macaúbas Group were deposited in the Neoproterozoic. This precursor basin system comprises an aborted continental rift of Early Tonian age and a Cryogenian rift that evolved to ocean-floor spreading up to the Early Ediacaran. The Jequitinhonha Complex is an extensive metasedimentary unit located in the northeastern Araçuaí Orogen, consisting of Al-rich paragneiss (kinzigite), sillimanite-graphite gneiss and associated economic deposits of flake graphite, quartzite and lenses of calc-silicate rock, metamorphosed to upper amphibolite or granulite facies around 570–550 Ma. U-Pb (LA-MC-ICP-MS) data of 110 detrital zircon grains from the paleosome of a migmatitic paragneiss yield five main age peaks at 2564 ±35 Ma (5% of the grains), 2012 ±21 Ma (7%), 1807 ±19 Ma (12%), 960 ±8 Ma (29%) and 662 ±6 Ma (48%), with the youngest grains around 630–609 Ma, and a major age gap from the Statherian to Stenian. The U-Pb age spectrum coupled

with Lu-Hf in zircon (LA-MC-ICP- MS) data for 106 zircon grains suggest the following sources: Neoarchean to Orosirian grains were sourced from the SFCP basement, Early Tonian grains from the anorogenic magmatic province, and Cryogenian to Early Ediacaran grains were provided by the Southern Bahia Alkaline Province and Rio Doce magmatic arc. The εHf(t) values show a predominant contribution from evolved crust, with minor involvement of moderately juvenile crust. The sedimentation of Jequitinhonha Complex protoliths developed from the Cryogenian to Early Ediacaran, partially within anoxic marine environments favorable to the preservation of organic matter that formed the huge graphite deposits and lots of smaller occurrences found in the region, accumulating probably more than one billion tons of raw graphite. The youngest detrital zircon population suggests that the deposition record of the Jequitinhonha Complex covers the Cryogenian continental rifting event followed by the development of oceanic crust to the onset of subduction and building of the Rio Doce magmatic arc in the Early Ediacaran. The regional accumulation and preservation of carbon-rich sediments (now graphite-rich gneiss) most probably represent one of the largest storages of Ediacaran carbon around the world.

Keywords: graphite; kinzigite; U-Pb and Lu-Hf isotopes; Araçuaí – West Congo Orogen; Gondwana; Ediacaran carbon

3.1. Introduction

The Araçuaí Orogen and its African counterpart, the West Congo Belt, lay together in the central part of West Gondwana until its break-up during the Lower Cretaceous (Alkmim et al., 2001). The Araçuaí – West Congo Orogenic System (AWCO) was the result of closure of a branch of the Neoproterozoic Adamastor Ocean, surrounded by the former São Francisco – Congo paleocontinent (Pedrosa-Soares et al., 2001; Cordani et al., 2003; Alkmim et al., 2006). On the current continental setting, the Brazilian AWCO counterpart, the Araçuaí Orogen, extends from the eastern margin of the São Francisco Craton to the Brazilian Atlantic coast (Fig. 3.1A).

The AWCO precursor basin system formed a large gulf within the São Francisco – Congo paleocontinent (Pedrosa-Soares et al., 2001, 2008), where sedimentary successions ascribed to the Jequitinhonha Complex, Macaúbas Group and correlated units were deposited in the Neoproterozoic (Fig. 3.1A). The AWCO precursor basin

system comprises an aborted continental rift of Early Tonian age (ca. 950–880 Ma) and a Cryogenian rift (ca. 720–675 Ma) that evolved to ocean-floor spreading until the Early Ediacaran (Pedrosa-Soares and Alkmim, 2011; Kuchenbecker et al., 2015; Castro et al., 2019; Amaral et al., 2020).

The last extensional episode evolved to a complete Wilson Cycle and led to a subduction-related convergent event with the development of the Rio Doce magmatic arc upon an active continental margin between 630-585 Ma (Pedrosa-Soares et al., 1998, 2001; 2011a; Nalini Jr. et al., 2000; Tedeschi et al., 2016) and broad development of orogenic basins with arc-related sedimentary contribution (Gradim et al., 2014; Richter et al., 2016; Novo et al., 2018; Deluca et al., 2019).

The Jequitinhonha Complex is an extensive metasedimentary terrane located in the northeastern Araçuaí Orogen, in the northeast portion of the Rio Doce magmatic arc (Fig. 3.1A). This complex consists of a series of Al-rich paragneisses, including kinzigite (i.e., sillimanite- cordierite-garnet-biotite gneiss with traces of graphite) (Mehnert, 1968), with intercalations of sillimanite-graphite gneiss, quartzite and paraderived calc-silicate rock, metamorphosed from high amphibolite to granulite facies at around 570–550 Ma (Gonçalves-Dias et al., 2016).

The presence of large economic deposits of flake graphite of sedimentary origin, comprising one of the largest graphite ore provinces around the world (Belém, 2006, 2018), probably reaching more than one billion tons of raw graphite, is an outstanding feature of the Jequitinhonha Complex, recording a huge accumulation of largely preserved Precambrian organic matter. Therefore, the Jequitinhonha paleobasin predominantly included quiet-water marine environments, indicated by the extensive Al-rich paragneiss layers representing clay-rich pelitic deposits, formed partially under anoxic conditions favorable to the preservation of large amounts of carbon-rich deposits now represented by thick layers of sillimanite-graphite-rich gneiss, bounded by more energic sedimentary environments represented by quartzite (metasandstone) layers.

This regional lithofacies association of sillimanite-graphite gneiss (metamorphosed carbon-rich mud), quartzite (metasandstone), kinzigitic gneiss (metapelite) and paraderived calc-silicate rock (metamarl), lacking any evidence of volcanic activity, suggests a sedimentary origin for the carbon-rich (i.e., organic matter-rich) layers

(Pedrosa-Soares and Wiedemann-Leonardos, 2000). Previous isotopic studies on the Jequitinhonha Complex have presented U-Pb isotope data from detrital grains of zircon extracted from quartzite layers and whole-rock Sm-Nd data from kinzigitic gneisses, suggesting mixed sediment sources with a possible maximum depositional age in the Cryogenian (Gonçalves-Dias et al., 2011, 2016). These data and interpretations are now revised in the light of new isotopic analysis.

This contribution is aimed to track the provenance of the fine- grained sedimentary fractions represented by the Al-rich paragneiss and also constraining the age of the deposition of the carbon-rich sediments precursor of graphite deposits. We selected a sample of kinzigitic paragneiss to recover detrital grains of zircon. From them, we obtained 110 new U-Pb ages and 106 Lu-Hf in-zircon analyses that allow us to better understand the sediment provenance and depositional setting of the Jequitinhonha Complex, as well as to constrain the depositional age of the extensive pelite layers rich in organic deposits.

3.2. Geological Setting

The Araçuaí Orogen is located between the São Francisco Craton and the Atlantic Ocean, between latitudes 15º S and 21º S (Fig. 3.1A). The orogen has the West Congo belt as a counterpart in southwestern Africa (Pedrosa-Soares et al., 2000, 2008; Tack et al., 2001), which encompasses a set of geotectonic components that define an accretionary orogen of active continental margin followed by a collision. These components can be exemplified by passive margin deposits, ophiolitic slivers, a suture zone, a continental magmatic arc, syn-collisional granites and post-collisional plutons (Pedrosa-Soares et al., 2007, 2008, 2011a,b; Gradim et al., 2014; Tedeschi et al., 2016; Serrano et al., 2018; Amaral et al. 2020).

The Macaúbas Group is the best preserved unit of the precursor basin of the Araçuaí Orogen. The basin has a volcano-sedimentary sequence of up to 10 km thickness, which mainly crops out on the northern sector of the orogen (Fig. 3.1A). The extensive Macaúbas diamictite-bearing units are coeval to at least one Cryogenian glacial event (Pedrosa-Soares et al., 2011b; Caxito et al., 2012). The Macaúbas Group has been divided into three successions in relation to the presence of glaciogenic diamictites (Pedrosa-Soares et al., 2011b): i) a diamictite-free preglacial succession deposited in

fluvial to shallow marine systems (Castro et al., 2019); ii) successions rich in glaciogenic diamictites (Babinski et al. 2012; Kuchenbecker et al., 2015); and iii) a post-glacial succession containing fine-grained turbidites and sedimentary exhalative deposits interleaved with metamafic and meta-ultramafic rocks that are interpreted as remnants of a Neoproterozoic oceanic lithosphere (Pedrosa-Soares et al. 1998, Amaral et al., 2020).

According to the U-Pb ages of anorogenic igneous rocks and detrital zircon data from associated rocks, the deposition in the Macaúbas basin can be related to two Neoproterozoic taphrogenic events (Pedrosa-Soares & Alkmim, 2011): (I) an Early Tonian (ca. 950–870 Ma) aborted continental rift event (e.g., Tack et al., 2001; Castro et al. 2019; Bitencourt et al., 2019; Souza et al., 2019); and (II) a Late Tonian to Early Cryogenian (ca. 735–675 Ma) continental rift event (Rosa et al., 2007; Straathof, 2011; Thiéblemont et al., 2009; Kuchenbecker et al., 2015) that evolved to a passive margin setting with seafloor spreading, thereby creating an inland-sea basin that was partially floored by oceanic crust (Pedrosa-Soares et al., 1998, 2008, 2011a; Amaral et al., 2020).

The detrital zircon U-Pb data of various units of the Macaúbas Group correspond to three main age peaks at 880–1000 Ma, 1900–2200 Ma and 2600–2800 Ma, besides some sparse grains dated at ca. 700 Ma (Babinski et al., 2012; Kuchenbecker et al., 2015; Bitencourt et al., 2019; Castro et al., 2019; Souza et al., 2019; Amaral et al., 2020). The lack of Archean zircon grains in the pre-glacial succession and the relative abundance of Tonian zircon grains in the upper succession reveal an important change of source areas, which is consistent with a shift of climatic conditions and the change of the tectonic setting from a rift-related to a passive margin basin.

Closure of the oceanic basin generated the Rio Doce magmatic arc (ca. 630–585 Ma) and arc-related basins (Nalini Jr. et al., 2000; Pedrosa-Soares et al., 2011a; Tedeschi et al., 2016; Novo et al., 2018). Peraluminous paragneiss with intercalations of calc-silicate rocks represents the pre-collisional deposition in the back-arc basin (Noce et al., 2004; Gradim et al., 2014; Richter et al., 2016; Araujo et al., 2019), and in the fore-arc and intra-arc basins (Degler et al., 2017). In addition to regional deformation and metamorphism, the collisional stage generated a large volume of S-type granitic rocks dated from ca. 585 Ma to ca. 540 Ma (Pedrosa Soares et al. 2011a; Gradim et al., 2014;

Melo et al., 2017), followed by a myriad of post-collisional intrusions (Campos et al., 2016; Serrano et al., 2018; Araujo et al., 2019) (Fig. 3.1A).

3.2.1. The Jequitinhonha Complex

The Jequitinhonha Complex (named by Almeida and Litwinski, 1984) represents one of the most extensive stratigraphic units of the Araçuaí Orogen. It occurs to the northeast of Minas Gerais and in the southeastern part of the state of Bahia (Fig. 3.1A, B). This complex is mostly composed of a series of paragneisses variably rich in biotite, garnet, cordierite and sillimanite in relation to quartz and feldspars, reflecting distinct contents of clay-rich fractions versus silt- to sand-rich fractions. The composition of the gneiss rich in Al-silicates resembles that of a true kinzigite (Mehnert, 1971). This gneiss is a sillimanite-cordierite-garnet-biotite gneiss with traces of graphite and sulphides. This regional package of paragneisses includes extensive and thick intercalations of sillimanite-graphite gneiss, representing carbon-rich mud, and orthoquartzite to graphite- and/or mica-bearing quartzite (metasandstones). There are small lenses of paraderived calc-silicate rock, representing pelite-carbonate mixtures like marls (Pedrosa-Soares & Wiedemann-Leonardos, 2000; Gonçalves Dias et al., 2011, 2016).

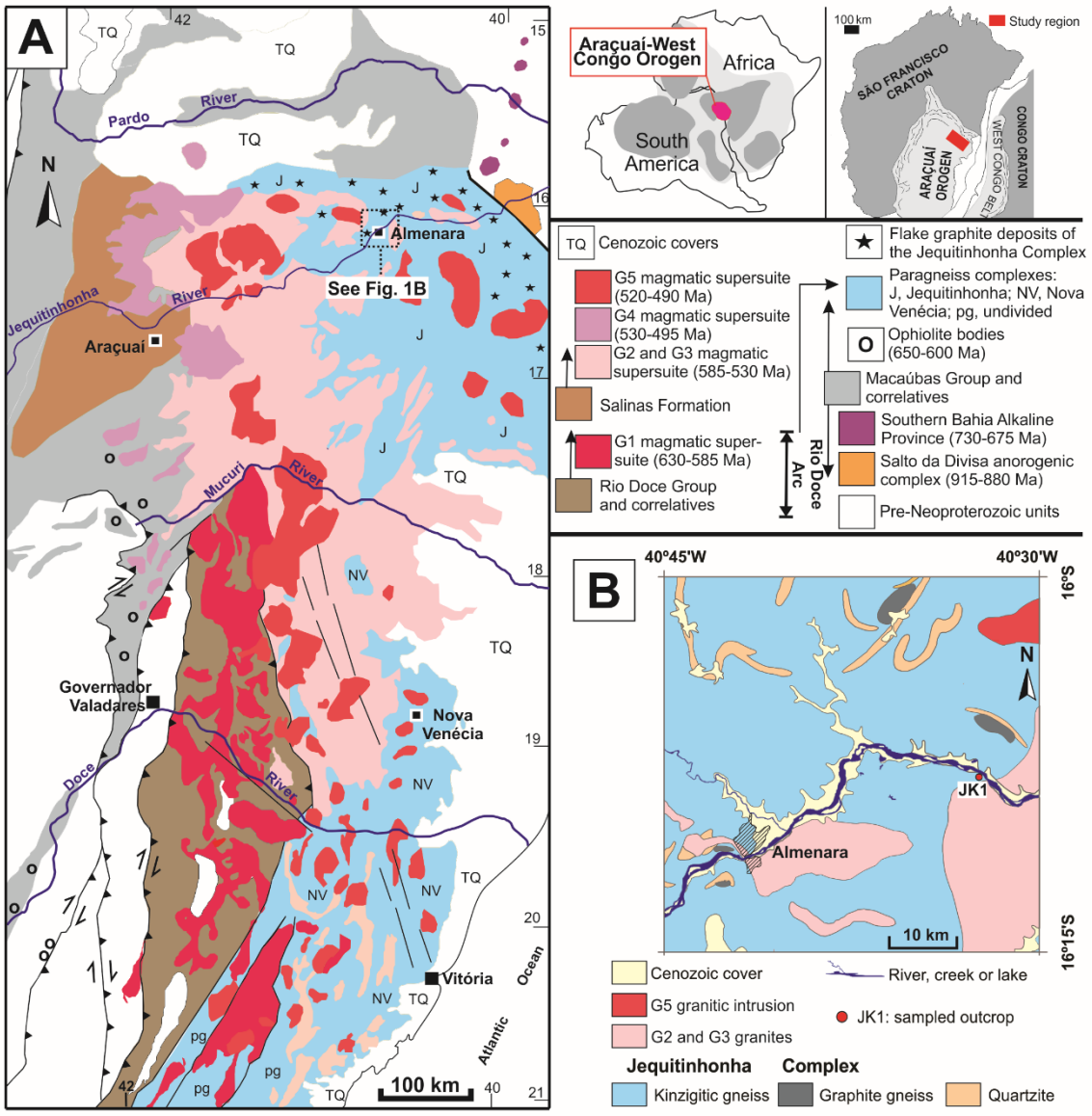

Figura 3.1 – A – Geotectonic setting and geological map of the Araçuaí Orogen (modified from Pedrosa-Soares et al., 2008). B – Geological map of the Jequitinhonha Complex close to the town of Almenara (modified from Paes et al., 2010). The location of sample JK1 is shown as a red dot (16◦7′57”S/40◦32′24”W/WGS84).

The Jequitinhonha Complex also includes large economic deposits of flake graphite and a great number of smaller deposits and occurrences of flake and lump graphite, reaching up to one billion tons of raw graphite, located on the extreme northeast of Minas Gerais and in southeast Bahia (e.g., Faria, 1997; Reis, 1999; Guimarães, 2000; Daconti, 2004; Belém, 2006, 2018). The graphite deposits generally occur as saprolites on sillimanite-graphite gneiss (to schist) that may grade into graphite-bearing quartzite. The graphite-rich gneiss is generally spatially associated with quartzite layers ranging from poor in graphite to begin barren. The layers of graphite-rich gneiss indicate low-energy anoxic sites in a marine environment (e.g., lagoons), whilst the associated quartzite layers point

a more energetic sedimentary environment (e.g., sand bars). The Jequitinhonha paragneisses form the paleosomes of migmatites with different degrees of partial melting, comprising metatexites and diatexites, that were metamorphosed under high amphibolite to granulite facies conditions (700-900 ºC at 5 to 7 kbar; Belém, 2006; Moraes et al., 2015).

Zircon U-Pb data from S-type leucosomes and other granitic bodies, formed from the partial melting of regional paragneisses, constrain the age of the collisional metamorphism and migmatization between 570-540 Ma, with a post-collisional episode at ca. 500 Ma (Gradim et al., 2014; Richter et al., 2016; Degler et al., 2017; Melo et al., 2017; Serrano et al., 2018). The Jequitinhonha Complex has been interpreted as part of the Neoproterozoic distal passive margin of the precursor basin of the Araçuaí Orogen, with sedimentation of the protoliths probably during the Cryogenian (Gonçalves-Dias et al., 2011, 2016).

3.3. Material and Methods

The paragneiss sample analyzed for this study is free of weathering and hydrothermal alteration. Sample preparation was done in the SEPURA (High Purity Mineral Separation) laboratories of the Centro de Pesquisa Manoel Teixeira da Costa (CPMTC), Federal University of Minas Gerais (UFMG). Zircon concentrates were extracted from the rock matrix using conventional magnetic (Frantz isodynamic separator) and gravimetric techniques, and through handpicking under a binocular microscope. The grains were mounted and polished in an epoxy disk. At MultiLab (UERJ), cathodoluminescence (CL) images were obtained on a scanning electron microscope (SEM, Quanta-250-FEI) to investigate morphological features and internal structures of zircon grains.

3.3.1. LA-MC-ICP-MS U-Pb in zircon

The zircon grains were analyzed with a Laser microprobe (Excimer Laser 193 μm by Photon – Machines Inc. Model ATLEX SI), pulsed with ArF, and attached to the MC-ICP-MS (Neptune-Plus) equipment in the multi-use isotopic laboratory (MULTILAB) at the University of Rio de Janeiro State (UERJ). Isotopic data were acquired in static from laser beam spots of 25 μm size. The acceleration voltage of the laser used for the

ablation of the grains varied between 5 and 100 Hz and applied energies were between 0 and 20 mJ. The applied parameters for the laser are: repletion rate of 6 Hz voltage of 5 – 7 mJ. The configuration for the MC-ICP-MS Neptune Collector are: i) Faradays: ^{206}Pb, ^{208}Pb, ^{232}Th, ^{238}U; ii) MIC's: ^{202}Hg, $^{204}Hg+^{204}Pb$, ^{207}Pb; iii) Gas injection: a)cooling liquid (Ar): 15 l/min; b) auxiliary liquid (Ar): 0.85 l/min; c) transport liquid: 0.85 l/min (Ar) + 0.75 l/min (He); iv) counting times: 50 cycles of 1.049 s.

Elemental fractionation in laser ablation and essential mass discrimination were monitored by analyses of external zircon standards GJ-1 ($^{207}Pb/^{206}Pb$ age of 608.5 ± 0.4 Ma; $^{207}Pb/^{206}Pb$ = 0.060136; $^{206}Pb/^{238}U$ = 0.098906; Jackson et al., 2004) and 91500 (1065 ± 0.3 Ma; $^{207}Pb/^{206}Pb$ = 0.07488; $^{206}Pb/^{238}U$ = 0.17917; Wiedenbeck et al., 1995) (Supplementary Data: SD-3.1). External uncertainties were propagated by quadratic addition of individual measurements of the external standard GJ-1 and individual measures of every sampled zircon (or spot). Detailed methodological conditions are described in Chemale Jr. et al. (2012). $^{207}Pb/^{206}Pb$ and $^{206}Pb/^{238}U$ dates are reported with 2σ errors, calculated using Isoplot 3.6 (Ludwig, 2008). We used $^{207}Pb/^{206}Pb$ dates for zircons older than 1.0 Ga and $^{206}Pb/^{238}U$ dates for zircons younger than 1.0 Ga.

3.3.2. LA-MC-ICP-MS Lu-Hf in zircon

The isotopic analyses for Lu-Hf in zircon were carried out by using the LA-MC-ICP-MS equipment of the MultiLab-UERJ, Rio de Janeiro, Brazil. In total, 107 Lu-Hf isotopic analyses were conducted for the paragneiss sample. It was attempted to analyze the same zircon grain domains analyzed for U-Pb dating. The laser was operated with a spot of 40 μm in diameter (65% power), fluence of 1.61 J/cm 250 s, and a pulse rate of 9 Hz. Helium was used as carrier gas to minimize oxide formation and increase Hf sensitivity (Bahlburg et al., 2011). For εHf(t) values calculation we adopted a decay constant of ^{176}Lu of 1.867×10^{-11} (Söderlund et al., 2004) and present-day chondritic ratios of $^{176}Hf/^{177}Hf$ = 0.282785 and $^{176}Lu/^{177}Hf$ = 0.0336 (Bouvier et al., 2008). The Hf evolution curve of the depleted mantle was determined from present-day depleted mantle values with $^{176}Hf/^{177}Hf$ ratio of 0.28325 and $^{176}Lu/^{177}Hf$ ratio of 0.0388 (Griffin et al., 2000; updated by Andersen et al., 2009). Following Pietranik et al. (2008), the continental model of felsic crust was calculated using the initial $^{176}Hf/^{177}Hf$ ratio of zircon and $^{176}Lu/^{177}Hf$ = 0.022.

3.4. Results

Sample JK1 of the Jequitinhonha Complex was collected ca. 20 km to the east of Almenara city (Fig. 3.1B). The rock is a banded migmatitic paragneiss with bands of paleosome alternately rich in cordierite and/or garnet and/or biotite, and bands richer in quartz and feldspars (Fig. 3.2). Accessory minerals include sillimanite (which can be essential in some bands, comprising more than 5% of the rock volume), hercynite, graphite, zircon, apatite, monazite, magnetite, pyrite and ilmenite. Foliated leucosome of garnet-biotite granite occurs parallel to the regional foliation, and leucosome of cordierite-garnet granite forms discordant veins and patches. Sample JK1 was collected from the paleosome, avoiding the leucosome

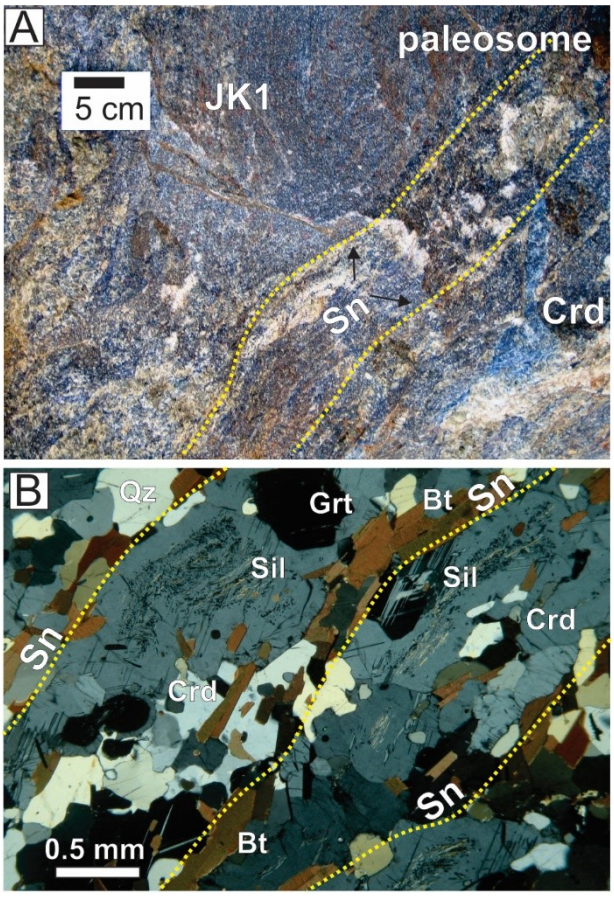

Figura 3.2 – Photos of the sampled sillimanite-garnet-cordierite paragneiss (Jequitinhonha kinzigite, JK1) showing (A) blueish bands rich in blue cordierite parallel to the regional foliation (Sn), and light veins of granitic leucosome; and the corresponding thin section (B) displaying elongated porphyroblasts of cordierite rich in oriented sillimanite inclusions, both parallel to the foliation highlighted by biotite flakes (modified from Gonçalves Dias et al., 2016). (Crd = cordierite, Sil = Sillimanite, Bt = biotite, Grt = garnet, Qz = quartz).

3.4.1. U-Pb detrital zircon ages

A total of 116 detrital zircon grains were recovered and analyzed. They range in lenght from 40 to 240 μm long. The concordances yielded by the 110 spots were within ±10% and with low common Pb (Supplementary Data: SD-3.2). Some grains are subhedral to euhedral, may even have acicular habits, but most of the grains have a rounded to subrounded shape, due to abrasion caused by erosion and transport processes (Fig. 3.3). U-Pb data of detrital zircon grains are displayed in a histogram and probability density plot calculated after Ludwig (2008) (Fig. 3.4).

Most Th/U values range from 0.11 to 1.76, with some as high as 3.51, and are consistent with a magmatic origin for these zircon grains (Rubatto, 2002). The concordant analyses yielded an age spectrum with five main peaks at 2564 ± 35 Ma (5% of the grains), 2012 ± 21 Ma (7%), 1807 ± 19 Ma (12%), 960 ± 8 Ma (29%) and 662 ± 6 Ma (48%) (Fig. 3.4A).

Figura 3.3– Selected cathodoluminescence images and spot placement for zircons grains from sample JK1. Quoted ages are $^{207}Pb/^{206}Pb$ dates for grains > 1.0 Ga and $^{206}Pb/^{238}U$ dates for grains < 1.0 Ga.

A histogram and probability density plot using only the Neoproterozoic grains (74 grains, with 9% from the Ediacaran, 61% from the Cryogenian, and 30% from the Tonian) yields a $^{206}Pb/^{238}U$ age spectrum with three main peaks at 953 ± 12 Ma, 881 ± 21 Ma and 662 ± 6 Ma (Fig. 3.4B & 3.4C). The age of the youngest zircon grain is 609 ± 26 Ma (spot number 47.1), with 100% concordance (Supplementary Data: SD-3.2).

3.4.2. Lu-Hf isotope analysis of detrital zircons

The Lu-Hf isotope analyses were performed on 106 dated detrital zircon grains of sample JK1 of the Jequitinhonha Complex (Supplementary Data: SD-3.3). The U-Pb ages obtained range from 2750 to 609 Ma with most grains falling between ca. 1018 and 638 Ma. The detrital zircon grains have $^{176}Lu/^{177}Hf$ ratios below 0.0025 and εHf(t)

values between 9.37 and -17.83. Present-day $^{176}Hf/^{177}Hf$ ratios are between 0.281032 and 0.282532.

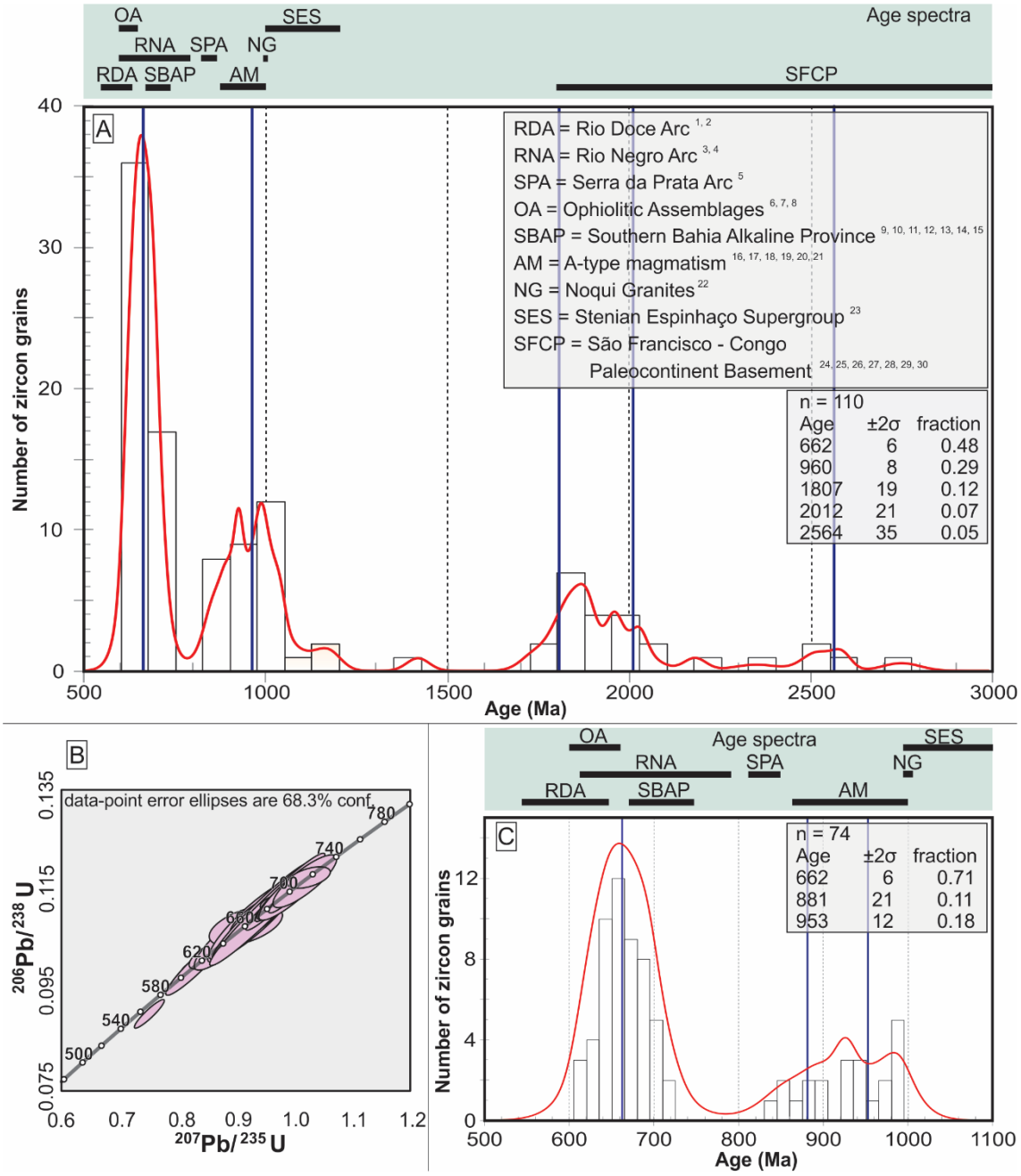

Figura 3.4 – A – Age histogram and probability density plot for all detrital zircon grains of sample JK1. Ages are 207Pb/206Pb dates for grains > 1.0 Ga and 206Pb/238U dates for grains < 1.0 Ga. B – Concordia age diagram for Neoproterozoic zircon grains (<800 Ma). C – Age histogram and probability density plot of all Neoproterozoic zircon grains. Interpretations of specific parts of this age spectrum are indicated at the top of the diagram, based on a detailed literature review: 1 – Tedeschi et al. (2016); 2 – Gonçalves et al. (2016); 3 – Heilbron & Machado (2003); 4 – Tupinambá et al. (2012); 5 – Peixoto et al. (2018); 6 – Pedrosa-Soares et al. (1998); 7 – Queiroga et al. (2007); 8 – Amaral et al. (2020); 9 – Rosa et al. (2004); 10 – Rosa et al. (2005a); 11 – Rosa et al. (2005b); 12 – Rosa et al. (2007); 13 – Menezes et al. (2012a); 14 – Rosa et al. (2015); 15 – Teixeira et al. (1997); 16 – Silva et al. (2008); 17 – McCourt et al. (2013); 18 – Menezes et al. (2012b); 19 – Chaves et al., 2019; 20 – Castro et al., 2019; 21 – Victoria et al., 2019; 22 – Tack et al. (2001); 23 – Chemale Jr et al. (2012); 24 – Vicat & Pouciet (2000); 25 – Noce

et al. (2007a); 26 – Noce et al. (2007b); 27 – Fernandes André et al. (2009); 28 – Heilbron et al. (2010); 29 – Albert et al. (2016); 30 – Silva et al. (2016).

Among the analyzed zircon grains, 53 represent a mean age peak of ca. 662 Ma (609 Ma to 717 Ma) with εHf(t) values of -14.69 to +3.82 and a common crustal evolution path projecting back to Hf_{TDM} between 1.2 and 1.8 Ga. The peak of ca. 960 Ma represents 27 zircon grains (836 Ma to 1180 Ma) with εHf(t) values of -16.13 to +9.37 and a common crustal evolution path projecting back to Hf_{TDM} between 1.0 and 2.1 Ga. The remaining 26 analyzed zircon grains represent three age groups of ca. 1807 Ma, ca. 2012 Ma, and ca. 2564 Ma, and present εHf(t) values of -17.83 to +9.36. These data may be grouped to form a common crustal evolution path projecting back to Hf_{TDM} between 1.5 and 3.0 Ma (Fig. 3.5).

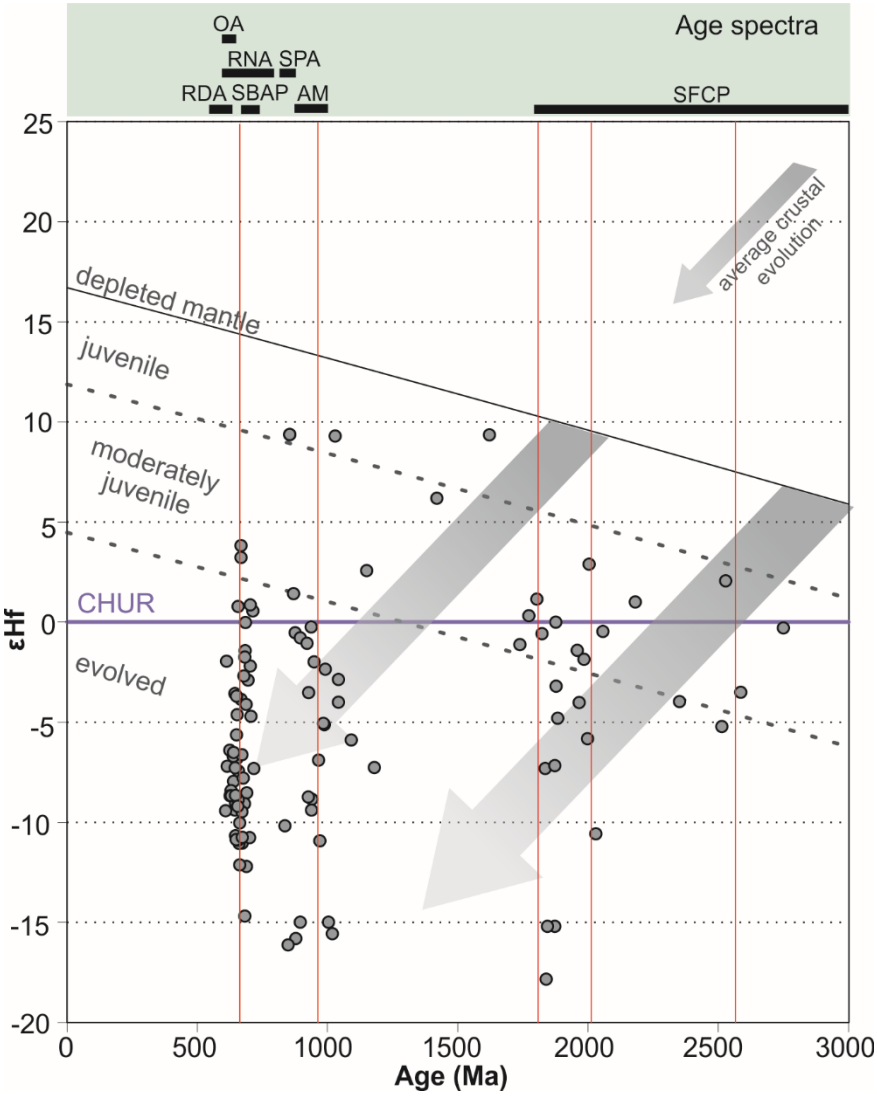

Figura 3.5 – Hf isotope data for detrital zircon grains from sample JK1. Reference lines on the Hf isotope plot after Bouvier et al. (2008). CHUR: chondritic uniform reservoir. Grey dashed lines classify fields of

juvenile (0–5 ε-units below DM), moderately juvenile (5–12 ε-units below DM), and evolved (12 ε-units below DM; Bahlburg et al., 2011). Age spectra references are the same as in Figure 3.4.

3.5. Discussion

The U–Pb data of detrital zircon grains from the Jequitinhonha Complex paragneiss sample indicates several possible sources of sediment as shown in the histograms (Fig. 3.4).

The São Francisco – Congo Paleocontinent and other paleoproterozoic basement terranes, such as the Mantiqueira Province, are the expected source for the Archean and Palaeoproterozoic zircon grains with ages ranging from 2.5 Ga to 1.8 Ga (e.g., Noce et al., 2007b; Heilbron et al., 2010, 2017; Caxito et al., 2015; Gonçalves-Dias et al., 2016; Degler et al., 2018; Silva et al., 2016). The 2.5 Ga, 2.0 Ga and 1.8 Ga peaks contain zircon grains with εHf(t) values between -10.57 and +2.89, with an outlier value of +17.82, suggesting sources of a recycled continental crust.

The 960 Ma peak includes most Tonian and some Stenian grains, which more probably represent a mixing of sources including the Stenian part of the Espinhaço Supergroup (Chemale-Junior et al., 2012), the ca. 1.0 Ga Noqui granites (Tack et al., 2001), and the Early Tonian (950 to 870 Ma) anorogenic igneous province (related to the Macaúbas Rift 1; Kuchenbecker et al., 2015) that includes the Salto da Divisa granitic suite (Silva et al., 2008; Menezes et al., 2012b; Victoria et al., 2019) and mafic rocks (Chaves et al., 2019; Castro et al., 2019) found in the Araçuaí orogen and São Francisco craton, and as well as the Zadinian-Mayumbian bimodal assemblage of the West Congo Belt (Tack et al., 2001). The 960 Ma peak may include contributions from more distant sources, like those found in northeastern Brazil (Caxito et al., 2016; Salgado et al., 2016; Santos et al., 2010; Santos et al., 2019) and in Angola (McCourt et al., 2013). Also, zircon populations from metasedimentary rocks of the São Francisco Craton and surrounding belts show similar Tonian peaks (e.g., Pedrosa-Soares et al., 2000; Figueiredo et al., 2009; Babinski et al., 2012; Caxito et al., 2012, 2014, 2016; Alcântara et al., 2017; Uhlein et al., 2017; Falci et al., 2018; Bitencourt et al., 2019; Castro et al., 2019; Souza et al., 2019). Although only one zircon grain (ca. 1021 Ma) represents a juvenile crustal contribution (εHf(t) = 9.37), the 960 Ma peak has zircon grains with εHf(t) values between -16.13 and 1.42, representing an evolved continental to moderately juvenile crustal contribution.

The Cryogenian peak of ca. 662 Ma also represents a mixture of sources, but it is important as a statiscal boundary of the maximum depositional age for the Jequitinhonha Complex protoliths. The U-Pb zircon grains ages from this peak range from ca. 609 to 717 Ma and Lu-Hf data suggest an overall evolved crustal source (εHf(t) values between -14.69 and 0.86), except for two grains with εHf(t) values of 3.24 and 3.82, possibly representing a moderately juvenile crustal source. The nearest source with similar ages would be the nearby Southern Bahia Alkaline Province (SBAP) composed of granites and syenites emplaced at the craton margin immediately to the north of the Jequitinhonha Complex (ca. 676 to 732 Ma; Teixeira et al., 1997, Rosa et al., 2004, 2005a, 2005b, 2007. 2015; Menezes et al., 2012a). Other relevant sources are the Rio Doce Arc (RDA, 630-585 Ma; Gonçalves et al., 2016 ; Tedeschi et al., 2016) just to the south, and the Rio Negro Arc (RNA) and Serra da Prata Arc (SPA) further south (ca. 600 to 860 Ma; Tupinambá et al., 2012; Peixoto et al., 2018). Although poor in zircon, alternative sources are the ophiolitic assemblages (OA) of the suture zone of the Araçuaí Orogen (600 to 660 Ma; Queiroga et al., 2007; Queiroga, 2010; Amaral et al., 2020).

The Southern Bahia Alkaline Province (SBAP) fulfills most of the criteria to be preferred as the main source area for the Cryogenian zircon grains recovered from JK1: it lies close to the Jequitinhonha Complex area, intruded into the cratonic margin upon which the Jequitinhonha Complex passive margin protoliths would have evolved, and has an age range of 675 to 735 Ma, consistent with the Cryogenian age range found in detrital zircon grains of sample JK1. Although Hf isotope data are not yet available for the SBAP, Rosa et al. (2005c) suggested the involvement of mantle-derived sources based on C and O isotopic analysis on calcite crystallized during late magmatism. As an alkaline suite intruded into thick cratonic continental crust, a scenario of magma emplacement involving mixing of mantle and crustal sources due to melting of the host crustal rocks is likely and could lead to the evolved and moderately juvenile values observed in the recovered zircon grains.

The Rio Doce Arc (RDA) lies relatively close to the sedimentary paleobasin of the Jequitinhonha Complex and zircon from the arc has yielded εHf(t) values between -30.15 and -4.31 (Gonçalves et al., 2016; Tedeschi et al., 2016). Although some plutons from the northernmost tip of the RDA are hosted by the Jequitinhonha Complex (Paes

et al., 2010; Gonçalves et al., 2016), suggesting the complex is older than the arc, 13 zircon grains gave ages in the RDA age range (630 to 585 Ma) with similar negative εHf(t) parameters. These facts suggest a shift in the geotectonic setting with respect to the Jequitinhonha basin from passive margin to active margin. Therefore, the Jequitinhonha basin would have received the major Neoproterozoic contributions from distinct Ediacaran (the RDA) and Cryogenian (SBAP) sources.

The sedimentation of the Jequitinhonha Complex was suggested to have occurred in a passive margin environment related to the Macaúbas Group (Pedrosa-Soares & Wiedemann-Leonardos, 2000; Gonçalves-Dias et al., 2016). Our new U-Pb zircon data indicate an statistical age peak for the Late Cryogenian, and a minor but significant amount of Early Ediacaran grains constraining the maximum sedimentation age around 610 Ma (Figs. 3.3 and 3.4; Supplementary data file). On the other hand, Paes et al. (2010) and Gonçalves et al. (2016) have demonstrated that some plutons of the northernmost end of the RDA intruded the Jequitinhonha complex. Therefore, the Jequitinhonha Complex seems to record a long period of sedimentation, as Sampaio et al. (2002) already supposed (without zircon data). The basin setting shifted from a passive margin to an orogenic basin that, later, would tectonically interleave rocks from both settings. Various other orogenic belts surrounding the São Francisco Craton has the same record (e.g., Caxito et al., 2014, 2016; Falci et al., 2018).

The data presented here also constrain the age of deposition of a large amount of organic matter that was later metamorphosed during the Brasiliano Orogeny, to become the giant graphite deposits and occurrences hosted by the Jequitinhonha kinzigitic gneisses and quartzites (Fig. 1). According to the detrital zircon data acquired and age constraints for the regional metamorphism (ca. 570 to 550 Ma, Pedrosa Soares et al., 2011a), the burial of that unprecedented amount of organic matter would have taken place during the Early Ediacaran on the internal margin of the AWCO gulf, shaped within the São Francisco-Congo Paleocontinent, accompanying the rising onset of the Rio Doce Arc, but before the climax of the collisional stage. This provides important constraints for life evolution, as the Ediacaran was a period of explosive complex life development, probably linked to the large climatic, paleogeographical, tectonic and geochemical changes recorded in the late Neoproterozoic (e.g., Caxito et al., 2019). The large amount of buried organic matter could also help to explain regional features such

as the large positive carbon isotope excursion recorded in the coeval Bambuí Group over the São Francisco-Congo Paleocontinent, with values of $\delta^{13}C$ up to ca. +14 ‰ (MIBE or Middle Bambuí Excursion; Uhlein et al., 2019) probably also developed in anoxic settings (Hippertt et al., 2019), as the corresponding ^{13}C-depleted carbon had decreased in the deep sea basin.

3.6. Conclusion

1. The U-Pb detrital zircon age spectra for a sample of kinzigitic paragneiss from the Jequitinhonha Complex contains main age peaks at ca. 662 Ma, 960 Ma, 1.8 Ga, 2.0 Ga and 2.5 Ga. The statistical peak at 662 Ma includes the maximum sedimentation age given by Early Ediacaran zircon grains at around 630-609 Ma. The main related source areas are the basement of the São Francisco – Congo paleocontinent and other paleoproterozoic terranes, Tonian anorogenic magmatism, the Cryogenian Southern Bahia Alkaline Province, and the Rio Doce Arc.

2. The Hf isotope data from zircon grains of the Jequitinhonha Complex show a contribution predominantly of evolved sources followed by moderately juvenile sources. Less than 2% of the analyzed zircon grains are from juvenile sources. This is in agreement with the mainly younger sources in the Southern Bahia Alkaline Province and Rio Doce Arc.

3. The sedimentation of the precursor basin of the Jequitinhonha Complex developed upon the internal margin of the AWCO gulf, close to the São Francisco paleocontinental region previously injected by a number of alkaline intrusions of the Southern Bahia Alkaline Province. This marks the Cryogenian rifting event of the precursor Macaúbas basin, which led to the development of Late Cryogenian to Early Ediacaran oceanic crust of the Adamastor Ocean further south, followed by the rising onset of the Rio Doce Arc. This suggests that the Jequitinhonha Complex records a basin setting shift from a passive margin to a syn-orogenic basin, which was later deformed and metamorphosed to high-grade, thus complicating the original stratigraphic relations.

4. The acquired data also constrain the burial of large amounts of organic matter that was later metamorphosed during the Basiliano Orogeny, to result in the giant flake graphite deposits and occurrences hosted by the Jequitinhonha Complex paragneisses

and quartzites to probably having been deposited during during the Ediacaran. Large-scale organic matter burialcould help to explain coeval features in regionally-related units such as the Bambuí Group which displays a striking positive $\delta^{13}C$ anomaly (MIBE). This development was probably linked to the major tectonic, paleogeographic, climatic and geochemical rearrangements taking place during the late Neoproterozoic.

3.7. Acknowledgements

This work was supported by FAPEMIG (Fundação de Amparo à Pesquisa do Estado de Minas Gerais) and CNPq (Conselho Nacional de Desenvolvimento Científico e Tecnológico). Fabrício de Andrade Caxito, Antônio Carlos Pedrosa-Soares and Ivo Antônio Dussin are Fellows of the CNPq and acknowledge the support received from CNPq. This paper is a contribution to Project MOBILE: Mountains Belts and the Inception of Complex Life on Earth (geolifemobile.com). This paper is a hommage to Márcio Pimentel, one of the first Brazilian researchers to conduct isotopic analysis of the Jequitinhonha Complex, as well as many other areas in Brazil. An original version was greatly improved after comments and suggestions by Prof. Lauro Cézar Montefalco de Lira Santos, Wolf Uwe Reimold, and an anonymous reviewer.

4. ARTIGO II - Detrital zircon U-Pb analysis constrains the depositional age and provenance of Cryogenian glacial successions of the Macaúbas Group in the northeastern Araçuaí Orogen, eastern Brazil

Fernando Estevão Rodrigues Crincoli Pacheco[1*]; Fabrício de Andrade Caxito[1#]; Maria Eugênia Souza[2]; Ciro Couto Bento[3]; Antônio Pedrosa-Soares[1#], Cristiano de Carvalho Lana[2]

[1]Programa de Pós-Graduação em Geologia, Universidade Federal de Minas Gerais, CPMTC-IGC-UFMG, Av. Antônio Carlos 6627, Pampulha, 31270-901 Belo Horizonte, MG, Brazil.

[2]Departamento de Geologia, Escola de Minas, Universidade Federal de Ouro Preto, Morro do Cruzeiro, 35400-000, Ouro Preto, MG, Brazil.

[3]Centro de Estudos em Geociências, Instituto de Ciência e Tecnologia, Universidade Federal dos Vales do Jequitinhonha e Mucuri, Rodovia MGT 367, Km 583 – Diamantina, 39100-000, Brazil.

*Corresponding author: ferodrigues@live.it

[#]Fellow of the Brazilian Research Council (CNPq)

Abstract

The precursor basin of the Araçuaí – West Congo Orogenic System (AWCO) formed a large gulf within the São Francisco – Congo Paleocontinent (SFCP), where the diamictite-bearing Macaúbas Group was deposited during the Neoproterozoic. However, the lack of robust age constraints on the Cryogenian glaciogenic successions prevents correlation to one or both of the Cryogenian Snowball Earth glaciations. The present study introduces new field and U-Pb detrital zircon data from diamictite-bearing units on the southern margin of the São Francisco Craton, in the northeastern Araçuaí Orogen. This region is much closer to possible Ediacaran-Cryogenian igneous rocks of the southern São Francisco craton than other regions previously studied for the Macaúbas Group, enhancing the probability of detecting detrital minerals from those rocks, if they were involved as source areas. In the studied region, the Macaúbas Group

is composed of metadiamictite with sparse clasts and schistified metagraywacke with bulk mineralogy similar to the quartz-muscovite-feldspar matrix of the metadiamictites. U-Pb (LA-MC-ICP-MS) dating of 182 detrital zircon grains from the Lower Chapada Acauã Formation forming the syn-glacial sequence yielded main age peaks at 939 ± 3 Ma, 1409 ± 10 Ma, 1822 ± 8Ma, 2044 ± 7 Ma, 2551 ± 9 Ma and 3103 ± 19 Ma. The youngest concordant zircon grain found in this study aged 753 ± 12 Ma. U-Pb (LA-MC-ICP-MS) dating of 104 zircon crystals from a granitic clast recovered from the diamictite exhibits highly discordant data plotting in distinct Discordia lines with upper intercept ages of 2.0 Ga, 2.5 Ga, 2.6 Ga and 3.2 Ga, indicating derivation from the adjacent cratonic basement. The U-Pb age spectra suggests important contribution from the Archean and Paleoproterozoic basement of the São Francisco – Congo paleocontinent and metamorphic complexes, from the Mesoproterozoic intrusive and volcanic rocks of São Francisco Craton, and from the Tonian Salto da Divisa Suite. Despite the relative abundance of Cryogenian zircon grains in the surrounding prospective source areas, the studied rocks lack this interval age. The glaciogenic events in the Macaúbas basin system probably did not sample rocks with these age intervals due to the general characteristics of this type of deposit or because the sources were not exposed. Thus, the lower diamictite-bearing units of the Macaúbas Group in the northeastern São Francisco craton were deposited after ca. 753 Ma, but their correlation to either the Sturtian or Marinoan global glaciations remain speculative.

Keywords: sedimentary provenance, U-Pb detrital zircon analysis, western Gondwana

4.1. Introduction

The Cryogenian Period is a pivotal time in Earth's history, especially during the transition from Rodinia to Gondwana. This reconfiguration of the lithospheric plates occurred contemporaneously with dynamic global environmental shifts, climatic extremes and, later, with the proliferation of eukaryotic and metazoan life (e.g. Halverson et al., 2009; Chen et al., 2014; Hoffman et al., 2017; Brocks et al, 2017; and references therein). During this period, the Sturtian (c. 717 – 660 Ma) and Marinoan (c. 657 – 635 Ma) glaciations extended from the low-latitudes to the equatorial zone and are known as "Snowball Earth events" (e.g. Kirschvink, 1992; Hoffman et al., 1998, 2017, MacDonald et al., 2010; Rooney et al., 2015, 2020).

During these global ice ages, glacial sediments were distributed all over the world (Hoffman et al., 2017). Geochronological constraints on glacially-related Neoproterozoic sequences are critical for understanding the chronology of the interactions between climatic, tectonics, biological and geochemical systems during this key time in Earth's story.

The Araçuaí – West Congo Orogenic system (AWCO) is a significant and singular tectonic piece that resulted from the assembly of western Gondwana (Fig. 4.1). This orogenic system comprises a large region bounded by the São Francisco – Congo craton along its northern, western and eastern margins, which makes up a confined segment of the Brasiliano – Pan African orogenic system (Pedrosa-Soares et al., 2011a; 2008; Alkmim et al., 2006). Two thirds of the AWCO are currently located in the Araçuaí Orogen, Southeast Brazil, and has a long evolutionary history including the precursor Neoproterozoic Macaúbas basin system (Pedrosa-Soares et al., 2011; Babinski et al., 2012; Kuchenbecker et al., 2015; Gonçalves-Dias et al., 2016; Castro et al., 2019; 2020; Souza et al., 2019). The Macaúbas Group comprises the record of the homonymous basin system in a volcano-sedimentary, up to 10 km thick pile, which includes an Early Tonian diamictite-free lower unit related to an aborted rift (c. 950 – 880 Ma; Castro et al., 2019; Souza et al., 2019). Overlapping this sequence, Cryogenian glacio-continental to glaciomarine diamictite-rich units occur, followed by diamictite-free (post-glacial) distal deposits (Pedrosa-Soares et al., 2011; Babinski et al., 2012; Kuchenbecker et al., 2015; Castro et al., 2020; Oliveira et al., 2021). This Cryogenian sequence was deposited in a rift that evolved into a passive margin with ophiolite remnants (Pedrosa-Soares et al., 1992; 1998; Queiroga et al., 2007; Peixoto et al., 2015; Amaral et al., 2020; Caxito et al., 2021a, 2022).

Despite the large number of detailed works on the Neoproterozoic glaciations in the São Francisco Craton (Jequitaí, Bebedouro and Carrancas formations), as well as in the Araçuaí Orogen (Macaúbas Group), until now detrital zircon geochronological studies have been unable to determine whether these deposits are related to Sturtian or Marinoan glaciation, or both. One of the reasons for the overall lack of Cryogenian detrital zircons is that most of these works were carried out in the western portion of the Araçuaí Orogen, near the eastern margin of São Francisco Craton, where basement source areas are devoid of rocks younger than 900 Ma. In contrast, in the northeastern

Araçuaí Orogen, near the southeast São Francisco Craton margin, Cryogenian sources were described such as the Southern Bahia Alkaline Province (Rosa et al., 2007). Thus, this is a key location that may shed light on the provenance and depositional age of the Macaúbas diamictites.

The aim of this study is to carry out detailed field work coupled with U-Pb geochronology and provenance analysis on a Cryogenian diamictite-rich unit of the Macaúbas basin system. This unit was study in a key-area located within the northeastern sector of the Araçuaí Orogen – southern margin of the São Francisco Craton (Fig. 1), where the geochronology of the Cryogenian diamictites was not previously studied. Our new data, together with a thorough compilation from the literature, provides a robust dataset that will allow us to better understand the Neoproterozoic Macaúbas Group evolution, as well as the deposits related to the Snowball glaciations in western Gondwana. Finally, we address tectonic implications of these results into the evolution of the Cryogenian period in the São Francisco – Congo paleocontinent.

4.2. Geological setting

The Araçuaí Orogen is located in southeast Brazil, between the São Francisco Craton and the Atlantic Ocean, and has the West Congo Belt as its counterpart in southwestern Africa (Pedrosa-Soares et al., 2000, 2008; Tack et al., 2001) (Fig. 4.1). The Araçuaí Orogen is an Ediacaran-Cambrian collisional orogen that preserves evidences of a complete Wilson Cycle (Pedrosa-Soares et al., 2007, 2008, 2011a,b; Gradim et al., 2014; Tedeschi et al., 2016; Serrano et al., 2018; Amaral et al. 2020; Caxito et al., 2022). Its main lithologic assemblages are: i) Archean-Paleoproterozoic basement; ii) Statherian-Mesoproterozoic sedimentary units and related magmatism; iii) Tonian-Cryogenian succession of the Macaúbas Group and correlated units (including the Jequitinhonha Complex), as well as Late Cryogenian – Early Ediacaran ophiolite slivers; iv) Ediacaran Rio Doce Magmatic Arc and related basins (including the orogenic Salinas Formation); v) collisional- to post-collisional granitic intrusions (Fig. 1).

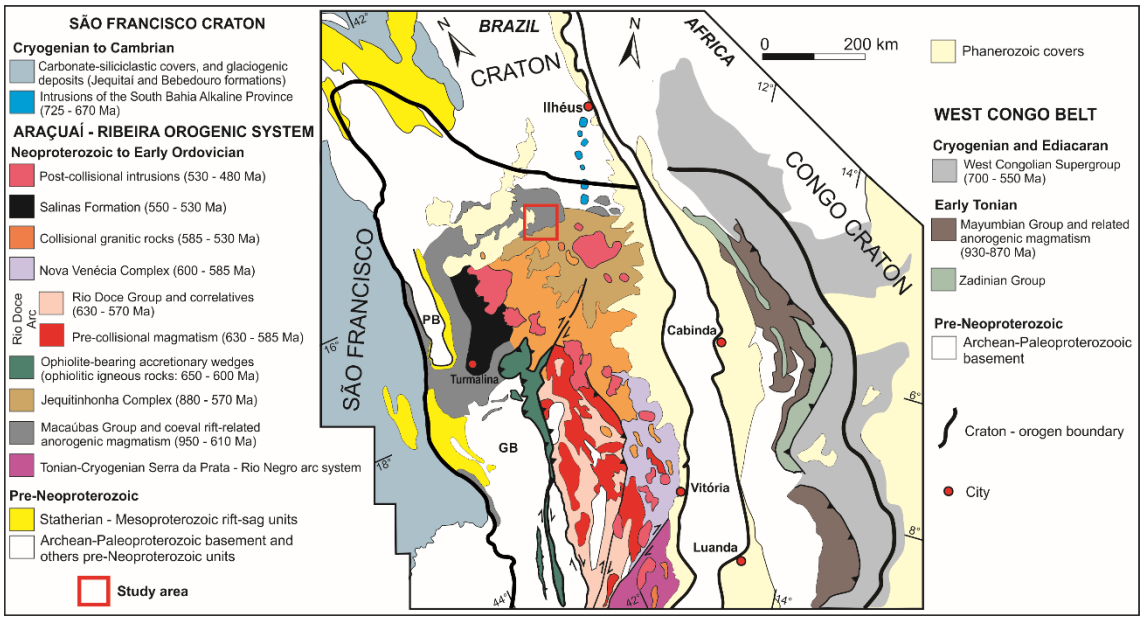

Figura 4.1 - Geotectonic setting and geological map of the Araçuaí – West Congo Orogenic System (AWCO) (modified and updated from Alkmim et al., 2006 and Pedrosa-Soares et al., 2008, 2011a, 2011b). GB = Guanhães Block, PB = Porteirinha Block. U-Pb age ranges for metasedimentary and metavolcanoclastic units are based on data from synsedimentary volcanic rocks or for the youngest detrital zircons, indicating the maximum sedimentation age, and the oldest metamorphic U-Pb age, constraining the minimum sedimentation age. See references for ages in Gradim et al. (2014), Pedrosa-Soares et al. (2016), Richter et al. (2016), Tedeschi et al. (2016), Degler et al. (2017), Peixoto et al. (2017), Araujo et al. (2019), and Castro et al. (2020).

The Araçuaí Orogen basement is represented by Archean – Paleoproterozoic greenstone belts and related TTG complexes, Siderian metasedimentary units and arc-related intrusions, and Rhyacian-Orosirian magmatic arcs and volcano-sedimentary successions related to the amalgamation of the São Francisco-Congo paleocontinent (Noce et al., 2007; Teixeira et al., 2000, 2017; Novo, 2013, Aguilar et al., 2017; Degler et al., 2018). During the Statherian – Mesoproterozoic occurred the deposition of sedimentary rocks related to Espinhaço rift-sag system and related volcanic rocks, as well as Statherian anorogenic granites (Chemale Jr et al., 2012; Guadagnin et al., 2015; Costa et al., 2018; Magalhães et al., 2019).

The Neoproterozoic Macaúbas Group records the homonymous precursor basin systems of the Araçuaí Orogen and could be subdivided in two major sequences. The lower sequence comprises an Early Tonian (c. 950 – 880 Ma) metavolcano-sedimentary succession delimited by unconformities at its base ad top, which record an aborted rift event (c. 957 – 880 Ma) by the Capelinha, Matão-Duas Barras, Planalto de Minas, Rio Peixe Bravo and Domingas formations (Fig. 4.2). This sequence is diamictite-free and ascribed as Lower Macaúbas Group (or pre-diamictite sequence) (Martins et al., 2008;

Pedrosa-Soares et al., 2011b; Babinski et al., 2012; Kuchenbecker et al., 2015; Castro et al., 2019; Souza et al., 2019).

The upper sequence comprises Early Cryogenian (c. 725-675 Ma) anorogenic magmatic assemblages in the São Francisco – Congo Craton margins (Texeira et al., 1997; Rosa et al., 2007; Thiéblemont et al., 2009a,b; Straathof, 2011), yielding time constraints for the second rift event related to the Macaúbas basin system. An unconformity occurs at the base of the Early Cryogenian continental rift, which includes the deposition of the diamictite-rich Serra do Catuni, Nova Aurora and Lower Chapada Acauã formations over at least one glacial event (Pedrosa-Soares et al., 2011b; Babinski et al., 2012; Caxito et al., 2012, 2021b; Kuchenbecker et al., 2015; Castro et al., 2020). This second rift evolved to the full development of the Macaúbas basin, with the establishment of a continental passive margin with ocean floor spreading (Pedrosa-Soares et al., 1992; 1998; 2001; 2011b; Queiroga et al., 2007; Peixoto et al., 2015; Amaral et al., 2020). The passive margin to the oceanic sequence comprises the Upper Chapada Acauã and Ribeirão da Folha formations. The latter hosts tectonic slices of ophiolitic mafic and ultramafic rocks, where U-Pb SHRIMP and LA-ICPMS ages for zircon from ophiolitic plagiogranites set the age of ocean-floor emplacement at around 645 ± 10 Ma (Queiroga et al., 2007; Amaral et al., 2020).

The Cryogenian – Early Ediacaran Jequitinhonha Complex, located in the northeastern Araçuaí Orogen, is an extensive metasedimentary unit essentially composed of Al- and graphite-rich paragneisses, quartzites and lenses of calc-silicate rocks, which is understand as a distal correlated of the passive margin of Macaúbas basin system (e.g. Gonçalves-Dias et al., 2016; Pacheco et al., 2021 and reference therein).

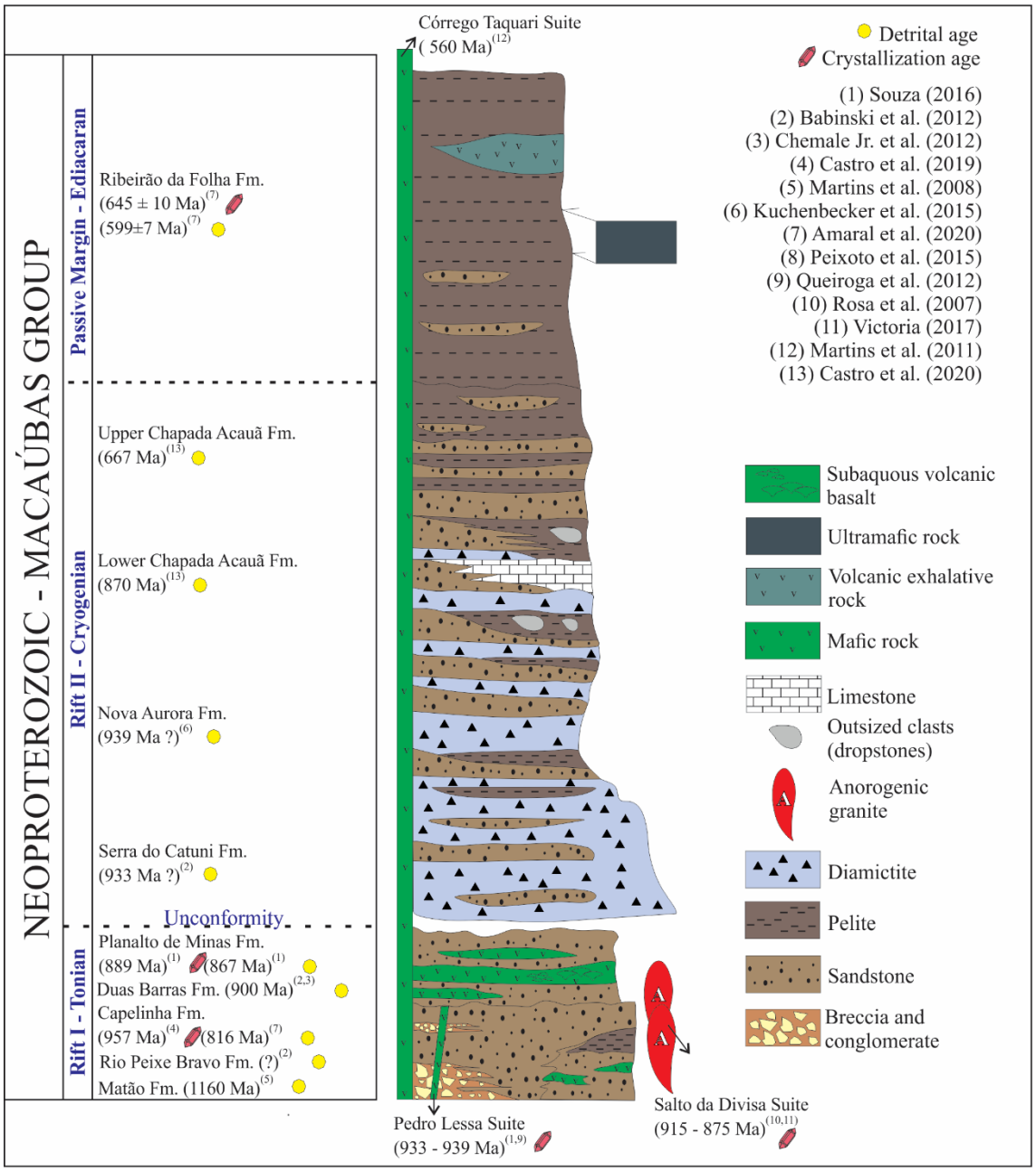

Figura 4.2 - Stratigraphic column and younger detrital zircon data available for the Macaúbas Group (modified from Pedrosa-Soares & Alkmim, 2011, adapted from Souza et al., 2019).

During the Ediacaran, the closure of the oceanic basin generated the Rio Doce magmatic arc and arc-related basins (e.g. Tedeschi et al., 2016), which encompass metasedimentary and metavolcanic rocks of the Rio Doce Group and paragneisses of the Andrelândia Complex (fore-arc and intra-arc regions – Degler et al., 2017; Novo et al., 2018; Schannor et al., 2018), as well as the migmatitic paragneisses of the Nova Venécia Complex (back-arc region – Gradim et al., 2014; Richter et al., 2016; Araújo et al., 2020) and other related paragnaissic units of the high-grade core of the Araçuaí Orogen (e.g. Santiago et al., 2022)

The Salinas Formation consists of a thick sequence of turbiditic wackes and pelites, containing lenses of conglomerates and calc-silicate rocks and covers different units of the Macaúbas Group, defining a regional unconformity (Lima et al., 2002; Peixoto et al., 2015; Deluca et al., 2019). It is a representative of orogenic sedimentation, with major detrital contribution from the Rio Doce Arc (Lima et al., 2002; Santos et al., 2009; Costa et al., 2018; Deluca et al., 2019; Kuchenbecker et al., 2020).

Widespread anatexis on paragneiss complexes during the collisional stage of the Araçuaí orogen generated a large volume of S-type granitic rocks (ca. 585 Ma – 540 Ma) (Pedrosa Soares et al. 2011a; Gradim et al., 2014; Melo et al., 2017), succeeded by a myriad of post-collisional I- and A- type intrusions, composed of granitic and mafic rocks (Pedrosa-Soares et al., 2011a; Gradim et al., 2014; Campos et al., 2016; Serrano et al., 2018; Araujo et al., 2019). These magmatic processes of the post-collisional phase have been associated to the extension and decompression of the crust and a gravitational collapse, related to mantle delamination, asthenosphere ascent and plume uprising (Serrano et al., 2018). Monazite data from granitic plutons related to the orogenic collapse indicate that this process might have lasted up to ca. 490 Ma (Gonçalves et al., 2019).

4.2.1. The Macaúbas Group syn-glacial deposits

The diamictite-bearing units of Macaúbas Group, interpreted as syn-glacial deposits, are the Serra do Catuni, Nova Aurora and Lower Chapada Acauã formations. The Serra do Catuni Formation is the oldest diamictitic unit of the Macaúbas Group, comprising a very extensive package of massive diamictite and minor sandstone and pelitic intercalations. Chaotic boulders and faceted/striated flat-iron-shaped clasts represent glacial features on this unit (Pedrosa-Soares et al., 2011; Kuchenbecker et al., 2015; Oliveira et al., 2021). Based on detrital zircon data, the maximum depositional age of the Serra do Catuni Formation is 933 ± 8 Ma (Babinski et al., 2012).

The Nova Aurora Formation represents another package of diamictites with minor intercalations of graded sandstone and scarce pelite. The basal unit shows predominantly a Fe-rich diamiticite with minor non-ferruginous diamictite. The grain size, matrix composition and clast/matrix ratio vary considerably on those diamictites. The upper unit presents a stratified diamictite with minor layers and lenses of fining-up

graded sandstone and thin intercalations of pelite (Pedrosa-Soares et al., 2011; Vilela et al., 2014; 2021). The maximum depositional age of the Nova Aurora Formation, based on detrital zircon data, is 879 ± 42 Ma (Vilela et al., 2021).

Lastly, the Lower Chapada Acauã Formation is essentially composed of fining-upward cycles of stratified diamictite, graded sandstone and pelitic rhythmite (Pedrosa-Soars et al., 2011; Kuchenbecker et al., 2015; Castro et al., 2020). The clast/matrix ratio shows great variations on the diamictite layers, with clasts ranging from granules to boulders. The sandstone layers and lenses show fining-up graded bedding and the pelitic rhythmite layers locally show isolated outsized clasts, mainly cobbles and boulders. This unit is interpreted as a glacio-marine deposit and corresponds to a more distal passive margin succession. The maximum depositional age of the Lower Chapada Acauã Formation is 870 ± 17 Ma with a younger grain at 667 ± 11 Ma (Castro et al., 2020).

All of these glaciogenic units yielded younger detrital zircons compatible with sources related to the late-stage magmatism of the Tonian rift of the Macaúbas basin system (Souza, 2019; Castro et al., 2020). The detrital zircon data alone is not sufficient to stablish a correlation with either the Sturtian or Marinoan global glacial events (e.g. Hoffman et al., 2017).

Over the São Francisco Craton, the hundred-meter thick diamictite-bearing Jequitaí Formation, locally covering striated pavements (Isotta et al., 1969) has been considered as a correlative to at least part of the diamictite-bearing units of the Macaúbas Group (e.g. Uhlein et al., 2001). Covering the Jequitaí Formation or overlapping the São Francisco Craton basement, the Pedro Leopoldo Member of the basal Sete Lagoas Formation, Bambuí Group in the São Francisco Craton has been recognized as a cap carbonate (c. 635 – 600 Ma) of the Marinoan glaciation (e.g. Caxito et al., 2012; 2021a) leaving the question open if the Cryogenian diamictites of Macaúbas Group are related to either the Sturtian or Marinoan glaciation, or both.

4.3. Analytical methods

Zircons were separated from five samples: three metadiamictite matrix (DF-4, DF-10 and DF-26); one granitoid clast within metadiamictite (DF-4D1); and one

metagreywacke (DF-18). They were all prepared in the High Purity Mineral Separation Laboratory (SEPURA) of the Centro de Pesquisa Manoel Teixeira da Costa (CPMTC) at the Federal University of Minas Gerais (UFMG). Concentrates were extracted from samples using conventional gravimetric and magnetic (Frantz isodynamic separator) techniques. Final separation was achieved by hand picking. Zircon grains were mounted and polished in an epoxy disk. All analysed grains were documented by cathodoluminescence (CL) imaging under a scanning electron microscope (SEM, JEOL 6510) using an acceleration voltage of 15kV. In sequence, the grains were analysed using an Excimer 193 μm Laser by Photon – Machines (Model ATLEX SI) attached to a Thermo-Finnigan Neptune-plus multi-collector ICP-MS hosted at Isotopic Geochemistry Laboratory in the Federal University of Ouro Preto (UFOP). All analyses are presented in Supplementary Material.

Isotopic data of all zircon grains were acquired using peak jumping mode with background measurement during 20 seconds, zircon ablation during 20 seconds and 30 μm spot size for U-Pb analyses. Element fractionation and mass discrimination were corrected using analyses of an external zircon reference material GJ-1 (608 Ma, Jackson et al., 2004). Reported uncertainties (2σ) were propagated by quadratic addition of the external reproducibility obtained from zircon standard GJ-1 during the analytical session (2SD in %) and within-run precision of each analysis (standard error in %). Accuracy and reproducibility were checked by repeated analyses of reference zircon Plesovice (Sláma et al., 2008) and Blue Berry (Santos et al., 2017). Data reduction was done in GLITTER Software, as well as the 204Pb common correction was applied using Ms Excel Spreadsheet program (Gerdes & Zeh, 2006) based on Stacey and Kramers (1975) Pb compostion model. Concordia ages, probability density plotter histograms and weighted average ages are reported with 2σ errors using Isoplot 3.75 (Ludwig, 2003). We used $^{207}Pb/^{206}Pb$ dates for zircons older than 1.0 Ga and $^{206}Pb/^{238}U$ dates for zircons younger than 1.0 Ga and discordance cut off of 10% (including for the literature dataset compilation). All analyses data are presented in Supplementary Material 1.

4.4. Results

4.1.The Lower Chapada Acauã setting in the northeastern Araçuaí Orogen

The studied area covers a portion of the northeastern sector of the Araçuaí Orogen – southern margin of the São Francisco Craton (Figs. 1 and 3). The metasedimentary succession of the study area is folded, with inverted flanks striking in the NW-SE direction and thrust over the cratonic basement units in the northeastern portion. This fault is part of a contractional shear zone and other transference shear zones are observed at the east/southeast area, striking NE-SW and both dextral and sinistral cinematic. This structural architecture is widely recognized as a crucial feature for the identification of inverted sedimentary basins in orogenic belt regions (e.g. Butler et al., 2006).

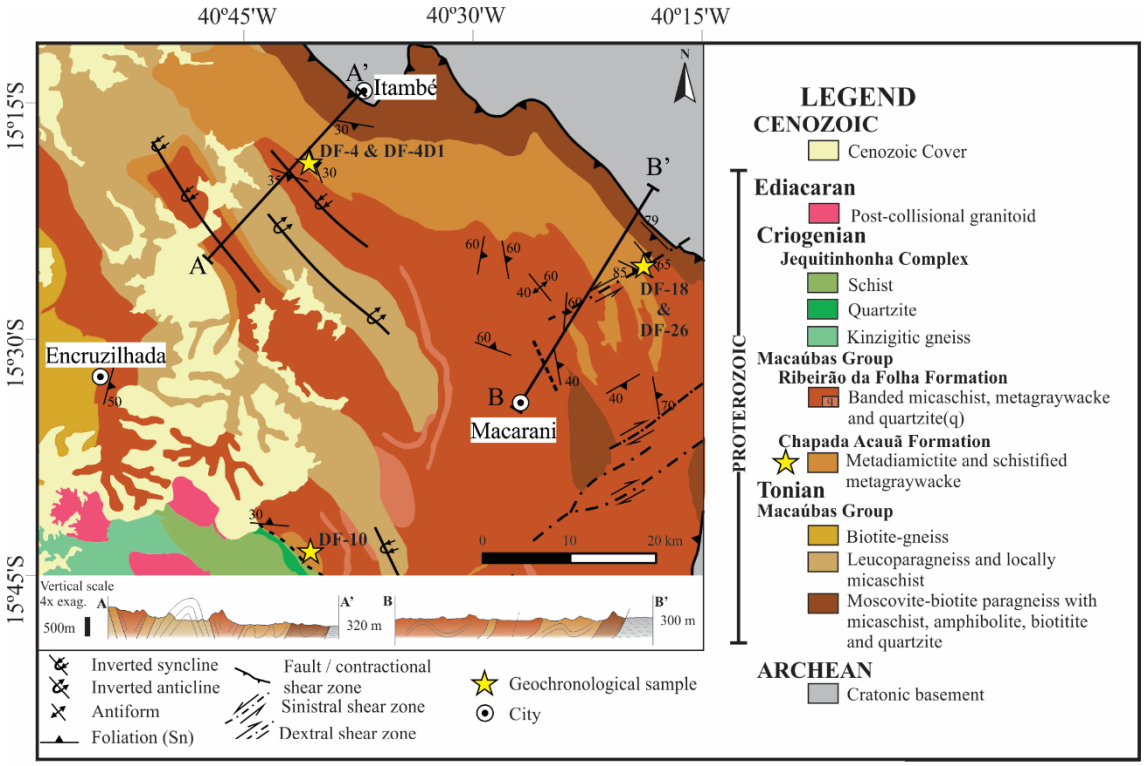

Figura 4.3 - Geological map of the study area with geochronological sample location, adapted from Araújo (2000), Drumond (2000) and Souza et al. (2003).

In the study area, the succession shows three lithotectonic sequences from northeastern to southwest (Fig 4.3): (i) the crystalline rocks of the São Francisco Craton basement; (ii) the metasedimentary rocks of the Macaúbas Group and the Jequitinhonha Complex; and (iii) the metagranitoids syn- and pos-collisional of the Araçuaí Orogen. This unit is composed of metadiamictite and schistified metagraywacke. The metadiamictite consists of a fine-grained quartz, feldspar and muscovite matrix with sparse clasts of varied angularity and size (Fig. 4a). Clast composition is predominantly granitic, but

limestone and quartz clasts are also common (Fig. 4b). Bedding of the diamictite unit commonly dips with high angles to the south (Fig. 4c) with down-dip stretched clasts due deformation (Fig. 4.4.d).

Diamictite matrix presents mainly quartz, feldspar and muscovite, with round to angular grains, moderately spherical, well- to- poorly sorted. The grains present long contacts, but concave-convex and sutured contacts also occur (Fig. 4e). The schistified metagraywacke is characterized by a poorly sorted matrix, with layers of fine to coarse quartz and mud (Fig. 4f). Sometimes the diamictite matrix is schistified, exhibiting one (Fig. 4g) or two directions (Fig. 4h) of mineral orientation.

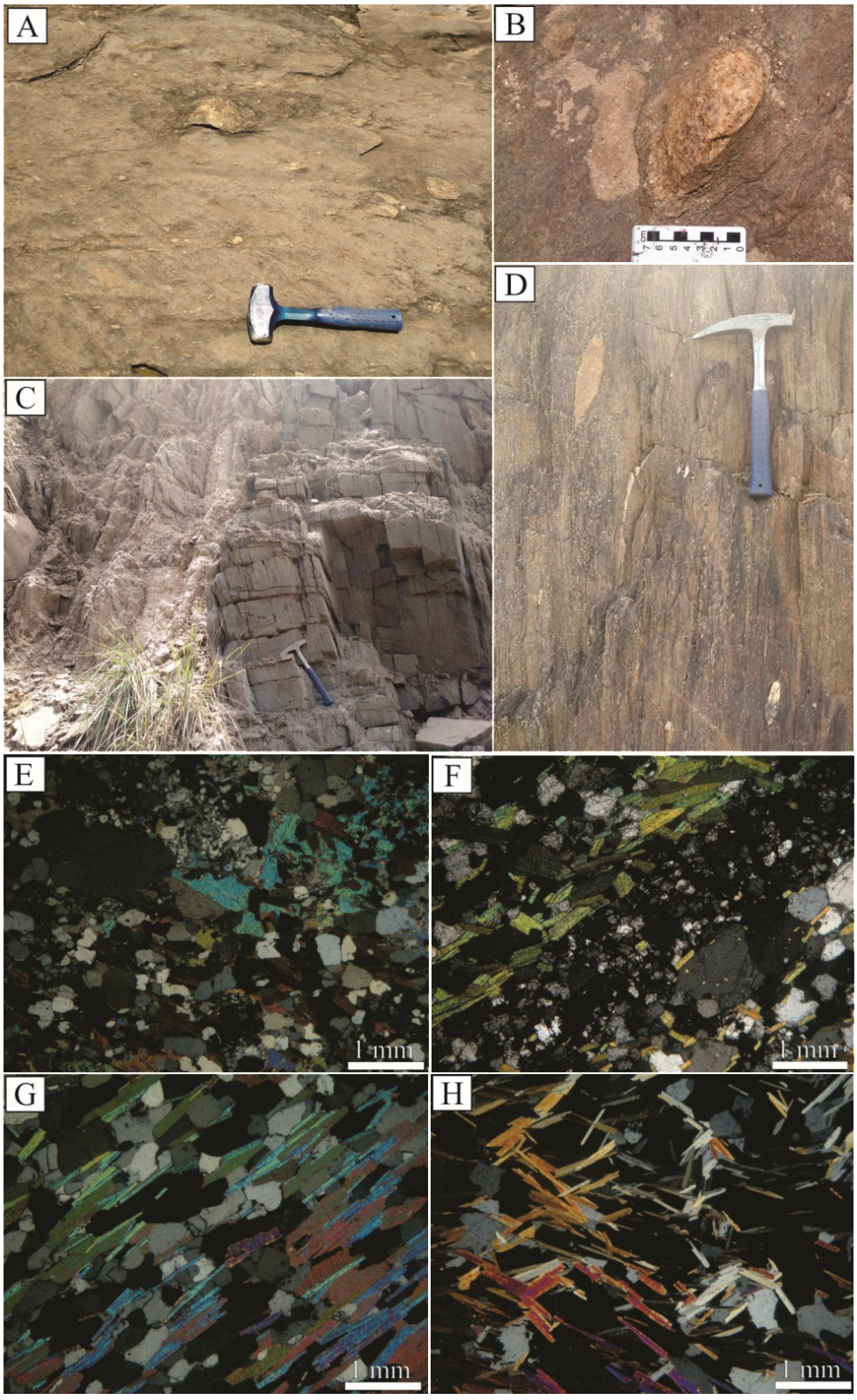

Figura 4.4 – A – Metadiamictite showing clasts with different sizes. B – Zoom of a granite clast. C – Schistified metagraywacke with high dip angle. D – Schistified diamictite with deformed clasts. E – Metadiamictite matrix without mineral orientation. F – Metagraywacke showing layers of medium quartz + muscovite, fine and coarse quartz, from the top left to bottom right. G & H – Schistified diamictite matrix showing one (G) or two (H) mineral orientations. Photomicrography under polarized lights, mineral assemblage composed of quartz and muscovite.

4.2. (LA-MC-ICP-MS) U-Pb zircon geochronology

Sample DF-26 – Metadiamictite matrix

The DF-26 sample was collected from a metadiamictite matrix, (UTM 416324E/8232060N; Zone 24K), and provided 11 zircon grains, ranging in size from 80 to 250 μm, with length/width ratio around 2:1. Zircon grains are prismatic, euhedral to subhedral, showing poorly developed zoning and, usually, dark cores embayed by a bright luminescent area followed by a low luminescence border (Fig. 4.5). Th/U ratios range from 0.001 and 0.60. Most grains are discordant and just two are concordant and considered. They are Paleoproterozoic and yielded 2350 ± 34 Ma and 2072 ± 44 Ma $^{207}Pb/^{206}Pb$ ages (Fig. 4.6).

Sample DF-4 – Metadiamictite matrix

The DF-4 sample was collected from a metadiamictite matrix (UTM 319331E/8305549N; Zone 24L), and provided 67 zircon grains ranging in size from 80 to 250 μm, also with length/width ratio around 2:1. Zircon grains are prismatic, euhedral to subhedral, showing poorly developed zoning and, usually, dark cores surrounded by a bright luminescent area followed by low luminescent border (Fig. 4.5). Th/U ratios range from 0.25 and 2.07. 67 grains were analyzed and 58 are concordant and considered. The probability histogram for the 58 zircon grains displays six peaks (Fig. 4.7b): 918 ± 10 Ma (21%); 1292 ± 24 Ma (18%); 1769 ± 28 Ma (17%); 2044 ± 15 Ma (20%); 2563 ± 19 Ma (11%); 3103 ± 38 Ma (2%). The youngest concordant zircon grain (#75; Supplementary Material 1) constrains the maximum depositional age at around 753 ± 12 Ma (Fig. 4.6).

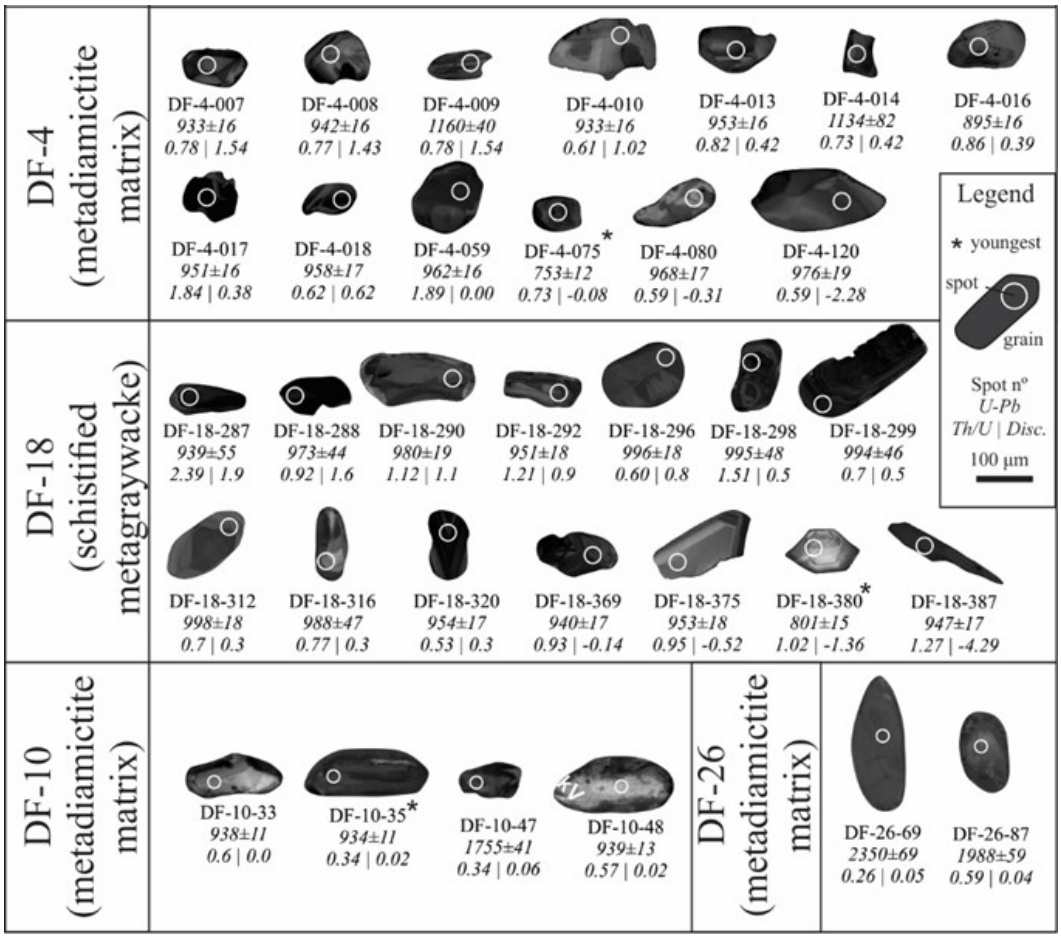

Figura 4.5 - Selected cathodoluminescence images and spot placement for zircons grains from analyzed samples.

Sample DF-18 – Metagreywacke

The DF-18 sample was collected from a schistified metagreywacke (UTM 358731E/8294306N; Zone 24L), and provided 78 zircon grains ranging in size from 100 to 300 µm, also with length/width ratio around 2:1. Zircon grains are prismatic, euhedral to subhedral, showing poorly developed zoning and, usually, dark cores surrounded by a bright luminescent area followed by low luminescent border (Fig. 4.5). Th/U ratios range from 0.20 and 2.38. 78 grains were analysed and 68 are concordant and considered. The probability histogram for the 68 zircon grains displays six peaks (Fig. 4.7c): 956 ± 11 Ma (34%); 1459 ± 37 Ma (12%); 1878 ± 39 Ma (13%); 2063 ± 27 Ma (21%); 2482 ± 36 Ma (10%); 2690 ± 32 Ma (11%). The youngest concordant zircon grain (#380; Supplementary Material 1) constrains the maximum depositional age at around 801 ± 15 Ma (Fig. 4.6).

Sample DF-10 – Metagreywacke

The DF-10 sample was collected from a metadiamictite matrix (UTM 319417E/8258730N; Zone 24L), and provided 26 zircon grains ranging in size from 80 to 250 μm, also with length/width ratio around 2:1. Zircon grains are prismatic, euhedral to subhedral, showing poorly developed zoning and, usually, dark cores surrounded by a bright luminescent area followed by low luminescent border (Fig. 4.5). Th/U ratios range from 0.35 and 1.06. 26 grains were analysed and 07 are concordant and considered. The probability histogram for the 07 zircon grains displays two peaks (Fig. 4.7d): 938 ± 10 Ma (71%); 1759 ± 57 Ma (29%). The youngest concordant zircon grain (#35; Supplementary Material 1) constrains the maximum depositional age at around 934 ± 11 Ma (Fig. 4.6).

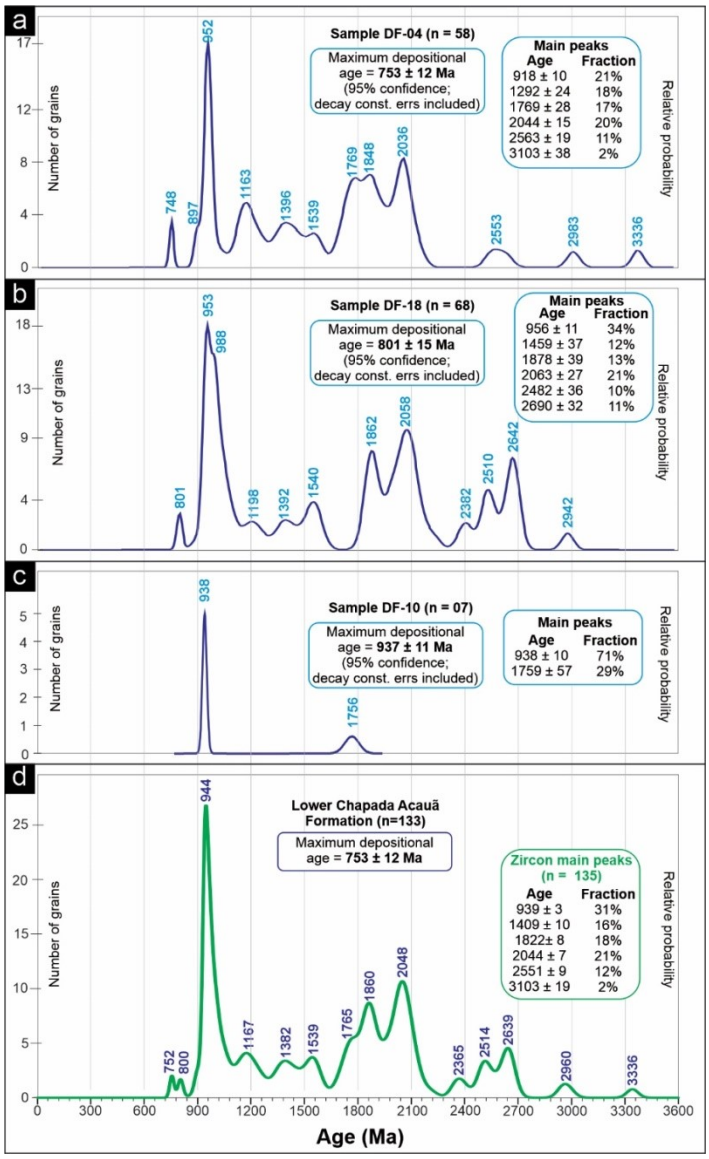

Figura 4.6– Age histogram of detrital zircon grain of individual samples DF-04 (A), DF-18 (B), DF-10 (C) and all analyzed detrital zircon grain from those samples (D).

4.5. Discussion

4.5.1. Maximum depositional ages and provenance assessment

The U–Pb data for detrital zircon grains from the Lower Chapada Acauã Formation are here discussed in the light of the novel data, together with a thorough compilation of U-Pb detrital zircon data from the literature (Figs. 4.6 and 4.7). Currently available U-Pb (LA-ICP-MS and SHRIMP) dataset for the Cryogenian units of the Macaúbas Group suggested that the sedimentation age of its diamictite-bearing units was constrained between 715 and 670 Ma (Castro et al., 2020). This is in agreement with the proposed

correlations between these glaciogenic units and the Lower Diamictite Formation, a glaciogenic unit of the West-Congo belt, which encloses volcanic rocks aged around 700 Ma (e.g. Pedrosa-Soares et a., 2008; 2011b; Straathof, 2011; Thiéblemont et al., 2009a,b). During the present study detrital zircon age spectra have been obtained for four samples of metadiamictite matrix and metagreywackes of the Lower Chapada Acauã Formation (with 133 zircons). The detrital zircons ages ranges from 753 ± 12 Ma to 3656 ± 8 Ma. The probability histogram for the 133 zircon grains displays six peaks (Fig. 4.7D): 939 ± 3 Ma (31%); 1409 ± 10 Ma (16%); 1822 ± 8Ma (18%); 2044 ± 7 Ma (21%); 2551 ± 9 Ma (12%); and 3103 ± 19 Ma (2%). The youngest concordant zircon grain found in this study aged 753 ± 12 Ma (Fig. 4.6).

In order to assess the possible source regions of the groups of zircon grains of the Cryogenian diamictite-bearing (Fig. 4.7), the large-scale setting of the Macaúbas basin system and the São Francisco – Congo paleocontinent was considered. There are many probable primary sources to have contributed to Lower Chapada Acauã Formation, as well as to correlate diamictite-bearing units that filled the Macaúbas basin. However, the spectra observed for these units probably resulted from a combination of primary and secondary sources.

Probable primary sources for Archean to Orosirian zircon grains are the migmatitic-gneissic complexes related to the São Francisco – Congo paleocontinent basement (Teixeira et al., 2000; Barbosa & Sabaté, 2004; Vicat and Pouclet, 2000; Noce et al., 2007; Silva et al., 2016; Bersan et al., 2018) and Guanhães Complex (Silva et al., 2002) (Fig. 4.7), as well as the relatively distant Eburnean and Kimezian basement (Begg et al., 2009) and the Borrachudos Suíte (Silva et al., 2002).

The Statherian-Stenian Espinhaço basin system probably is an important primary as well as secondary sedimentary source. Primary sources are related to the anorogenic magmatism of this basin and secondary sources to the reworking of its sedimentary rocks. Possible Calymmian sources are thick felsic volcanics of the Bomba Formation and mafic dykes from the intracratonic rift phase of the Espinhaço basin within the São Francisco Craton (Danderfer et al., 2009; Silveira et al., 2013) From the Ectasian, volcanic rocks from the Sopa-Brumadinho Formation (Chemale Jr et al., 2012) are closer to the study area than the distant sources such as Namaqua-Natal metavolcanic rocks from southern Africa (Evans et al., 2007) or bimodal magmatism from the

southeast Congo Craton (Fernandez-Alonso et al., 2012; Debruyne et al., 2015) (Fig. 4.7).

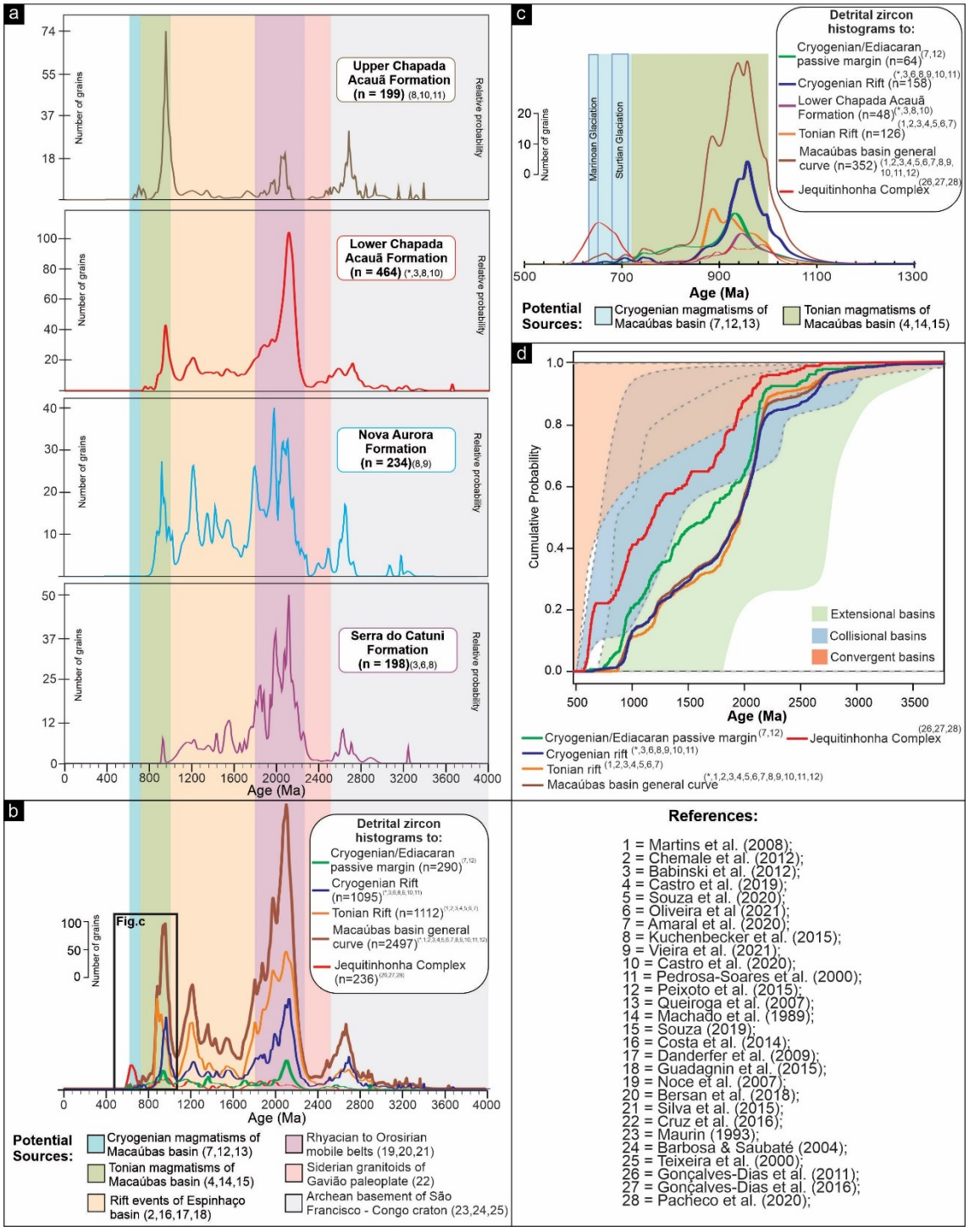

Figura 4.7 – Summary of principal zircon grains sources of the Macaúbas Basin passive margin stage and collisional basin related to the Araçuaí Orogen.

Detrital zircon grains from the Tonian comprise an important source to the Lower Chapada Acauã Formation related units. The possible sources from the Tonian could be from the anorogenic rift-related bimodal magmatism widespread in the São Francisco craton and surrounding areas (Tack et al., 1990; Renne et al., 1990; Heaman, 1991; Silva et al., 2008; Danderfer et al., 2009; Menezes et al., 2012b; Queiroga et al., 2012; McCourt et al., 2013; Souza et al., 2022; Victoria et al., 2019; Castro et al., 2019; Chaves et al., 2019), especially considering that A-type granites of the Salto da Divisa Suite are the nearest source (Figs. 4.1, 4.2, 4.7 and 4.8). The similarity between the Tonian rift and the Cryogenian rift spectra age (Fig. 4.7b), also suggests the Tonian rift sedimentary rocks as an important secondary source to the Cryogenian rift.

The youngest detrital zircon group is Cryogenian, with the Southern Bahia Alkaline Province (Rosa et al., 2004, 2005a, 2005b, 2007, 2015; Menezes et al., 2012a; Teixeira et al., 1997) as a most probable source due to the proximity to the area. A contribution of Sumbi-type dolerite sills and dykes (Straathof, 2011) and volcanic rocks of the La Louila Formation (Thiéblemont et al., 2009a, 2009b), in central SW Africa, could be alternatively considered as far-sourced (Fig. 4.8).

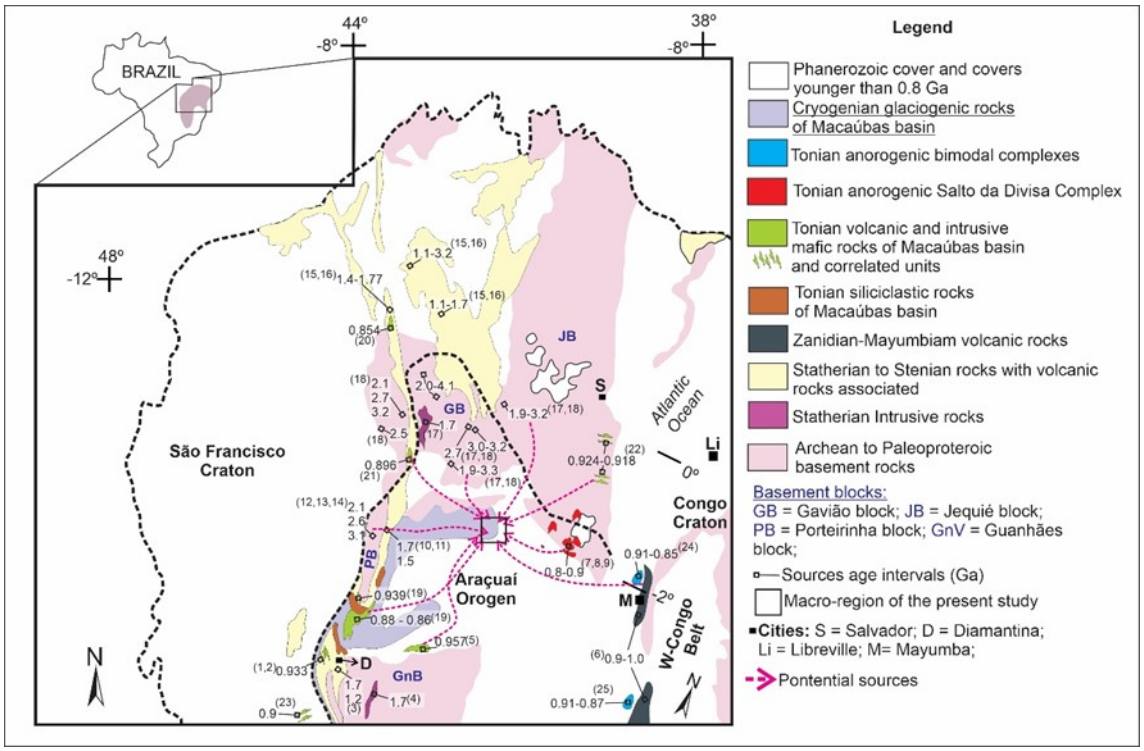

Figura 4.8- Schematic map showing the location of the potential primary and secondary sources areas of the detrital zircons of the entirely siliciclastic Tonian basal deposits of the Macaúbas Group rift I sequence (the reader is referred to the web version of this article). Modified from Cruz et al. (2016). 1 = Machado et al. (1989); 2 = Souza (2016); 3 = Chemale et al. (2012a,b); 4 = Magalhães et al. (2018); 5 = Castro et al. (2019); 6 = Tack et al. (2001); 7 = Rosa et al. (2007); 8 = Menezes et al. (2012); 9 = Victoria (2017); 10 = Costa et al. (2018a,b); 11 = Danderfer et al. (2015); 12 = Noce et al. (2007); 13 = Silva et al. (2015); 14 = Bersan et al. (2018); 15 = Danderfer et al. (2009); 16 = Guadagnin et al. (2015); 17 = Cordani et al. (1992); 18 = Cruz et al. (2016 and references therein); 19 = Souza et al. (2022); 20 = Danderfer et al. (2009); 21 = Moreira et al. (2020); 22 = Evans et al. (2016); 23 = Caxito et al. (2020); 24 = Thiéblemont et al. (2009); 25 = Pedrosa-Soares et al. (2016).

4.5.2. Tectonic implications

Fig. 4.8d shows the cumulative distribution of zircon ages versus the difference between crystallization age of the grains for the Tonian and Cryogenian rift, the Cryogenian-Early Ediacaran passive margin, the Macaúbas basin general curve, and the correlated Jequitinhonha Complex. Since detrital zircon spectra reflect the tectonic setting in which they are deposited, we can observe that the Cryogenian diamictite-bearing units of the Macaúbas Group was deposited in a rift- to- passive margin stage, as previously proposed in the literature (e.g. Pedrosa-Soares and Alkmim, 2011; Kuchenbecker et al., 2015; Castro et al., 2020; Oliveira et al., 2021; Vilela et al., 2021).

The spectra age of the diamictite-bearing units of the Macaúbas (Figs. 7 and 8) reflects the strong influence of the basement rocks of the São Francisco – Congo paleocontinent during the onset of the Cryogenian rift and throughout Macaúbas basin system's other

evolutionary stages. In addition, few Cryogenian-Early Ediacaran zircon grains are found in these sequences, as their sources are unavailable nearby. The comparison of the spectra age of Macaúbas basin and Jequitinhonha Complex (Fig. 4.8) reinforces the correlation between these units. However, the Jequitinhonha Complex exhibit more Cryogenian zircons than the Macaúbas basin. This could be explained considering that the post-glacial metasedimentary units of the Macaúbas basin grade laterally and upward to the metasedimentary units of the Jequitinhonha Complex (e.g. Gonçalves-Dias et al., 2016). In fact, the Jequitinhonha Complex detrital zircons are smaller than the Macaúbas basin zircons, which probably reflects the change in the sedimentary energy between both systems. Moreover, the Jequitinhonha Complex is closer to Rio Doce Arc and the Southern Bahia Alkaline Province than the Macaúbas basin, both of which are important zircon sources for the syn-orogenic basins and the passive margin of the percussor basin.

Thus, the lower diamictite-bearing units of the Macaúbas Group could be chrono-correlated to the Sturtian glaciation. This interpretation is permitted by the observed detrital zircon content, although definitive proof for this chrono-correlation (e.g. dating of ash levels) needs yet to be found. The upper diamictite-bearing units could be either chrono-correlated with the Sturtian or to the Marinoan glacial events, in which case, the cap carbonate to the Sturtian glaciation is missing in this region, probably due to the higher sedimentation rates influenced by a normal fault-bounded rift-to-passive margin basin. The Pedro Leopoldo Member of the Sete Lagoas Formation (Lower Bambuí Group), in the São Francisco Craton, was interpreted as a cap carbonate (c. 635 – 600 Ma) of the Marinoan glaciation, probably recorded in the cratonic Jequitaí Formation. In this case, while in the Araçuaí Orogen diamictite-bearing units related both to the Sturtian and Marinoan glaciations are widely preserved, over the São Francisco craton the Marinoan-related units are better preserved, with only scattered, if present, Sturtian remnants.

This situation is similar to that of the adjoining cratonic margin where the West Congo belt developed, and is coherent with the greater accommodation space in the Macaúbas basin system during the Cryogenian, in fault-bounded rift to passive-margin basins. Over the São Francisco craton, on the other hand, accommodation space for the development of a widespread sedimentary basin was only achieved after development

of the Brasília fold belt during the early Ediacaran, causing flexure of the cratonic lithosphere and development of the foreland basin where the Bambuí Group would be deposited from ca. 635 Ma on (e.g. Caxito et al., 2012; 2021).

4.6. Conclusions

The Macaúbas Group diamictite-bearing basal unit – Lower Chapada Acauã Formation – was systematically studied for the first time at the northern margin of AWCO. The U-Pb data of detrital zircon grains from this unit yielded ages ranging from 753 ± 12 Ma to 3656 ± 8 Ma. This suggests that the lower units of Macaúbas Group could be correlated to the Sturtian ice age, although upper units could be correlated to Marinoan ice age.

As postulated by Caxito et al. (2012), the spatial distribution of Macaúbas diamictite-bearing units and the presence of a cap carbonate associated with the Bambuí Group in the São Francisco Craton indicate that its rifted margin was a large sink that allowed the deposition of sequences throughout the entire Cryogenian, including the Sturtian and Marinoan. The accommodation space in the cratonic area, on the other hand, was formed concurrently with the formation of the Brasília and Aracuaí orogens, which generated the lithospheric flexure necessary for the development of a foreland basin after c. 635 Ma, as indicated by the presence of a Marinoan cap carbonate. However, this scenario must be better understood and supported by new data.

The related source areas of the Lower Chapada Acauã Formation in the northeastern Araçuaí Orogen are the basement of the São Francisco – Congo paleocontinent and Paleoproterozoic metamorphic complexes, Mesoproterozoic intrusive and volcanic rocks from the Espinhaço rift-sag basin, Tonian anorogenic magmatism, and the Cryogenian Southern Bahia Alkaline Province. This study demonstrates the importance of conducting research in distinct areas when sedimentary provenance of widely dispersed units such as the Macaúbas Group is envisaged, as local source areas easily overlooked in distant regions might be relevant to the detrital zircon contents.

4.7. Acknowledgements

This work is supported by Instituto Serrapilheira (Serra-1912-31510), Brazil, through Project MOBILE (geolifemobile.com), by FAPEMIG (Fundação de Amparo à Pesquisa do Estado de Minas Gerais through grant PPM-00618-18) and CNPq (Conselho

Nacional de Desenvolvimento Científico e Tecnológico through grant 408815/2021-3). Fabrício de Andrade Caxito and Antônio Pedrosa-Soares are recipients of Research Productivity grants from CNPq and acknowledge the support received.

5. Considerações finais e conclusões

A região de abrangência da pesquisa possibilitou o levantamento de dados importantes referentes ao Complexo Jequitinhonha e o Grupo Macaúbas. Para o Complexo Jequitinhonha, dados geocronológicos de U-Pb em zircão detrítico retirado de uma amostra de paragnaisse kinzigítico indicaram como possíveis fontes rochas do embasamento do Paleocontinente São Francisco-Congo além de outros terrenos paleoproterozóicos, rochas do magmatismo anorogênico Toniano, rochas da Província Alcalina do Sul do Estado da Bahia (PASEBA), do Criogeniano, e rochas do Arco do Rio Doce, do Ediacarano.

A idade de sedimentação máxima do Complexo Jequitinhonha pelo pico estatístico é de 662 Ma, com grãos mais jovens entre 630-609 Ma. Essa idade restringe o soterramento de um grande volume de matéria orgânica que, posteriormente seria metamorfizada durante a Orogenia Brasiliana, resultando em grandes depósitos de grafita do tipo flake que ocorrem em rochas do Complexo Jequitinhonha.

Dados isotópicos de Lu-Hf em zircão detrítico da mesma amostra do Complexo Jequitinhonha mostraram que, durante a sedimentação da unidade, a contribuição foi predominantemente de fontes diferenciadas, seguidas por fontes moderadamente juvenis. Existe pouca contribuição (menos de 2%) de fontes estritamente juvenis. Esses dados corroboram a contribuição principal de fontes mais jovens, como rochas da PASEBA e do Arco do Rio Doce.

No Grupo Macaúbas, a Formação Chapada Acauã Inferior foi estudada pela primeira vez na margem norte do Orógeno Araçuaí-Congo Ocidental. Os dados geocronológicos de U-Pb em zircão detrítico mostraram idades entre 753 ± 12 Ma a 3656 ± 8 Ma. Essas idades sugerem que as unidades basais, ricas em diamictitos, do Grupo Macaúbas poderiam ser correlacionadas com a Glaciação Sturtiana, enquanto unidades superiores poderiam se correlacionar com a Glaciação Marinoana.

As áreas fonte para a Formação Chapada Acauã Inferior, na porção norte do Orógeno Araçuaí-Congo Ocidental, são semelhantes às evidenciadas nesse trabalho para o Complexo Jequitinhonha. As possíveis fontes para a unidade são rochas do

embasamento do Paleocontinente São Francisco-Congo e outros complexos metamóficos, rochas intrusivas e vulcânicas do Mesoproterozóico encontradas na bacia rifte-sag do Espinhaço e rochas do magmatismo anorogênico Toniano, rochas da Província Alcalina do Sul do Estado da Bahia (PASEBA). Apesar de a região ser geograficamente próxima de onde foram coletadas amostras do Complexo Jequitinhonha, não foram encontradas evidências de contribuição de fontes do Criogeniano superior e Ediacaranas nas amostras coletadas.

A sedimentação da bacia precursora do Complexo Jequitinhonha se desenvolveu sobre a margem interna do golfo do Orógeno Araçuaí-Congo Ocidental, próximo à região do paleocontinente São Francisco, onde haviam ocorrido as instruões alcalinas da PASEBA. Essas intrusões marcam o evento de rifteamento do Criogeniano responsável pela bacia precursora do Grupo Macaúbas e que levou ao desenvolvimento da crosta oceânica do Oceano Adamastor mais ao sul, durante o final do Criogeniano e início do Ediacarano, seguido pelo início da formação do Arco do Rio Doce. Esse contexto sugere que o Complexo Jequitinhonha registrou a mudança da configuração da bacia de margem passiva para bacia sin-orogênica e que, posteriormente, essa unidade foi deformada e metamorfizada em alto grau, complicando as relações estratigráficas originais.

A distribuição das unidades diamictitícas do Grupo Macaúbas e a presença de uma capa de carbonato associada ao Grupo Bambuí no Cráton do São Francisco indica que a margem do rifte formou uma extensa depressão topográfica que permitiu a deposição ao longo de todo o Criogeniano, incluindo durante o Sturtiano e Marinoano, no espaço de acomodação da bacia precursora do Orógeno Araçuaí. Em contraste, o espaço de acomodação para sedimentação sobre a região cratônica se formou concomitantemente à formação dos orógenos Brasília e Araçuaí, gerando a flexura litosférica necessária para o desenvolvimento de uma bacia de antepaís somente após cerca de 635 Ma atrás, conforme indicado pela presença de carbonato de capa Marinoano na base do Grupo Bambuí.

REFERÊNCIAS

Aguilar, C., Alkmim, F. F., Lana, C., & Farina, F. (2017). Palaeoproterozoic assembly of the São Francisco craton, SE Brazil: New insights from U–Pb titanite and monazite dating. *Precambrian Research*, *289*, 95-115.

Albert, C., Farina, F., Lana, C., Stevens, G., Storey, C., Gerdes, A., & Dopico, C. M. (2016). Archean crustal evolution in the Southern São Francisco craton, Brazil: constraints from U-Pb, Lu-Hf and O isotope analyses. *Lithos*, *266*, 64-86.

Alcântara, D.C.B.G., Uhlein, A., Caxito, F.A., Dussin, I.A., & Pedrosa-Soares, A.C. (2017). Stratigraphy, tectonics and detrital zircon U-Pb (LA-ICP-MS) geochronology of the Rio Preto Belt and northern Paramirim corridor, NE, Brazil. *Brazilian Journal of Geology, 47* (2), 261–273.

Alkmim, F. F., Marshak, S., & Fonseca, M. A. (2001). Assembling West Gondwana in the Neoproterozoic: clues from the Sao Francisco craton region, Brazil. Geology, 29(4), 319-322.

Alkmim, F. F., Marshak, S., Pedrosa-Soares, A. C., Peres, G. G., Cruz, S. C. P., & Whittington, A. (2006). Kinematic evolution of the Araçuaí-West Congo orogen in Brazil and Africa: Nutcracker tectonics during the Neoproterozoic assembly of Gondwana. *Precambrian research, 149*(1-2), 43-64.

Almeida, F.F.M., & Litwinski, N., 1984. Província Mantiqueira: setor setentrional. In: Almeida F.F.M. Hasui Y. (Eds.) *O Pré-Cambriano do Brasil*. São Paulo, Editora Edgar Blücher, p. 282-307.

Amaral, L., Caxito, F. A., Pedrosa-Soares, A. C., Queiroga, G., Babinski, M., Trindade, R., Lana, C., & Chemale, F. (2020). The Ribeirão da Folha ophiolite-bearing accretionary wedge (Araçuaí orogen, SE Brazil): New data for Cryogenian plagiogranite and metasedimentary rocks. *Precambrian Research, 336*, January 2020, 105522.

Andersen, T., Andersson, U.B., Graham, S., Åberg, G., & Simonsen, S. L. (2009). Granitic magmatism by melting of juvenile continental crust: new constraints on the source of Palaeoproterozoic granitoids in Fennoscandia from Hf isotopes in zircon. Journal of the *Geological Society, 166*, 233–247.

Araujo, C., Pedrosa-Soares, A., Lana, C., Dussin, I., Queiroga, G., Serrano, P., & Medeiros-Júnior, E. (2019). Zircon in emplacement borders of post-collisional plutons compared to country rocks: A study on morphology, internal texture, U–Th–Pb geochronology and Hf isotopes (Araçuaí orogen, SE Brazil). *Lithos*, 105252.

Araújo, M. C. (2000). Projeto Leste: Folhas Jacinto/Salto da Divisa/Itarantim – SE.24-V-B-I/SE.24-V-B-II/SD.24-Y-D-IV, escala 1:100.000. Belo Horizonte: SEME/COMIG/CPRM.

Babinski, M., Gradim, R. J., Pedrosa-Soares, A. C., de Alkmim, F. F., Noce, C. M., & Liu, D. (2005). Geocronologia U-Pb (SHRIMP) e Sm-Nd de xistos verdes basálticos do

Orógeno Araçuaí: implicações para a idade do Grupo Macaúbas. *Revista Brasileira de Geociências, 35*(4 sup), 77-81.

Babinski M., Pedrosa-Soares A.C., Trindade R.I.F., Martins M., Noce C.M., & Liu D. (2012). Neoproterozoic glacial deposits from the Araçuaí orogen, Brazil: Age, provenance and correlations with the São Francisco craton and West Congo belt. *Gondwana Research, 21*(2-3):451-465.

Barbosa, J. S. F., & Sabaté, P. (2004). Archean and Paleoproterozoic crust of the São Francisco craton, Bahia, Brazil: geodynamic features. *Precambrian Research, 133*(1-2), 1-27.

Bahlburg, H., Vervoort, J. D., DuFrane, S. A., Carlotto, V., Reimann, C., & Cárdenas, J. (2011). The U-Pb and Hf isotope evidence of detrital zircons of the Ordovician Ollantaytambo Formation, southern Peru, and the Ordovician provenance and paleogeography of southern Peru and northern Bolivia. *Journal of South American Earth Sciences, 32*, 196–209.

Begg, G. C., Griffin, W. L., Natapov, L. M., O'Reilly, S. Y., Grand, S. P., O'Neill, C. J., . . . Bowden, P. (2009). The lithospheric architecture of Africa: seismic tomography, mantle petrology, and tectonic evolution. *Geosphere, 5*, 23–50.

Belém, J. (2006). *Caracterização mineralógica, física e termobarométrica de minérios de grafita da Província Grafítica Bahia-Minas* (Dissertação de Mestrado) Instituto de Geociências, Universidade Federal de Minas Gerais, Belo Horizonte, MG, Brasil.

Belém, J. (2018). Grafita. In: Pedrosa-Soares, A.C; Voll, E; Cunha, E.C. (Org.). *Recursos Minerais de Minas Gerais*. (1a ed., pp. 1-24). Belo Horizonte: Companhia de Desenvolvimento de Minas Gerais (CODEMGE).

Bersan, S. M., Danderfer Filho, A., Abreu, F., & Lana, C. (2018). Geoquímica e geocronologia da Suíte Paciência: implicações para o fim da evolução riaciana do Bloco Itacambira-Monte Azu. Geologia USP. *Série Científica, 18*(1), 185-206.

Bitencourt, C. N., Cruz, S. C. P., Cruz, V. A., Pedrosa-Soares, A. C., Paquette, J. L., Alkmim, A. R., & Barbosa, J. S. F. (2019). Rifting events in the southern sector of the Paramirim Aulacogen, NE Brazil: New geochronological data and correlations for the São Francisco–Congo paleocontinent. *Precambrian Research, 326*, 417-446.

Bouvier, A., Vervoort, J. D., & Patchett, P. J. (2008). The Lu–Hf and Sm-Nd isotopic composition of CHUR: constraints from unequilibrated chondrites and implications for the bulk composition of terrestrial planets. *Earth and Planetary Science Letters, 273*, 48–57.

Brito-Neves, B. B., Campos Neto, M.C., & Fuck, R. A. (1999). From Rodinia to Western Gondwana: An approach to the Brasiliano-Pan African Cycle and orogenic collage. *Episodes, 22(*3):155-166.

Brocks, J. J., Jarrett, A. J., Sirantoine, E., Hallmann, C., Hoshino, Y., & Liyanage, T. (2017). The rise of algae in Cryogenian oceans and the emergence of animals. *Nature, 548*(7669), 578-581.

Butler, R. W., Tavarnelli, E., & Grasso, M. (2006). Structural inheritance in mountain belts: an Alpine–Apennine perspective. *Journal of structural geology, 28*(11), 1893-1908.

Campos, C. P., Medeiros, S. R., Mendes, J. C., Pedrosa-Soares, A. C., Dussin, I., Ludka, I. P., & Dantas, E. L. (2016). Cambro-Ordovician magmatism in the Araçuaí Belt (SE Brazil): snapshots from a post-collisional event. *Journal of South American Earth Sciences, 68*, 248-268.

Castro, M. P., Queiroga, G., Martins, M., Alkmim, F. F., Pedrosa-Soares, A. C., Dussin, I. A., & Souza, M. E. (2019). An Early Tonian rifting event affecting the São Francisco-Congo paleocontinent recorded by the Lower Macaúbas Group, Araçuaí Orogen, SE Brazil. *Precambrian Research, 331*, 105351.

Castro, M. P., Queiroga, G. N., Martins, M., Pedrosa-Soares, A. C., Dias, L., Lana, C., . . . Silva, M. A. (2020). Provenance shift through time in superposed basins: From Early Cryogenian glaciomarine to Late Ediacaran orogenic sedimentations (Araçuaí Orogen, SE Brazil). *Gondwana Research, 87*, 41-66.

Caxito, F. A., Halverson, G. P., Uhlein, A., Stevenson, R., Gonçalves-Dias, T., & Uhlein, G. J. (2012). Marinoan glaciation in east central Brazil. *Precambrian Research, 200*, 38-58.

Caxito, F. A., Dantas, E. L., Stevenson, R., & Uhlein, A. (2014). Detrital zircon (U–Pb) and Sm–Nd isotope studies of the provenance and tectonic setting of basins related to collisional orogens: The case of the Rio Preto fold belt on the northwest São Francisco Craton margin, NE Brazil. *Gondwana Research, 26*(2), 741-754.

Caxito, F.A., Uhlein, A., Dantas, E.L., Stevenson, R., & Pedrosa-Soares, A.C. (2015). Orosirian (ca. 1.96 Ga) mafic crust of the northwestern São Francisco Craton margin: Petrography, geochemistry and geochronology of amphibolites from the Rio Preto fold belt basement, NE Brazil. *Journal of South American Earth Sciences, 59*, 95-111.

Caxito, F.A., Uhlein, A., Dantas, E.L., Stevenson, R., Salgado, S.S., Dussin, I.A., & Sial, A.N. (2016). A complete Wilson Cycle recorded within the Riacho do Pontal Orogen, NE Brazil: Implications for the Neoproterozoic evolution of the Borborema Province at the heart of West Gondwana. *Precambrian Research, 282*, 97-120.

Caxito, F. A., Uhlein, G. J., Uhlein, A., Pedrosa-Soares, A.C., Kuchenbecker, M, Reis, . . . Paula, J. R., (2019). Isotope stratigraphy of Precambrian sedimentary rocks from Brazil: Keys to unlock Earth's hydrosphere, biosphere, tectonic, and climate evolution. *In Stratigraphy & Timescales, 4*, 73-132. Academic Press.

Caxito, F. A., Hagemann, S., Dias, T.G., Barrote, V., Dantas, E.L., Chaves, A. de O., Campello, M.S., &Campos, F.C. (2020). A magmatic barcode for the São Francisco Craton: Contextual in-situ SHRIMP U–Pb baddeleyite and zircon dating of the Lavras,

Pará de Minas and Formiga dike swarms and implications for Columbia and Rodinia reconstructions. *Lithos* 374–375, 105708. https://doi.org/10.1016/j.lithos.2020.105708

Caxito, F. A., Heilbron, M., Valeriano, C. M., Bruno, H., Pedrosa-Soares, A., Alkmim, F. F., . . . Basei, M. A. S. (2021a). Integration of elemental and isotope data supports a neoproterozoic adamastor ocean realm. *Brazilian Journal of Geology*, *44*, 493-518.

Caxito, F., Lana, C., Frei, R., Uhlein, G. J., Sial, A. N., Dantas, E. L., . . . Ganade, C. E. (2021b). Goldilocks at the dawn of complex life: mountains might have damaged Ediacaran–Cambrian ecosystems and prompted an early Cambrian greenhouse world. *Scientific reports*, *11*(1), 1-15.

Caxito, F. A., Hartmann, L. A., Heilbron, M., Pedrosa-Soares, A. C., Bruno, H., Basei, M. A., & Chemale, F. (2022). Multi-proxy evidence for subduction of the Neoproterozoic Adamastor Ocean and Wilson cycle tectonics in the South Atlantic Brasiliano Orogenic System of Western Gondwana. *Precambrian Research*, *376*, 106678.

Chaves, A. O., Ernst, R. E., Söderlund, U., Wang, X., & Naeraa, T. (2019). The 920–900 Ma Bahia-Gangila LIP of the São Francisco and Congo cratons and link with Dashigou-Chulan LIP of North China craton: new insights from U-Pb geochronology and geochemistry. *Precambrian Research, 329*, 124-137.

Chemale Jr., F., Dussin, I. A., Alkmim, F. F., Martins, M. S., Queiroga, G. N., Armstrong, R., & Santos, M.N. (2012). Unravelling a Proterozoic basin history through detrital zircon geochronology: the case of the Espinhaco Supergroup, Minas Gerais, Brazil. *Gondwana Research, 22*, 200–206.

Chen, D. F., Dong, W. Q., Zhu, B. Q., & Chen, X. P. (2004). Pb–Pb ages of Neoproterozoic Doushantuo phosphorites in South China: constraints on early metazoan evolution and glaciation events. *Precambrian Research, 132*(1-2), 123-132.

Cordani, U. G., D'Agrella-Filho, M. S., Brito-Neves, B. B. D., & Trindade, R. I. F., (2003). Tearing up Rodinia: the Neoproterozoic palaeogeography of South American cratonic fragments. *Terra Nova, 15*(5), 350-359.

Costa, A. F. O., & Danderfer, A. (2017). Tectonics and sedimentation of the central sector of the Santo Onofre rift, north Minas Gerais, Brazil. *Brazilian Journal of Geology, 47*(3), 491-519.

Costa, A. F. O., Danderfer, A., & Lana, C. (2018a). Stratigraphic and geochronological characterization of the Mato Verde group, Central Espinhaço (Brazil): An Eocalymmian rifting record in the western domain of the Congo-São Francisco paleocontinent. *Journal of South American Earth Sciences, 84*, 16-33.

Costa, F. G. D., Alkmim, F. F., & Magalhães, P. M. (2018b). The Ediacaran Salinas turbidites, Araçuaí Orogen, MG: tectonics and sedimentation interplay in a syn-orogenic basin. *Brazilian Journal of Geology, 48*(4), 783-804.

Cruz, S. C. P., Barbosa, J. S. F., Pinto, M. S., Peucat, J. J., Paquette, J. L., de Souza, J. . . . Carneiro, M. A. (2016). The Siderian-Orosirian magmatism in the Gavião Paleoplate, Brazil: U–Pb geochronology, geochemistry and tectonic implications. *Journal of South American Earth Sciences, 69*, 43-79.

Daconti, B. C. (2004). *Contexto geológico, controle e correlação regional das mineralizações de grafita da região de Almenara, Província Grafítica do Nordeste de Minas Gerais* (Dissertação de Mestrado) Instituto de Geociências, Universidade Federal de Minas Gerais, Belo Horizonte, MG, Brasil.

Danderfer, A., De Waele, B., Pedreira, A. J., & Nalini, H. A. (2009). New geochronological constraints on the geological evolution of Espinhaço basin within the São Francisco Craton—Brazil. *Precambrian Research, 170*(1-2), 116-128.

Debruyne, D., Hulsbosch, N., Van Wilderode, J., Balcaen, L., Vanhaecke, F., & Muchez, P. (2015). Regional geodynamic context for the Mesoproterozoic Kibara Belt (KIB) and the Karagwe-Ankole Belt: Evidence from geochemistry and isotopes in the KIB. *Precambrian Research, 264*, 82-97.

Degler, R., Pedrosa-Soares, A., Dussin, I., Queiroga, G., & Schulz, B. (2017). Contrasting provenance and timing of metamorphism from paragneisses of the Araçuaí-Ribeira orogenic system, Brazil: Hints for Western Gondwana assembly. *Gondwana Research, 51*, 30-50.

Degler, R., Pedrosa-Soares, A. C., Novo, T., Tedeschi, M., Silva, L. C., Dussin, I. A., & Lana, C. (2018). Rhyacian-Orosirian isotopic records from the basement of the Araçuaí-Ribeira orogenic system (SE Brazil): Links in the Congo-São Francisco palaeocontinent. *Precambrian Research, 317*, 179-195.

Deluca, C., Pedrosa-Soares, A., Lima, S., Cordani, U., & Sato, K. (2019). Provenance of the Ediacaran Salinas Formation (Araçuaí Orogen, Brazil): Clues from lithochemical data and zircon U-Pb (SHRIMP) ages of volcanic clasts. *Brazilian Journal of Geology, 49*(2).

Drumond, J. B. V. (2000). *Projeto Leste: Folha Encruzilhada – SD.24-Y-C-VI, escala 1:100.000.* Belo Horizonte: SEME/COMIG/CPRM.

Evans, D. M., Windrim, D. P., & Armstrong, R. A. (2007). Age of Metavolcanic rocks at the northern margin of the Namaqua-Natal Metamorphic Province in the Karas Mountains, Namibia, defined by SHRIMP U-Pb dating of zircons. *South African Journal of Geology, 110*(1), 47-54.

Falci, A., Caxito, F. A., Seer, H. J., Valeriano, C. M., Dias, P. H. A., & Pedrosa-Soares, A. C. (2018). Provenance shift from a continental margin to a syn-orogenic basin in the Neoproterozoic Araxá nappe system, southern Brasília belt, Brazil. *Precambrian Research, 306*, 209-219.

Faria, L. F. (1997). *Controle e tipologia de mineralizações de grafita flake do nordeste de Minas Gerais e sul da Bahia: uma abordagem regional* (Dissertação de Mestrado)

Instituto de Geociências, Universidade Federal de Minas Gerais, Belo Horizonte, MG, Brasil.

Fernandes André, J. L., Valladares, C. S., & Duarte, B. P. (2009). O Complexo Juiz de Fora na região de Três Rios (RJ): litogeoquímica, geocronologia U-Pb (LA-ICPMS) e geoquímica isotópica de Nd e Sr. *Revista Brasileira de Geociências, 39*(4), 773-793.

Fernandez-Alonso, M., Cutten, H., De Waele, B., Tack, L., Tahon, A., Baudet, D., & Barritt, S. D. (2012). The Mesoproterozoic Karagwe-Ankole Belt (formerly the NE Kibara Belt): The result of prolonged extensional intracratonic basin development punctuated by two short-lived far-field compressional events. *Precambrian Research, 216*, 63-86.

Figueiredo, F.T., Almeida, R.P., Tohver, E., Babinski, M., Liu, D., & Fanning, C.M., (2009). Neoproterozoic glacial dynamics revealed by provenance of diamictites of the Bebedouro Formation, São Francisco Craton, Central Eastern Brazil. *Terra Nova, 21*, 375–385.

Frimmel, H. E., Tack, L., Basei, M. S., Nutman, A. P., & Boven, A. (2006). Provenance and chemostratigraphy of the Neoproterozoïc West congolian Group in the Democratic Republic of Congo. *Journal of African Earth Sciences, 46*(3), 221-239.

Gerdes, A., & Zeh, A. (2006). Combined U-Pb and Hf isotope LA-(MC)ICP-MS analyses of detrital zircons: comparison with SHRIMP and new constraints for the provenance and age of an Armorican metasediment in Central Germany. *Earth Planet. Sci. Lett. 249*, 47–61.

Gonçalves, L., Alkmim, F. F., Pedrosa-Soares, A. C., Dussin, I. A., Valeriano, C. D. M., Lana, C., & Tedeschi, M. (2016). Granites of the intracontinental termination of a magmatic arc: an example from the Ediacaran Araçuaí orogen, southeastern Brazil. Gondwana Research, 36, 439-458.

Gonçalves, L., Alkmim, F. F., Pedrosa-Soares, A., Gonçalves, C. C., & Vieira, V. (2017). From the plutonic root to the volcanic roof of a continental magmatic arc: a review of the Neoproterozoic Araçuaí orogen, southeastern Brazil. *International Journal of Earth Sciences, 107*(1), 337-358.

Gonçalves, G. O., Lana, C., Buick, I. S., Alkmim, F. F., Scholz, R., & Queiroga, G. (2019). Twenty million years of post-orogenic fluid production and hydrothermal mineralization across the external Araçuaí orogen and adjacent São Francisco craton, SE Brazil. *Lithos, 342*, 557-572.

Gonçalves-Dias, T., Pedrosa-Soares, A. C., Dussin, I. A., Alkmim, F. F., Caxito, F.A., Silva, L.C., & Noce, C.M. (2011). Idade máxima de sedimentação e proveniência do Complexo Jequitinhonha na áreatipo (Orógeno Araçuaí): primeiros dados U–Pb (LA-ICP-MS) de grãos detríticos de zircão. *Geonomos, 19*(2), 121-130.

Gonçalves-Dias, T. (2012). *Caracterização geoquímica e geocronológica do complexo Jequitinhonha na área tipo, Orógeno Araçuaí* (Dissertação de Mestrado) Instituto de Geociências, Universidade Federal de Minas Gerais, Belo Horizonte, MG,

Brasil.Gonçalves-Dias, T., Caxito, F. A., Pedrosa-Soares, A. C., Stevenson, R., Dussin, I., Silva, L. C., Alkmim, F. F., & Pimentel, M. (2016). Age, provenance and tectonic setting of the high-grade Jequitinhonha Complex, Araçuaí Orogen, eastern Brazil. *Brazilian Journal of Geology, 46*(2), 199-219.

Gradim, R.J., Alkmim, F.F., Pedrosa-Soares, A.C., Babinski, M., Noce, C.M. (2005). Xistos Verdes do Alto Araçuaí, Minas Gerais: Vulcanismo Básico do Rifte Neoproterozóico Macaúbas. *Revista Brasileira de Geociências 35* (4-suplemento), 59–69.

Gradim, C., Roncato, J., Pedrosa-Soares, A. C., Cordani, U. G., Dussin, I. A., Alkmim, F. F., . . . Babinski, M. (2014). The hot back-arc zone of the Araçuaí orogen, Eastern Brazil: from sedimentation to granite generation. *Brazilian Journal of Geology, 44*(1), 155-180.

Griffin,W. L., Pearson,N. J., Belousova, E., Jackson, S. E., van Achterbergh, E., O'Reilly, S. Y., & Shee, S. R. (2000). The Hf isotope composition of cratonicmantle: LAM-MC-ICPMS analysis of zircon megacrysts in kimberlites. *Geochimica et Cosmochimica Acta, 64*, 133–147.

Guadagnin, F., Chemale Jr, F., Magalhães, A. J., Santana, A., Dussin, I., & Takehara, L. (2015). Age constraints on crystal-tuff from the Espinhaço Supergroup—Insight into the Paleoproterozoic to Mesoproterozoic intracratonic basin cycles of the Congo–São Francisco Craton. *Gondwana Research, 27*(1), 363-376.

Guimarães, F. R. (2000). *Uso de Imagem de Satélite Landsat 5/TM e Sistema de Informações Geográficas no Estudo Geológico da Província Grafítica Minas-Bahia: Setor Noroeste* (Dissertação de Mestrado) Instituto de Geociências, Universidade Federal de Minas Gerais, Belo Horizonte, MG, Brasil.

Heaman, L. (1991). U–Pb dating of giant radiating dyke swarms: potential for global correlation of mafic magmatic events. In *International Symposium of mafic dykes. Extended abstracts*, São Paulo, Brazil (pp. 7-9).

Heilbron, M., & Machado, N. (2003). Timing of terrane accretion in the Neoproterozoic–Eopaleozoic Ribeira orogen (SE Brazil). *Precambrian Research, 125*(1-2), 87-112.

Heilbron, M., Duarte, B. P., Valeriano, C. M., Simonetti, A., Machado, N., & Nogueira, J. R. (2010). Evolution of reworked Paleoproterozoic basement rocks within the Ribeira belt (Neoproterozoic), SE-Brazil, based on U–Pb geochronology: Implications for paleogeographic reconstructions of the São Francisco-Congo paleocontinent. *Precambrian Research, 178*(1-4), 136-148.

Heilbron, M., Cordani, U. G., & Alkmim, F. F. (2017). The São Francisco craton and its margins. In *São Francisco Craton, Eastern Brazil*. Springer, Cham. 3-13.

Hippertt, J. P., Caxito, F. A., Uhlein, G. J., Nalini, H. A., Sial, A. N., Abreu, A. T., & Nogueira, L. B. (2019). The fate of a Neoproterozoic intracratonic marine basin: Trace

elements, TOC and IRON speciation geochemistry of the Bambuí Basin, Brazil. *Precambrian Research 330*, 101–120.

Hoffman, P. F., Abbot, D. S., Ashkenazy, Y., Benn, D. I., Brocks, J. J., Cohen, P. A., . . . Warren, S.G. (2017). Snowball Earth climate dynamics and Cryogenian geology-geobiology. *Science Advances, 3*(11), e1600983.

Jackson, S. E., Pearson, N. J., Griffin,W. L., & Belousova, E. A. (2004). The application of laser ablation-inductively coupled plasma-mass spectrometry to in situ U-Pb zircon geochronology. *Chemical Geology, 211*, 47–69.

Jaffey, A. H., Flynn, K. F., Glendenin, L. E., Bentley, W. T., & Essling, A. M. (1971). Precision measurement of half-lives and specific activities of U^{235} and U^{238}. *Physical review C, 4*(5), 1889.

Kirschvink, J. L. (1992). Late Proterozoic low-latitude global glaciation: the snowball Earth.

Kuchenbecker, M., Pedrosa-Soares, A. C., Babinski, M., & Fanning, M. (2015). Detrital zircon age patterns and provenance assessment for pre-glacial to post-glacial successions of the Neoproterozoic Macaúbas Group, Araçuaí orogen, Brazil. *Precambrian Research, 266*, 12-26.

Kuchenbecker, M., Pedrosa-Soares, A. C., Babinski, M., Reis, H. L. S., Atman, D., & Costa, R. D. (2020). Towards an integrated tectonic model for the interaction between the Bambuí basin and the adjoining orogenic belts: Evidences from the detrital zircon record of syn-orogenic units. *Journal of South American Earth Sciences, 104*, 102831.

Lima, S.A.A., Martins-Neto, M.A., Pedrosa-Soares, A.C., Cordani, U.G., & Nutman, A. (2002). A Formação Salinas na área-tipo, NE de Minas Gerais: uma proposta de revisão da estratigrafia da Faixa Araçuaí com base em evidências sedimentares, metamórficas e de idades U-Pb SHRIMP. *Revista Brasileira de Geociências.* 32 (4), 491–500.

Ludwig, K. R., (2008). User's manual for Isoplot 3.6. A geochronological toolkit for Microsoft Excel. Berkeley Geochronologic Center, *Special Publication No. 4*, Berkeley, USA.

Ludwig, K. R. (2012). User's manual for Isoplot 3.75. Berkeley Geochronology Center. *Special Publication, 5*, 1-75.

Macdonald, F. A., Schmitz, M. D., Crowley, J. L., Roots, C. F., Jones, D. S., Maloof, A. C., . . . Schrag, D. P. (2010). Calibrating the cryogenian. *Science, 327(*5970), 1241-1243.

Magalhaes, J. R., Pedrosa-Soares, A., Dussin, I., Müntener, O., Pinheiro, M. A. P., Silva, L. C., . . . Baumgartner, L. (2019). First Lu-Hf, δ18O and trace elements in zircon signatures from the Statherian Espinhaço anorogenic province (Eastern Brazil): geotectonic implications of a silicic large igneous province. *Brazilian Journal of Geology, 48*(4), 735-759.

Martins, V. T. S., Teixeira, W., Noce, C. M., & Pedrosa-Soares, A. C. (2004). Sr and Nd characteristics of Brasiliano-Pan African granitoid plutons of the Araçuaí orogen, southeastern Brazil: Tectonic implications. *Gondwana Research, 7*, 75-89.

Martins, M., Karfunkel, J., Noce, C. M., Babinski, M., Pedrosa-Soares, A. C., Sial, A. N., & Liu, D. (2008). A sequência pré-glacial do Grupo Macaúbas na área-tipo e o registro da abertura do rifte Araçuaí. *Brazilian Journal of Geology, 38*(4), 761-772.

Martins, M., Babinski, M., Noce, C.M., Queiroga, G.N., Pedrosa-Soares, A.C., Trindade, R., Liu, D. (2011). A Suíte Córrego Taquari na Anticlinal de Itacambira, Bacia do Rio Macaúbas (MG): magmatismo básico tardi-ediacarano (ca. 560 Ma) no domínio externo do Orógeno Araçuaí. *Geonomos 19*, 78–89.

McCourt, S., Armstrong, R. A., Jelsma, H., & Mapeo, R. B. M. (2013). New U–Pb SHRIMP ages from the Lubango region, SW Angola: insights into the Palaeoproterozoic evolution of the Angolan Shield, southern Congo Craton, Africa. *Journal of the Geological Society, 170*(2), 353-363.

Mehnert, K. R. (1968). *Migmatites and the Origin of Granitic Rocks*. New York: Elsevier.

Melo, M. G., Lana, C., Stevens, G., Pedrosa-Soares, A. C., Gerdes, A., Alkmin, L. A., Nalini Jr., H. A., & Alkmim, F. F. (2017). Assessing the isotopic evolution of S-type granites of the Carlos Chagas Batholith, SE Brazil: Clues from U–Pb, Hf isotopes, Ti geothermometry and trace element composition of zircon. *Lithos, 284*, 730-750.

Menezes, R. C. L., Conceição, H., Rosa, M. L. S., Galarza, M. A., Rios, D. C., & Macambira, M. J. B. (2012a). O Stock Nefelina-Sienítico Rio Pardo, Província Alcalina do Sul do Estado da Bahia. *Geonomos, 20*(1), 14-22.

Menezes, R. C. L., Conceição, H., Rosa, M. L. S., Macambira, M. J. B., Galarza, M. A., & Rios, D. C. (2012b). Geoquímica e geocronologia de granitos anorogênicos tonianos (ca. 914–899 ma) da Faixa Araçuaí no sul do Estado da Bahia. *Revista Geonomos, 20*(1), 1-13.

Moreira, H.F., Danderfer, A., Costa, A.F.O., Bersan, S.M., Lana, C.C., & Queiroga, G.N. (2020). Record of Early Tonian mafic magmatism in the central Espinhaço (Brazil): New insights for break-up of the Neoproterozoic landmass ancestor of São Francisco-Congo paleocontinent. *Geoscience Frontiers, 11*(6), 2323-2337.

Nalini Jr., H. A., Bilal, E., & Neves, J. M. C. (2000). Syn-collisional peraluminous magmatism in the Rio Doce region: mineralogy, geochemistry, and isotopic data of the Neoproterozoic Urucum Suite (eastern Minas Gerais State, Brazil). *Revista Brasileira de Geociências, 30*, 120-125.

Noce, C. M., Pedrosa-Soares, A. C., Piuzana, D., Armstrong, R., Laux, J. H., Campos, C. M., & Medeiros, S. R. (2004). Ages of sedimentation of the kinzigitic complex and of a late orogenic thermal episode in the Araçuaí orogen, northern Espírito Santo State, Brazil: Zircon and monazite U-Pb SHRIMP and ID-TIMS data. *Revista Brasileira de Geociências, 349*, 587-592.

Noce, C. M., Soares, A. C. P., Silva, L. C. D., & Alkmim, F. F. (2007a). O embasamento arqueano e paleoproterozóico do orógeno Araçuaí. *Geonomos, 15*, 17-23.

Noce, C. M., Pedrosa-Soares, A. C., Silva, L. C., Armstrong, R., & Piuzana, D. (2007b). Evolution of polycyclic basement complexes in the Araçuaí Orogen, based on U–Pb SHRIMP data: Implications for Brazil–Africa links in Paleoproterozoic time. *Precambrian Research, 159*(1-2), 60-78.

Novo, T. A. (2013). *Caracterização do Complexo Pocrane, magmatismo básico mesoproterozóico e unidades neoproterozóicas do Sistema Araçuaí Ribeira, com ênfase em geocronologia U-Pb (SHRIMP e LA-ICP-MS)* (Tese de Doutorado) Instituto de Geociências, Universidade Federal de Minas Gerais, Belo Horizonte, MG, Brasil.

Novo, T. A., Pedrosa-Soares, A., Vieira, V. S., Dussin, I. A., & Silva, L. C., (2018). The Rio Doce Group revisited: an Ediacaran arc-related volcano-sedimentary basin, Araçuaí orogen (SE Brazil). *Journal of South American Earth Sciences, 85*, 345-361.

Oliveira, R. G., Martins, M., Queiroga, G., de Souza, M. E. S., Lana, C., Alkmim, A. R., . . . Linhares, D. (2021). Sedimentary provenance and role of tectonic inheritance on the control of the Macaúbas group, eastern margin of São Francisco Craton (SE Brazil). *Journal of South American Earth Sciences, 109*, 103210.

Pacheco, F. E. R. C., Caxito, F. A., Pedrosa-Soares, A. C., Dussin, I. A., & Gonçalves-Dias, T. (2021). Detrital zircon U-Pb and Lu-Hf data for a kinzigitic gneiss (Jequitinhonha Complex, Araçuaí Orogen, SE Brazil) constrain the age of a huge storage of Ediacaran carbon. *Journal of South American Earth Sciences, 105*, 102709.

Paes, V. J. C., Raposo, F. O., Pinto, C. P., & Oliveira, F. A. R. (2010). *Projeto Jequitinhonha, Estados de Minas Gerais e Bahia: texto explicativo. Geologia e Recursos Minerais das Folhas Comercinho, Jequitinhonha, Almenara, Itaobim, Joaíma e Rio do Prado*. Programa Geologia do Brasil. Belo Horizonte: CPRM.

Pedrosa-Soares A. C., Noce C. M., Vidal P., Monteiro R., & Leonardos O. H. (1992). Toward a new tectonic model for the Late Proterozoic Araçuaí (SE Brazil)-West Congolian (SW Africa) Belt. *Journal of South American Earth Science, 6*(1-2):33-47.

Pedrosa-Soares, A. C., Vidal, P., Leonardos, O. H., & Brito-Neves, B. B. (1998). Neoproterozoic oceanic remnants in eastern Brazil: further evidence and refutation of an exclusively ensialic evolution for the Araçuaí–West Congo Orogen. *Geology, 26*(6), 519-522.

Pedrosa-Soares, A. C., Cordani, U. G., & Nutman, A. (2000). Constraining the age of Neoproterozoic glaciation in eastern Brazil: first U-Pb (SHRIMP) data of detrital zircons. *Revista Brasileira de Geociências, 30*(1), 058-061.

Pedrosa-Soares, A. C., & Wiedemann-Leonardos, C. M. (2000). Evolution of the Araçuaí Belt and its connection to the Ribeira Belt, Eastern Brazil. *Tectonic Evolution of South America, 31*, 265-310.

Pedrosa-Soares, A. C., Noce, C. M., Wiedemann, C. M., & Pinto, C. P. (2001). The Araçuaí–West Congo orogen in Brazil: An overview of a confined orogen formed during Gondwanland assembly. *Precambrian Research, 110*, 307-323.

Pedrosa-Soares, A. C., Noce, C. M., Alkmim, F. F., Silva, L. C. D., Babinski, M., Cordani, U. G., & Castañeda, C. (2007). Orógeno Araçuaí: síntese do conhecimento 30 anos após Almeida 1977. *Geonomos, 15*, 1-16.

Pedrosa-Soares, A. C., Alkmim, F. F., Tack, L., Noce, C. M., Babinski, M., Silva, L. C., Martins-Neto, M. A. (2008). Similarities and differences between the Brazilian and African counterparts of Neoproterozoic Araçuaí-West Congo orogen. In: Pankhrust R., Trouw R., Brito- Neves B B., Wit M. (eds). *The Gondwana Peleocontinent in the South Atlantic Region*. Geological Society of London, Special Publications, 294, 153-172.

Pedrosa-Soares, A. C., Campos, C. P., Noce, C., Silva, L. C., Novo, T., Roncato, J., . . . Alkmim, F. F. (2011a). Late Neoproterozoic-Cambrian granitic magmatism in the Araçuaí orogen (Brazil), the Eastern Brazilian Pegmatite Province and related mineral resources. In: Sial A.N., Bettencourt J.S., De Campos C.P., Ferreira V.P. (eds). *Granite-Related Ore Deposits*. Geological Society, London, Special Publications, 350, 25-51.

Pedrosa-Soares, A. C., Babinski, M., Noce, C., Martins, M., Queiroga, G., & Vilela, F. (2011b). The Neoproterozoic Macaúbas Group, Araçuaí orogen, SE Brazil. Geological Society, London, *Memoirs, 36*(1), 523-534.

Pedrosa-Soares, A. C., & Alkmim F. F. (2011). How many rifting events preceded the development of the Araçuaí-West Congo orogen? *Geonomos, 19*(2), 244-251.

Pedrosa-Soares, A.C., Dussin, I., Nseka, P., Baudet, D., Fernandez-Alonso, M., & Tack, L. (2016). Tonian rifting events on the Congo-São Francisco palaeocontinent: new evidence from U-Pb and Lu-Hf data from the Shinkakasa plutonic complex (Boma region, West Congo Belt, Democratic Republic of Congo). *5th International Geologica Belgica Meeting*, Mons, Belgium, Abstract Book, p. 44.

Peixoto, C. A., Heilbron, M., Ragatky, D., Armstrong, R., Dantas, E., Valeriano, C. M., & Simonetti, A. (2017). Tectonic evolution of the Juvenile Tonian Serra da Prata magmatic arc in the Ribeira belt, SE Brazil: Implications for early west Gondwana amalgamation. *Precambrian Research, 302*, 221-254.

Peixoto, E., Pedrosa-Soares, A. C., Alkmim, F. F. D., & Dussin, I. A. (2015). A suture–related accretionary wedge formed in the Neoproterozoic Araçuaí orogen (SE Brazil) during Western Gondwanaland assembly. *Gondwana Research, 27*(2), 878-896.

Peixoto, E., Alkmim, F. F., & Pedrosa-Soares, A. C. (2018). The Rio Pardo salient, northern Araçuaí orogen: an example of a complex basin-controlled fold-thrust belt curve. *Brazilian Journal of Geology, 48*(1), 25-49.

Peres, G. G., Alkimim, F. F., & Jordt-Evangelista, H. (2004). The southern Araçuaí belt and the Dom Silvério Group: geologic architecture and tectonic significance. *Anais da Academia Brasileira de Ciências, 76*(4), 771-790.

Pietranik, A. B., Hawkesworth, C. J., Storey, C. D., Kemp, A. I. S., Sircombe, K. N., Whitehouse, M. J., & Bleeker, W. (2008). Episodic, mafic crust formation from 4.5 to 2.8 Ga: new evidence from detrital zircons, Slave craton, Canada. *Geology, 36*, 875–878.

Queiroga, G. N., Pedrosa-Soares, A. C., Noce, C. M., Alkmim, F. F., Pimentel, M. M., Dantas, E., . . . Prichard, H. (2007). Age of the Ribeirão da Folha ophiolite, Araçuaí Orogen: The U-Pb zircon dating of a plagiogranite. *Geonomos,, 15*, 61-65.

Queiroga, G.N. (2010). *Caracterização de restos de litosfera oceânica do Orógeno Araçuaí entre os paralelos 17° e 21° S* (Tese de Doutorado) Instituto de Geociências, Universidade Federal de Minas Gerais, Belo Horizonte, MG, Brasil.

Queiroga, G. N., Dussin, I. A., Martins, M., Machado, M. C., Kawashita, K., & Chemale, F. (2012). Capítulo 9. Roteiro de Campo – Rochas Meta-ígneas. In: Dussin, I.A.; Chemale Jr., F.. (Org.). *Geologia Estrutural e Estratigrafia do Sistema Espinhaço-Chapada Diamantina e sua aplicação nas Bacias Mezocenozóicas da Margem Passiva Brasileira*. Belo Horizonte: FUNDEP/PETROBRÁS.

Reis, L. B. (1999). *Estudos de mineralizações de grafita no extremo nordeste de Minas Gerais* (Dissertação de Mestrado) Instituto de Geociências, Universidade Federal de Minas Gerais, Belo Horizonte, MG, Brasil.

Renne, P. R., Onstott, T. C., D'Agrella-Filho, M. S., Pacca, I. G., & Teixeira, W. (1990). 40Ar/39Ar Dating of 1.0–1.1 Ga magnetizations from the Sa˜ o Francisco and Kalahari cratons: tectonic implications for Pan-African and Brasiliano mobile belts. *Earth and Planetary Science Letters, 101*(2-4), 349-366.

Richter, F., Lana, C., Stevens, G., Buick, I., Pedrosa-Soares, A. C., Alkmim, F. F., & Cutts, K. (2016). Sedimentation, metamorphism and granite generation in a back-arc region: Records from the Ediacaran Nova Venécia Complex (Araçuaí Orogen, Southeastern Brazil). *Precambrian Research, 272*, 78-100.

Rooney, A. D., Strauss, J. V., Brandon, A. D., & Macdonald, F. A. (2015). A Cryogenian chronology: Two long-lasting synchronous Neoproterozoic glaciations. *Geology, 43*(5), 459-462.

Rooney, A. D., Yang, C., Condon, D. J., Zhu, M., & Macdonald, F. A. (2020). U-Pb and Re-Os geochronology tracks stratigraphic condensation in the Sturtian snowball Earth aftermath. *Geology, 48*(6), 625-629.

Rosa, M. L. S., Conceição, H., Oberli, F., Meir, M., Martin, H., Macambira, M. J. B., . . . Leal, L. R. B. (2000). Geochronology (U-Pb/Pb-Pb) and isotopic signature (Rb-Sr/Sm-Nd) of the Paleoproterozoic Guanambi Batholith, southwest Bahia State (NE Brazil). *Revista Brasileira de Geociências, 30*, 62–65.

Rosa, M. L. S., Conceição, H., Macambira, M. J. B., Marinho, M. M., Cunha, M. P., & Menezes, R. C. L. (2004). Idade Pb-Pb E Aspectos Petrológicos Da Mineralização Em Sodalita Azul Do Maciço Nefelina-Sienítico Itarantim, Sul Do Estado Da Bahia. *Revista Brasileira de Geociências, 34*(3), 347-354.

Rosa, M. L. S., Conceição, H., Leal, R. C. M., Macambira, M. J. B., Galarza, M. A., Oliveira, E. C., . . . Rios, D. C. (2005a). Idade U-Pb da mineralização de sodalita-sienito (Azul-Bahia) no stock litchfieldítico Itaju do Colônia, sul do estado da Bahia. *Revista Brasileira de Geociências, 35*(3), 433-436.

Rosa, M. L. S., Conceição, H., Macambira, M. J. B., Menezes, R. C. L., Cunha, M. P., Rios, D. C., & Marinho, M. M. (2005b). Magmatismo alcalino intraplaca neoproterozóico no sul do estado da Bahia: o batólito nefelina-sienítico Itarantim. *Revista Brasileira de Geociências, 35*(4 sup), 47-58.

Rosa, M. L. S., Conceição, H., Moura, C. A. V., Macambira, M. J. B., Marinho, M. M., Leal, R. C. M., Cunha, M. P., & Rios, D. C. (2005c). Assinatura mantélica de isótopos de carbono e oxigênio em cristais de calcita de rochas foid-sieníticas da Província Alcalina do Sul do Estado da Bahia. *Revista Brasileira de Geociências, 35*(4 sup), 71-76.

Rosa, M. L. S., Conceição, H., Macambira, M., Galarza, M. C., Cunha, M., Menezes, R., . . . Rios, D. C. (2007). Neoproterozoic anorogenic magmatism in the Southern Bahia Alkaline Province of NE Brazil: U-Pb and Pb-Pb ages of the blue sodalite syenites. *Lithos, 97*, 88-97.

Rosa, M. L. S., Oliveira, J. A., Conceição, H., Conceição, J. A., Macambira, M. J. B., & Galarza, M. A. (2015). Idade Pb-Pb do Stock Nefelina Sienítico Serra da Gruta, Província Alcalina do Sul do Estado da Bahia. *Scientia Plena, 11*(3), 1-5.

Rubatto, D. (2002). Zircon trace element geochemistry: partitioning with garnet and the link between U–Pb ages and metamorphism. *Chemical geology, 184*(1-2), 123-138.

Salgado, S. S., Ferreira Filho, C. F., Caxito, F. A., Uhlein, A., Dantas, E. L., & Stevenson, R. (2016). The Ni-Cu-PGE mineralized Brejo Seco mafic-ultramafic layered intrusion, RPO: onset of Tonian (ca. 900 Ma) continental rifting in Northeast Brazil. *J. South Am. Earth Sci. 70,* 324–339. http://dx.doi.org/10.1016/j.jsames.2016.06.001.

Sampaio, A. R., Martins, A. M., Loureiro, H. C., Arcanjo, J. B., Moraes Filho, J. C., Souza, J. D., . . . Borges, V. P. (2002). *Projeto Extremo Sul da Bahia*. Salvador: CPRM, CBPM.

Santiago, R., Caxito, F. A., Pedrosa-Soares, A., Neves, M. A., Calegari, S. S., & Lana, C. (2022). Detrital zircon U–Pb and Lu–Hf constraints on the age, provenance and tectonic setting of arc-related high-grade units of the transition zone of the Araçuaí and Ribeira orogens (SE Brazil). *Journal of South American Earth Sciences*, 103861.

Santos, E. J., Van Schmus, W. R., Kozuch, M., & de Brito Neves, B. B. (2010). The Cariris Velhos tectonic event in northeast Brazil. *Journal of South American Earth Sciences, 29*(1), 61-76.

Santos, M. M., Lana, C., Scholz, R., Kamo, S. L., Gerdes, A., Corfu, F., & Tapster, S. (2017). A new appraisal of Sri Lankan BB Zircon as reference material for LA- ICP-MS U-Pb geochronology and Lu-Hf isotope tracing. *Geostandards and Geoanalytical Research, 41*(3), 335–358.

Santos, L. C. M. L., Dantas, E. L., Cawood, P. A., Lages, G. D. A., Lima, H. M., Santos, E. J., & Caxito, F. A. (2019). Early to late Neoproterozoic subduction-accretion episodes in the Cariris Velhos Belt of the Borborema Province, Brazil: Insights from isotope and whole-rock geochemical data of supracrustal and granitic rocks. *Journal of South American Earth Sciences, 96,* 102384.

Santos, M. M., Lana, C., Scholz, R., Kamo, S. L., Gerdes, A., Corfu, F., & Tapster, S. (2017). A new appraisal of Sri Lankan BB Zircon as reference material for LA- ICP-MS U-Pb geochronology and Lu-Hf isotope tracing. *Geostandards and Geoanalytical Research, 41*(3), 335–358.

Santos, R.F., Alkmim, F.F., & Pedrosa-Soares, A.C. (2009). A Formação Salinas, Orógeno Araçuaí (MG): história deformacional e significado tectônico. *Revista Brasileira de Geociências, 39*, 81–100.

Schannor, M., Lana, C., & Fonseca, M.A. (2018). São Francisco-Congo break-up delimited by U-Pb-Hf isotopes and trace-elements of zircon from metasediments of the Araçuaí Belt. *Geoscience Frontiers, 10*, 611–628.

Serrano, P., Pedrosa-Soares, A. C., Medeiros-Júnior, E., Fonte-Boa, T., Araujo, C., Dussin, I., Queiroga, G., & Lana, C. (2018). A-type Medina batholith and post-collisional anatexis in the Araçuaí orogen (SE Brazil). *Lithos, 320*, 515-536.

Silva, L. C., Armstrong, R., Noce, C. M., Pimentel, M., Pedrosa-Soares, A. C., Leite, C., . . . Paes, V. C. (2002). Reavaliação U-Pb SHRIMP em terrenos pré-cambrianos brasileiros. Parte II: Orógeno Araçuaí, Cinturão Mineiro e Cráton São Francisco Meridional. *Revista Brasileira de Geociências, 32*(4), 513-528.

Silva, L. C., Pedrosa-Soares, A. C., Teixeira, L., & Armstrong, R. (2008). Tonian rift-related, A-type continental plutonism in the Araçuaí Orogen, eastern Brazil: New evidence for the breakup stage of the São Francisco Congo Paleocontinent. *Gondwana Research, 13*, 527-537.

Silva, L. C., Pedrosa-Soares, A. C., Armstrong, R., & Noce, C. M. (2011). Determinando a duração do período colisional do Orógeno Araçuaí com base em geocronologia U-Pb de alta resolução em zircão: uma contribuição para a história da amalgamação do Gondwana Ocidental. *Geonomos, 19*(2), 180-197.

Silva, L. C., Pedrosa-Soares, A. C., Armstrong, R., Pinto, C. P., Magalhães, J. T. R., Pinheiro, M. A. P., & Santos, G. G. (2016). Disclosing the Paleoarchean to Ediacaran history of the São Francisco craton basement: The Porteirinha domain (northern Araçuaí orogen, Brazil). *Journal of South American Earth Sciences, 68*, 50-67.

Silveira, E. M., Söderlund, U., Oliveira, E. P., Ernst, R. E., & Leal, A. M. (2013). First precise U–Pb baddeleyite ages of 1500 Ma mafic dykes from the São Francisco Craton, Brazil, and tectonic implications. *Lithos, 174*, 144-156.

Sláma, J., Košler, J., Condon, D. J., Crowley, J. L., Gerdes, A., Hanchar, J. M. . . . Whitehouse, M. J. (2008). Plešovice zircon—a new natural reference material for U–Pb and Hf isotopic microanalysis. *Chemical Geology, 249*(1-2), 1-35.

Söderlund, U., Patchett, J. P., Vervoort, J. D., & Isachsen, C. E. (2004). The 176 Lu decay constant determined by Lu–Hf and U–Pb isotope systematics of Precambrian mafic intrusions. *Earth and Planetary Science Letters, 219*, 311–324.

Souza, J. D. D., Melo, R. C. D., & Kosin, M. (2003). *Mapa geológico do estado da Bahia*. Salvador: CPRM.

Souza, M. E. S. (2016). *Caracterização litoestrutural e geocronológica dos xistos verdes e metagabros do grupo macaúbas na faixa terra branca-planalto de Minas, Minas Gerais* (Tese de Doutorado). Departamento de Geologia, Universidade Federal de Ouro Preto, Ouro Preto, MG, Brasil.

Souza, M. E., Martins, M., Queiroga, G., Leite, M., Oliveira, R. G., Dussin, I., & Pedrosa-Soares, A. C. (2019). Paleoenvironment, sediment provenance and tectonic setting of Tonian basal deposits of the Macaúbas basin system, Araçuaí orogen, southeast Brazil. *Journal of South American Earth Sciences, 96*, 102393.

Souza, M. E., Martins, M., Queiroga, G., Pedrosa-Soares, A., Dussin, I., de Castro, M. P., & Serrano, P. (2022). Time and isotopic constraints for Early Tonian basaltic magmatism in a large igneous province of the São Francisco–Congo paleocontinent (Macaúbas basin, Southeast Brazil). *Precambrian Research,* 106621.

Stacey, J. T., & Kramers, I. (1975). Approximation of terrestrial lead isotope evolution by a two-stage model. *Earth and planetary science letters, 26*(2), 207-221.

Straathof, G.B. (2011). *Neoproterozoic Low Latitude Glaciations: An African Perspective* (Tese de Doutorado). University of Edinburg, Scotland.

Tack, L., Wingate, M. T. D., Liégeois, J. P., Fernandez-Alonso, M., & Deblond, A., (2001). Early Neoproterozoic magmatism (1000-910 Ma) of the Zadinian and Mayumbian groups (Bas-Congo): Onset of Rodinian rifting at the western edge of the Congo craton. *Precambrian Research, 110*, 277-306.

Tassinari, C. C. G., Munhá, J. M., Ribeiro, A., & Correia, C. T. (2001). Neoproterozoic oceans in the Ribeira Belt (southeastern Brazil): the Pirapora do Bom Jesus ophiolitic complex. *Episodes, 24*(4), 245-251.

Tedeschi, M., Novo, T., Pedrosa-Soares, A. C., Dussin, I., Tassinari, C., Silva, L. C., . . . Heilbron, M. (2016). The Ediacaran Rio Doce magmatic arc revisited (Araçuaí-Ribeira orogenic system, SE Brazil). *Journal of South American Earth Sciences, 68*, 167-186.

Teixeira, W., Kamo, S. L., & Arcanjo, J. B. A. (1997). U-Pb zircon and baddeleyite age and tectonic interpretation of the Itabuna alkaline suite, São Francisco Cráton, Brazil. *Journal of South American Earth Sciences, 10*(1), 91-98.

Teixeira, W., Sabaté, P., Barbosa, J., Noce, C. M., & Carneiro, M. A. (2000). Archean and Paleoproterozoic tectonic evolution of the São Francisco craton, Brazil. In *Tectonic Evolution of South America* (Vol. 31, pp. 101-137). Rio de Janeiro: SBG.

Teixeira, W., Oliveira, E.P., & Marques, L.S. (2017). Nature and evolution of the Archean Crust of the São Francisco craton. In: Heilbron, M., Cordani, U.G., Alkmim, F.F. (Eds.), *São Francisco Craton, Eastern Brazil, Tectonic Genealogy of a Miniature Continent.* Springer International Publishing Co., pp. 29–56.

Thiéblemont, D., Castaing, C., Billa, M., Bouton, A., & Préat, A. (2009). *Notice explicative de la carte géologique et des ressources minérales de la République Gabonaise à 1/1000000*. Programme Sysmin 8 ACP GA 017, Ministère des Mines, du Pétrole, des Hydrocarbures. Direction Générale des Mines et de la Géologie (384 pp.).

Thiéblemont, D., Prian, J. P., Goujou, J. C., Boulingui, B., Ekogha, H., Kassadou, A. B., . . . Guerrot, C. (2011). Timing and characteristics of Neoproterozoic magmatism in SW-Gabon: First geochronogical and geochemical data on the West-Congolian orogen in Gabon (SYSMIN project, Gabon 2005-2009). In: *23 Colloquium of African Geology*, Posters and Abstracts.

Tupinambá, M., Heilbron, M., Valeriano, C., Júnior, R. P., Dios, F. B., Machado, N., Silva, L. G., & Almeida, J. C. H. (2012). Juvenile contribution of the Neoproterozoic Rio Negro magmatic arc (Ribeira Belt, Brazil): implications for western Gondwana amalgamation. *Gondwana Research, 21*(2-3), 422-438.

Uhlein, A., Egydio-Silva, M., Bouchez, J. L., & Vauchez, A. (1998a). The Rubim pluton (Minas Gerais, Brazil): a petrostructural and magnetic fabric study. *Journal of South American Earth Sciences, 11*(2), 179-189.

Uhlein, A., Trompette, R., & Egydio-Silva, M. (1998). Proterozoic rifting and closure, SE border of the São Francisco craton, Brazil. *Journal of South American Earth Sciences, 11*, 191–203.

Uhlein, G. J., Uhlein, A., Stevenson, R., Halverson, G. P., Caxito, F. A., & Cox, G. (2017). Early to late Ediacaran conglomeratic wedges from a complete foreland basin cycle in the southwest São Francisco Craton, Bambuí Group, Brazil. *Precambrian Research, 299,* 101–116.

Uhlein, G. J., Uhlein, A., Pereira, E., Caxito, F. A., Okubo, J., Warren, L., & Sial, A.N. (2019). Ediacaran paleoenvironmental changes recorded in the mixed carbonate-siliciclastic Bambuí Basin, Brazil. *Palaeogeogr. Palaeoclimatol. Palaeoecol. 517*, 39–51.

Van Achterbergh, E., Ryan, C. G., Jackson, S. E., & Griffin, W. L. (2001). Data reduction software for LA-ICP-MS: Appendix. *Laser Ablation-ICP Mass Spectrometry in the Earth Sciences: Principles and Applications*; Sylvester, PJ, Ed, 239-243.

Vicat, J. P., & Pouclet, A. (2000). Palaeo-and Neoproterozoic granitoids and rhyolites from the West Congolian Belt (Gabon, Congo, Cabinda, north Angola): chemical composition and geotectonic implications. *Journal of African Earth Sciences, 31*(3-4), 597-617.

Victoria, A. M. (2017). *A província anorogência toniana da região sul da Bahia, divisa nordeste com Minas Gerais: Novos dados para a bacia rifte precursora ao Orógeno*

Araçuaí-Oeste Congo (Dissertação de Mestrado) Universidade Federal da Bahia, Salvador, BA, Brasil.

Victoria, A. M., Pedrosa-Soares, A. C., & Cruz, S. C. P. (2019). Os riftes neoproterozóicos precursores ao Orógeno Araçuaí – Congo Ocidental: atualização dos limites de tempo com base em Idades (U-Pb e Pb-Pb) do magmatismo anorogênico. In: *Anais do XVII Simpósio de Nacional de Estudos Tectônicos*, Bento Gonçalves, RS, Brasil.

Vieira, V.S. (2007). *Significado do Grupo Rio Doce no Contexto do Orógeno Araçuaí* (Tese de Doutorado) Instituto de Geociências, Universidade Federal de Minas Gerais, Belo Horizonte, MG, Brasil.

Vilela, F. T., Pedrosa-Soares, A. C., Carvalho, M. T. N., Arimateia, R.., Santos, E., & Voll, E. (2014). Metalogênese da Faixa Araçuaí: O Distrito Ferrífero Nova Aurora (Grupo Macaúbas, Norte de Minas Gerais) no contexto dos recursos minerais do Orógeno Araçuaí. *Metalogênese das Províncias Tectônicas Brasileiras, Rio de Janeiro, Brazil*, 415-430.

Vilela, F. T., Pedrosa-Soares, A., Babinski, M., Lana, C., Trindade, R. F., & Santos, E. (2021). Diamictitic iron formation (DIF) deposits of the Neoproterozoic Nova Aurora iron district (Macaúbas Group, Southeast Brazil). *Journal of South American Earth Sciences*, 103614.

Wiedenbeck, M., Alle, P., Corfu, F., Griffin, W. L., Meier, M., Oberli, F. . . . Spiegel, W. (1995). 3 natural zircon standards for U-Th-Pb, Lu-Hf, traceelement and REE analyses. *Geostandards Newsletter, 19*, 1–23.

ANEXO A – SUPPLEMENTARY DATA

Supplementary Data 3.1. Results for the zircon standards used for instrumental calibration

Sample JK-01 - LA-MC-ICPMS/UERJ - reduction considering ratios from the GJ-1 standard, measured by TIMS - GJ-1 - Primary Ref. Mat.

	$^{207}Pb/^{206}Pb$	StDv	$^{206}Pb/^{238}U$	StDv	$^{232}Th/^{238}U$	StDv	$^{208}Pb/^{206}Pb$	StDv	U (cps)	Th (cps)	Th (ppm)	U238 (ppm)	^{206}Pb	^{207}Pb	^{208}Pb	^{204}Pb	*f* 206/204	Pb (cps)	Pb (in ppm)
Dating Campaign 02/02/2016																			
JK-1(I)-1st serie																			
002-GJ1 (1)	0,06012	0,00036	0,09882	0,0007	0,01753	0,0008	0,0055	0,0001	4137379	72233	6,3	317,3	457276	27501	2515	23	0,0009	487314	31,6
016-GJ1 (2)	0,06002	0,00040	0,09870	0,0007	0,01782	0,0011	0,0055	0,0002	3462996	61505	6,3	317,3	379665	22769	2087	16	0,0007	404536	31,6
JK-1(II)-2nd serie																			
002-GJ1 (3)	0,06000	0,00042	0,09791	0,0014	0,01782	0,0011	0,0055	0,0002	3462996	61505	6,3	317,3	379665	22769	2087	16	0,0007	404536	31,6
016-GJ1 (4)	0,06003	0,00042	0,09715	0,0009	0,01772	0,0010	0,0054	0,0002	3259289	57635	6,3	317,3	363138	21778	1981	12	0,0006	386909	31,6
JK-1(III)-3rd serie																			
002-GJ1 (5)	0,05997	0,00047	0,09646	0,0007	0,01772	0,0010	0,0054	0,0002	3259289	57635	6,3	317,3	363138	21778	1981	12	0,0006	386909	31,6
016-GJ1 (6)	0,06000	0,00038	0,09614	0,0011	0,01769	0,0009	0,0055	0,0001	3473816	61320	6,3	317,3	383186	22993	2114	17	0,0008	408310	31,6
JK-1(IV)-4th serie																			
002-GJ1 (7)	0,06002	0,00036	0,09602	0,0011	0,01769	0,0009	0,0055	0,0001	3473816	61320	6,3	317,3	383186	22993	2114	17	0,0008	408310	31,6
016-GJ1 (8)	0,06014	0,00044	0,09626	0,0012	0,01756	0,0011	0,0055	0,0001	3553934	61987	6,3	317,3	399461	24022	2190	16	0,0007	425689	31,6
JK-1(V)-5th serie																			
002-GJ1 (9)	0,06011	0,00043	0,09801	0,0013	0,01765	0,0011	0,0055	0,0001	3552924	62495	6,3	317,3	399459	24021	2190	12	0,0005	425681	31,6
016-GJ1 (10)	0,06001	0,00033	0,09810	0,0017	0,01749	0,0012	0,0055	0,0002	3468745	60357	6,3	317,3	392103	23541	2160	22	0,0010	417826	31,6
JK-1(VI)-6th serie																			
002-GJ1 (11)	0,06003	0,00035	0,09718	0,0015	0,01749	0,0012	0,0055	0,0002	3468745	60357	6,3	317,3	392103	23541	2160	22	0,0010	417826	31,6
016-GJ1 (12)	0,06007	0,00033	0,09704	0,0017	0,01764	0,0010	0,0055	0,0002	3492111	61279	6,3	317,3	389150	23372	2151	23	0,0010	414696	31,6

	$^{207}Pb/^{206}Pb$	StDv	$^{206}Pb/^{238}U$	StDv	$^{232}Th/^{238}U$	StDv	$^{208}Pb/^{206}Pb$	StDv	U (cps)	Th (cps)	Th (ppm)	U238 (ppm)	^{206}Pb	^{207}Pb	^{208}Pb	^{204}Pb	*f* 206/204	Pb (cps)	Pb (in ppm)
Dating Campaign 29/02/2016																			
JK-1(VII)-7th serie																			
GJ-1 (1)	0,06004	0,00038	0,09752	0,0008	0,01610	0,0013	0,0056	0,0002	3388001	54947	6,3	317,3	370575	22257	2064	27	0,0013	394923	31,6
GJ-1 (2)	0,06024	0,00043	0,09725	0,0011	0,01646	0,0013	0,0056	0,0001	3074802	50654	6,3	317,3	333439	20090	1873	17	0,0009	355420	31,6
JK-1(VIII)-8th serie																			
GJ-1 (3)	0,06027	0,00046	0,09598	0,0010	0,01646	0,0013	0,0056	0,0001	3074802	50654	6,3	317,3	333439	20090	1873	17	0,0009	355420	31,6
GJ-1 (4)	0,06051	0,00049	0,09579	0,0010	0,01725	0,0013	0,0056	0,0002	2421037	41551	6,3	317,3	251879	15255	1417	14	0,0010	268566	31,6
JK-1(IX)-9th serie																			
GJ-1 (5)	0,06053	0,00048	0,09411	0,0004	0,01773	0,0012	0,0055	0,0002	2828153	49822	6,3	317,3	297369	18014	1653	24	0,0014	317060	31,6
GJ-1 (6)	0,06052	0,00046	0,09490	0,0007	0,01723	0,0016	0,0052	0,0015	2496531	42726	6,3	317,3	261335	15780	1400	18	0,0012	278532	31,6
JK-1(X)-10th serie																			
GJ-1 (7)	0,06052	0,00046	0,09515	0,0006	0,01723	0,0016	0,0052	0,0015	2496531	42726	6,3	317,3	261335	15780	1400	18	0,0012	278532	31,6
GJ-1 (8)	0,06046	0,00042	0,09505	0,0007	0,01746	0,0016	0,0056	0,0002	2415001	41737	6,3	317,3	256324	15501	1428	15	0,0010	273267	31,6
JK-1(XI)-11th serie																			
GJ-1 (9)	0,06049	0,00044	0,09380	0,0008	0,01746	0,0016	0,0056	0,0002	2415001	41737	6,3	317,3	256324	15501	1428	15	0,0010	273267	31,6
GJ-1 (10)	0,06067	0,00044	0,09385	0,0004	0,01716	0,0015	0,0056	0,0001	2241977	38679	6,3	317,3	236222	14326	1320	18	0,0014	251886	31,6
JK-1(XII)-12th serie																			
GJ-1 (11)	0,06056	0,00060	0,09573	0,0012	0,01717	0,0016	0,0054	0,0010	2644409	45300	6,3	317,3	290062	17579	1562	27	0,0017	309231	31,6
GJ-1 (12)	0,06055	0,00051	0,09579	0,0010	0,01723	0,0020	0,0061	0,0028	2428387	41831	6,3	317,3	264185	16007	1514	23	0,0016	281729	31,6
JK-1(XIII)-13th serie																			
GJ-1 (13)	0,06052	0,00047	0,09579	0,0010	0,01723	0,0020	0,0061	0,0028	2428387	41831	6,3	317,3	264185	16007	1514	23	0,0016	281729	31,6
GJ-1 (14)	0,06053	0,00046	0,09572	0,0011	0,01738	0,0013	0,0056	0,0002	2479175	42849	6,3	317,3	271857	16449	1512	26	0,0017	289844	31,6

SD-3.1(cont.) - 91.500 - Secundary Ref. Mat.

	$^{207}Pb/^{206}Pb$	StDv	$^{206}Pb/^{238}U$	StDv	$^{232}Th/^{238}U$	StDv	$^{208}Pb/^{206}Pb$	StDv	U (cps)	Th (cps)	Th (ppm)	U238 (ppm)	^{206}Pb	^{207}Pb	^{208}Pb	^{204}Pb	*f* 206/204	Pb (cps)	Pb (in ppm)
Dating Campaign 02/02/2016																			
JK-1(I)-1st serie																			
91500 (1)	0,07534	0,00095	0,17189	0,00366	0,32500	0,00936	0,09856	0,00130	420719	136211	28,6	80,6	81763	6149	8065	22	0,0046	95999	14,8
JK-1(II)-2nd serie																			
91500 (2)	0,07468	0,00080	0,17655	0,00289	0,33075	0,00866	0,09715	0,00107	535750	176589	28,6	80,6	113727	8494	11052	14	0,0021	133288	14,8
JK-1(III)-3rd serie																			
91500 (3)	0,07477	0,00073	0,17441	0,00379	0,33005	0,00739	0,09753	0,00124	588356	193435	28,6	80,6	121259	9085	11835	15	0,0021	142194	14,8
JK-1(IV)-4th serie																			
91500 (4)	0,07468	0,00099	0,17486	0,00376	0,32354	0,00696	0,09743	0,00107	580406	187437	28,6	80,6	120965	9037	11787	14	0,0020	141803	14,8
JK-1(V)-5th serie																			
91500 (5)	0,07487	0,00094	0,17802	0,00296	0,32389	0,00804	0,09713	0,00096	579899	187096	28,6	80,6	121384	9105	11795	10	0,0014	142295	14,8
JK-1(VI)-6th serie																			
91500 (6)	0,07478	0,00086	0,17734	0,00331	0,32411	0,00731	0,09819	0,00246	613403	198423	28,6	80,6	127518	9551	12509	30	0,0040	149609	14,8

SD-3.1 (cont.)

	$^{207}Pb/^{206}Pb$	StDv	$^{206}Pb/^{238}U$	StDv	$^{232}Th/^{238}U$	StDv	$^{208}Pb/^{206}Pb$	StDv	U (cps)	Th (cps)	Th (ppm)	U238 (ppm)	^{206}Pb	^{207}Pb	^{208}Pb	^{204}Pb	*f* 206/204	Pb (cps)	Pb (in ppm)
Dating Campaign 29/02/2016																			
JK-1(VII)-7th serie																			
95100 (1)	0,07515	0,00091	0,17769	0,00110	0,30951	0,00682	0,09830	0,00127	531835	164334	28,6	80,6	102384	7695	10067	21	0,0035	120166	14,8
JK-1(VIII)-8th serie																			
95100 (2)	0,07527	0,00089	0,17324	0,00148	0,31591	0,01441	0,09863	0,00176	396281	125038	28,6	80,6	75210	5664	7421	12	0,0027	88307	14,8
JK-1(IX)-9th serie																			
95100 (3)	0,07534	0,00095	0,17189	0,00366	0,32500	0,00936	0,09856	0,00130	420719	136211	28,6	80,6	81763	6149	8065	22	0,0046	95999	14,8
JK-1(X)-10th serie																			
95100 (4)	0,07536	0,00106	0,17256	0,00274	0,31973	0,01011	0,09746	0,00581	408799	130201	28,6	80,6	78878	5905	7707	22	0,0048	92512	14,8
JK-1(XI)-11th serie																			
95100 (5)	0,07553	0,00084	0,17076	0,00265	0,32369	0,01226	0,09866	0,00116	386197	124158	28,6	80,6	75332	5706	7431	21	0,0047	88490	14,8
JK-1(XII)-12th serie																			
95100 (6)	0,07541	0,00117	0,17425	0,00405	0,32032	0,00860	0,09787	0,00361	425479	136026	28,6	80,6	87250	6546	8534	14	0,0028	102345	14,8
JK-1(XIII)-13th serie																			
95100 (7)	0,07543	0,00091	0,17450	0,00370	0,31773	0,01051	0,09855	0,00109	424398	134233	28,6	80,6	85878	6487	8466	19	0,0038	100850	14,8

SD-3.2						Isotope ratios[c]							Ages (Ma)								
Spot number		**Pb**	**Th**	**U**		$^{207}Pb/$	**1 s**	$^{206}Pb/$	**1 s**		$^{207}Pb/$	**1 s**	$^{206}Pb/$	**1 s**	$^{207}Pb/$	**1 s**	$^{207}Pb/$	**1 s**	**%**		
	f_{206}[a]	**ppm**	**ppm**	**ppm**	**Th/U**[b]	^{235}U	**[%]**	^{238}U	**[%]**	**Rho**[d]	^{206}Pb[e]	**[%]**	^{238}U	**abs**	^{235}U	**abs**	^{206}Pb	**abs**	**Disc.**	**Conc.Age**	**Error**
1,1	0,0005	54	64	147	0,43	5,3208	2,95	0,337010	2,79	0,95	0,114507	0,95	1872	52	1872	55	1872	18	0	1872	33
2,1	0,0045	3	26	23	1,13	0,8768	2,22	0,104292	1,33	0,60	0,060974	1,78	640	9	639	14	638	11	0	639	16
5,1	0,0016	19	65	113	0,58	1,3580	3,23	0,144833	3,03	0,94	0,068002	1,12	872	26	871	28	869	10	0	870	34
6,1	0,0037	9	66	73	0,90	0,8595	2,03	0,102656	1,48	0,73	0,060727	1,38	630	9	630	13	630	9	0	630	17
7,1	0,0028	11	37	93	0,39	0,9202	4,10	0,108200	3,71	0,90	0,061682	1,75	662	25	662	27	663	12	0	663	40
8,1	0,0023	18	15	38	0,39	11,0592	2,39	0,472707	1,61	0,67	0,169679	1,77	2495	40	2528	60	2554	45	2	2528	45
9,1	0,0005	66	222	549	0,41	0,9214	1,65	0,108322	1,43	0,87	0,061693	0,82	663	9	663	11	663	5	0	663	16
10,1	0,0011	47	413	323	1,28	0,9405	3,28	0,110100	3,09	0,94	0,061954	1,08	673	21	673	22	673	7	0	673	30
11,1	0,0009	38	84	263	0,32	1,4165	1,40	0,149173	1,13	0,81	0,068871	0,82	896	10	896	13	895	7	0	896	17
12,1	0,0019	23	248	154	1,62	0,9167	1,86	0,108169	1,48	0,79	0,061462	1,13	662	10	661	12	655	7	-1	661	17
13,1	0,0013	34	161	169	0,96	1,6894	2,64	0,168731	2,48	0,94	0,072616	0,90	1005	25	1005	27	1003	9	0	1004	29
14,1	0,0007	63	234	547	0,43	0,8876	2,21	0,105331	2,02	0,91	0,061114	0,92	646	13	645	14	643	6	0	645	21
15,1	0,0025	31	218	253	0,86	0,9724	1,90	0,112903	1,67	0,88	0,062466	0,92	690	11	690	13	690	6	0	690	19
16,1	0,0004	68	495	491	1,01	0,9026	1,86	0,106641	1,67	0,90	0,061383	0,81	653	11	653	12	653	5	0	653	18
17,1	0,0011	56	155	476	0,33	0,9702	1,60	0,112833	1,25	0,78	0,062361	0,99	689	9	689	11	687	7	0	689	15
18,1	0,0012	18	82	148	0,55	0,8877	2,14	0,105237	1,82	0,85	0,061181	1,14	645	12	645	14	646	7	0	645	20
19,1	0,0006	75	107	167	0,64	10,8321	2,37	0,472828	1,97	0,83	0,166153	1,31	2496	49	2509	59	2519	33	1	2514	39
20,1	0,0005	71	273	587	0,47	0,8917	2,95	0,105622	2,83	0,96	0,061231	0,84	647	18	647	19	647	5	0	647	25
21,1	0,0019	15	125	119	1,05	0,8500	1,59	0,101851	1,06	0,67	0,060530	1,19	625	7	625	10	623	7	0	625	12
22,1	0,0035	10	63	56	1,12	1,3738	3,03	0,145752	2,30	0,76	0,068361	1,98	877	20	878	27	880	17	0	878	34
23,1	0,0021	79	688	501	1,37	0,9306	2,47	0,109216	2,29	0,93	0,061799	0,93	668	15	668	16	667	6	0	668	23
24,1	0,0008	61	180	229	0,79	5,0992	1,74	0,328668	1,57	0,90	0,112523	0,74	1832	29	1836	32	1841	14	0	1839	24
25,1	0,0039	9	97	28	3,51	1,6540	1,35	0,165885	0,73	0,54	0,072316	1,14	989	7	991	13	995	11	1	990	13
26,1	0,0011	32	89	264	0,34	0,9614	1,89	0,111812	1,58	0,83	0,062361	1,05	683	11	684	13	686	7	0	684	19

27,1	0,0004	57	71	103	0,69	11,8251	2,19	0,496183	2,05	0,93	0,172847	0,79	2597	53	2591	57	2585	20	0	2586	26
28,1	0,0013	15	53	85	0,63	1,5887	2,55	0,161869	2,21	0,87	0,071185	1,27	967	21	966	25	963	12	0	966	32
29,1	0,0019	23	127	193	0,66	0,9117	2,27	0,107575	1,65	0,73	0,061466	1,57	659	11	658	15	656	10	0	658	20
30,1	0,0011	19	65	179	0,36	0,9006	2,98	0,106546	2,59	0,87	0,061306	1,48	653	17	652	19	650	10	0	652	29
31,1	0,0035	22	58	153	0,38	1,6022	3,36	0,162790	2,78	0,83	0,071384	1,88	972	27	971	33	968	18	0	971	42
32,1	0,0009	29	60	165	0,36	1,4865	1,21	0,154504	0,82	0,68	0,069778	0,89	926	8	925	11	922	8	0	926	13
33,1	0,0012	28	80	148	0,54	1,7357	2,61	0,171941	2,39	0,91	0,073214	1,06	1023	24	1022	27	1020	11	0	1021	31
35,1	0,0015	45	69	402	0,17	0,9640	2,13	0,112039	1,90	0,89	0,062405	0,96	685	13	685	15	688	7	0	685	21
36,1	0,0001	74	55	234	0,23	4,8992	1,78	0,321989	1,56	0,88	0,110354	0,85	1799	28	1802	32	1805	15	0	1804	26
37,1	0,0004	45	38	131	0,29	6,5832	2,47	0,375558	1,86	0,75	0,127133	1,63	2055	38	2057	51	2059	33	0	2057	43
38,1	0,0010	70	603	344	1,76	1,6465	1,89	0,165643	1,72	0,91	0,072092	0,79	988	17	988	19	989	8	0	988	23
39,1	0,0005	53	75	392	0,19	1,3688	2,53	0,145508	2,35	0,93	0,068227	0,94	876	21	876	22	875	8	0	876	27
41,1	0,0012	22	33	135	0,24	1,9318	3,61	0,184280	2,40	0,66	0,076030	2,70	1090	26	1092	39	1096	30	1	1091	44
42,1	0,0017	12	113	89	1,26	0,8985	1,91	0,106346	1,60	0,84	0,061275	1,05	651	10	651	12	649	7	0	651	18
43,1	0,0024	45	49	435	0,11	0,8747	2,60	0,103980	2,37	0,91	0,061010	1,07	638	15	638	17	640	7	0	638	24
44,1	0,0023	11	77	45	1,71	1,6283	1,84	0,164300	1,43	0,78	0,071878	1,16	981	14	981	18	982	11	0	981	23
45,1	0,0015	14	45	108	0,41	0,9997	1,79	0,115130	1,30	0,73	0,062975	1,23	702	9	704	13	707	9	1	703	16
46,1	0,0031	5	43	44	0,98	0,8524	2,54	0,102056	1,76	0,69	0,060577	1,83	626	11	626	16	624	11	0	626	20
47,1	0,0031	16	127	129	0,98	0,8222	2,80	0,099164	2,54	0,91	0,060133	1,18	610	15	609	17	608	7	0	609	26
48,1	0,0009	49	99	107	0,93	6,2165	2,90	0,366031	2,68	0,92	0,123176	1,12	2011	54	2007	58	2003	23	0	2004	37
49,1	0,0035	12	37	72	0,51	1,4169	1,84	0,149259	1,38	0,75	0,068849	1,23	897	12	896	17	894	11	0	896	21
50,1	0,0047	8	59	46	1,28	1,3071	2,70	0,140627	2,27	0,84	0,067412	1,47	848	19	849	23	851	12	0	849	31
51,1	0,0019	18	72	88	0,82	1,7264	1,34	0,171030	0,97	0,73	0,073209	0,91	1018	10	1018	14	1020	9	0	1018	16
52,1	0,0013	32	130	284	0,46	0,8611	2,38	0,102675	2,13	0,90	0,060823	1,05	630	13	631	15	633	7	0	631	22
53,1	0,0009	71	98	174	0,56	5,8965	1,67	0,355887	1,58	0,94	0,120166	0,55	1963	31	1961	33	1959	11	0	1959	19
54,1	0,0030	19	128	156	0,82	0,8334	4,25	0,100192	4,01	0,94	0,060327	1,41	616	25	615	26	615	9	0	615	37
55,1	0,0031	8	30	88	0,34	1,0184	3,55	0,116824	2,97	0,84	0,063223	1,94	712	21	713	25	716	14	0	713	36

56,1	0,0036	15	51	38	1,35	5,2565	4,24	0,334037	4,14	0,98	0,114131	0,89	1858	77	1862	79	1866	17	0	1866	32
57,1	0,0033	4	51	36	1,42	0,8910	4,64	0,105578	4,04	0,87	0,061207	2,27	647	26	647	30	647	15	0	647	44
58,1	0,0036	12	103	127	0,81	0,9936	2,09	0,115036	1,64	0,78	0,062641	1,30	702	12	701	15	696	9	-1	701	20
59,1	0,0047	5	15	15	1,02	5,3338	3,88	0,336888	3,48	0,90	0,114829	1,71	1872	65	1874	73	1877	32	0	1876	54
60,1	0,0027	3	25	37	0,67	0,9716	2,03	0,112679	1,02	0,50	0,062538	1,76	688	7	689	14	693	12	1	688	13
61,1	0,0029	3	16	12	1,42	5,1440	3,44	0,328507	2,54	0,74	0,113568	2,33	1831	46	1843	63	1857	43	1	1844	59
63,1	0,0028	7	38	64	0,59	0,9388	4,01	0,109868	3,71	0,92	0,061974	1,54	672	25	672	27	673	10	0	672	38
64,1	0,0045	12	23	78	0,30	1,5532	2,20	0,159316	1,42	0,65	0,070707	1,68	953	14	952	21	949	16	0	952	24
65,1	0,0025	6	24	69	0,35	0,9313	5,46	0,109268	4,91	0,90	0,061816	2,38	668	33	668	36	668	16	0	668	53
66,1	0,0021	13	106	105	1,01	0,9212	4,97	0,108414	4,67	0,94	0,061626	1,71	664	31	663	33	661	11	0	663	46
67,1	0,0035	5	15	39	0,40	1,5427	3,24	0,158355	2,78	0,86	0,070657	1,65	948	26	948	31	948	16	0	948	40
68,1	0,0042	10	17	26	0,68	5,9367	1,53	0,355503	1,01	0,66	0,121115	1,15	1961	20	1967	30	1973	23	1	1966	26
69,1	0,0026	8	29	68	0,42	0,9997	3,99	0,115234	3,54	0,89	0,062921	1,83	703	25	704	28	706	13	0	704	40
70,1	0,0019	31	60	108	0,56	5,0083	4,20	0,325849	3,99	0,95	0,111474	1,33	1818	72	1821	77	1824	24	0	1823	45
71,1	0,0031	9	18	61	0,30	1,2719	5,81	0,137703	5,69	0,98	0,066989	1,18	832	47	833	48	837	10	1	836	43
72,1	0,0014	33	85	74	1,15	5,3955	1,25	0,339494	1,02	0,82	0,115265	0,72	1884	19	1884	24	1884	14	0	1884	21
73,1	0,0028	18	49	94	0,52	2,1975	2,29	0,201280	1,93	0,84	0,079181	1,23	1182	23	1180	27	1177	14	0	1180	32
74,1	0,0044	6	14	58	0,24	0,9100	3,32	0,107315	2,65	0,80	0,061504	1,99	657	17	657	22	657	13	0	657	31
75,1	0,0049	8	52	72	0,73	0,9540	6,85	0,111212	6,65	0,97	0,062217	1,63	680	45	680	47	682	11	0	681	54
76,1	0,0042	3	14	14	0,97	1,7899	2,77	0,176253	2,14	0,77	0,073651	1,76	1046	22	1042	29	1032	18	-1	1043	36
77,1	0,0048	5	27	47	0,58	0,9107	3,01	0,107247	2,38	0,79	0,061584	1,83	657	16	657	20	660	12	0	657	28
78,1	0,0030	9	81	81	1,00	0,9104	3,26	0,107399	2,66	0,82	0,061477	1,89	658	18	657	21	656	12	0	657	31
79,1	0,0035	19	30	61	0,50	5,5341	3,11	0,344694	2,71	0,87	0,116442	1,53	1909	52	1906	59	1902	29	0	1904	47
80,1	0,0040	7	20	22	0,93	4,5431	2,23	0,310242	1,58	0,71	0,106207	1,57	1742	28	1739	39	1735	27	0	1739	37
81,1	0,0018	32	50	90	0,55	6,4047	1,32	0,371811	1,15	0,87	0,124933	0,65	2038	24	2033	27	2028	13	0	2030	20
82,1	0,0025	26	56	74	0,76	6,1574	3,81	0,363501	3,57	0,94	0,122855	1,32	1999	71	1998	76	1998	26	0	1998	44
83,1	0,0033	7	6	18	0,37	7,5127	3,01	0,399008	2,86	0,95	0,136557	0,91	2164	62	2175	65	2184	20	1	2182	31

84,1	0,0022	22	18	93	0,19	3,0643	3,56	0,247722	3,45	0,97	0,089715	0,86	1427	49	1424	51	1419	12	-1	1420	31
85,1	0,0027	18	91	180	0,51	0,9820	3,07	0,113799	2,69	0,87	0,062583	1,49	695	19	695	21	694	10	0	695	31
86,1	0,0042	8	16	23	0,70	4,7250	3,22	0,315653	2,71	0,84	0,108565	1,74	1768	48	1772	57	1775	31	0	1773	51
87,1	0,0030	34	88	378	0,23	1,0028	3,04	0,115510	2,86	0,94	0,062965	1,03	705	20	705	21	707	7	0	706	29
88,1	0,0043	7	26	38	0,67	1,7919	1,48	0,175332	0,75	0,51	0,074124	1,27	1041	8	1043	15	1045	13	0	1042	14
89,1	0,0042	14	41	95	0,43	1,4789	2,46	0,153479	1,45	0,59	0,069886	1,99	920	13	922	23	925	18	0	921	24
90,1	0,0042	4	16	22	0,72	2,1050	2,95	0,195264	2,08	0,70	0,078186	2,09	1150	24	1150	34	1152	24	0	1150	39
91,1	0,0041	4	15	26	0,59	1,6970	3,41	0,169206	2,78	0,82	0,072738	1,97	1008	28	1007	34	1007	20	0	1007	44
92,1	0,0043	6	11	45	0,25	1,5155	2,83	0,156577	1,87	0,66	0,070200	2,13	938	18	937	27	934	20	0	937	31
93,1	0,0038	5	30	48	0,63	0,9377	3,42	0,109814	2,67	0,78	0,061932	2,14	672	18	672	23	672	14	0	672	32
94,1	0,0031	6	5	22	0,23	5,3306	3,28	0,337873	2,74	0,83	0,114425	1,81	1876	51	1874	62	1871	34	0	1873	53
95,1	0,0047	4	10	10	1,00	5,3693	3,71	0,339213	3,28	0,88	0,114800	1,75	1883	62	1880	70	1877	33	0	1878	54
96,1	0,0047	8	34	82	0,41	0,8908	4,09	0,105493	3,80	0,93	0,061245	1,52	647	25	647	26	648	10	0	647	38
98,1	0,0031	4	7	8	0,92	14,0620	3,29	0,534782	2,84	0,86	0,190708	1,67	2762	78	2754	91	2748	46	0	2750	51
99,1	0,0010	45	110	311	0,35	1,6358	1,81	0,164966	1,55	0,86	0,071918	0,94	984	15	984	18	984	9	0	984	23
100,1	0,0016	7	30	47	0,64	1,3199	2,80	0,141865	1,39	0,50	0,067476	2,43	855	12	854	24	852	21	0	855	22
101,1	0,0043	13	49	117	0,42	0,9472	2,57	0,110560	1,96	0,77	0,062135	1,65	676	13	677	17	679	11	0	676	24
102,1	0,0017	13	35	72	0,49	1,6567	2,24	0,166575	1,73	0,77	0,072132	1,43	993	17	992	22	990	14	0	992	28
103,1	0,0030	7	59	60	0,98	0,9067	2,57	0,107209	1,63	0,64	0,061339	1,98	657	11	655	17	651	13	-1	656	20
104,1	0,0029	12	14	51	0,28	9,0590	3,64	0,432192	2,82	0,78	0,152020	2,29	2316	65	2344	85	2369	54	2	2351	64
105,1	0,0042	7	26	41	0,62	1,5157	3,03	0,156756	1,63	0,54	0,070128	2,55	939	15	937	28	932	24	-1	938	27
106,1	0,0038	8	43	72	0,60	1,0253	2,37	0,117561	1,20	0,51	0,063254	2,04	717	9	717	17	717	15	0	717	16
107,1	0,0021	5	12	27	0,43	1,7918	3,47	0,175550	2,78	0,80	0,074027	2,08	1043	29	1042	36	1042	22	0	1042	45
108,1	0,0022	27	386	151	2,56	0,8750	1,84	0,104197	1,35	0,74	0,060904	1,24	639	9	638	12	636	8	0	639	16
109,1	0,0008	98	196	789	0,25	0,9564	2,72	0,111375	2,55	0,94	0,062279	0,96	681	17	681	19	684	7	0	682	26
110,1	0,0015	56	402	429	0,94	0,8949	1,77	0,105966	1,29	0,73	0,061249	1,21	649	8	649	11	648	8	0	649	15
111,1	0,0007	67	380	469	0,81	0,9416	1,35	0,110025	1,02	0,76	0,062072	0,88	673	7	674	9	677	6	1	673	12

112,1	0,0009	49	128	389	0,33	0,9519	1,99	0,111031	1,71	0,86	0,062176	1,01	679	12	679	14	680	7	0	679	20
113,1	0,0043	7	62	55	1,13	0,8894	2,73	0,105325	1,61	0,59	0,061244	2,21	646	10	646	18	648	14	0	646	19
114,1	0,0014	60	193	512	0,38	0,9313	1,95	0,109020	1,73	0,89	0,061957	0,90	667	12	668	13	673	6	1	668	19
115,1	0,0006	80	375	418	0,90	1,4931	1,10	0,154736	0,69	0,63	0,069982	0,86	927	6	928	10	928	8	0	927	11
116,1	0,0017	40	436	280	1,56	0,8276	1,70	0,099699	1,04	0,61	0,060208	1,35	613	6	612	10	611	8	0	613	12

SD-3.3

Spot number	$^{176}Lu/^{177}Hf$ [a]	±2s	$^{176}Hf/^{177}Hf$	±2s [c]	age [f] (Ma)	±2s	$^{176}Hf/^{177}Hf_{(t)}$ [d]	eHf(t) [d]	±2s [c]	TDM (Hf) (Ga)
1,1	0,000437	2,72	0,281178	19,88	1872	33	0,281162	-15,20	3,70	2,8
2,1	0,000553	3,50	0,282164	16,83	639	16	0,282157	-7,95	1,81	1,5
5,1	0,001338	11,51	0,282297	14,40	870	34	0,282275	1,42	0,42	1,3
6,1	0,001402	9,43	0,282166	15,41	630	17	0,282150	-8,42	2,32	1,5
7,1	0,000699	4,86	0,282092	16,80	663	40	0,282084	-10,02	2,77	1,6
8,1	0,000779	4,89	0,281257	22,62	2528	45	0,281219	2,07	0,60	2,7
9,1	0,00125	7,59	0,281955	16,59	683	16	0,281939	-14,69	3,90	1,8
10,1	0,001156	12,36	0,282063	15,58	673	30	0,282049	-11,03	3,57	1,7
11,1	0,000791	5,40	0,281809	15,68	896	17	0,281795	-14,99	3,44	2,0
12,1	0,002072	13,40	0,282081	23,26	661	17	0,282056	-11,05	4,34	1,7
13,1	0,00073	5,05	0,281740	20,94	1004	29	0,281727	-14,98	4,33	2,1
14,1	0,000923	11,11	0,282124	21,24	645	21	0,282113	-9,39	3,34	1,6
15,1	0,001216	7,97	0,282124	29,13	690	19	0,282109	-8,53	3,40	1,6
16,1	0,002346	20,01	0,282271	18,65	653	18	0,282242	-4,63	1,92	1,4
17,1	0,001292	8,49	0,282022	20,58	689	15	0,282005	-12,21	3,81	1,7
18,1	0,001225	7,62	0,282292	17,97	645	20	0,282277	-3,57	1,02	1,3
19,1	0,000682	4,24	0,281056	14,13	2514	19	0,281024	-5,22	1,00	3,0
20,1	0,001497	11,63	0,282140	25,62	647	25	0,282122	-9,03	3,71	1,6
21,1	0,001198	8,43	0,282224	20,42	625	12	0,282210	-6,40	1,97	1,4
22,1	0,000394	5,14	0,281790	22,96	878	34	0,281784	-15,80	5,05	2,0
23,1	0,001475	16,11	0,282273	25,32	668	23	0,282254	-3,86	1,73	1,4
24,1	0,000493	8,84	0,281126	21,45	1839	24	0,281109	-17,83	5,63	2,9
25,1	0,001138	8,60	0,281961	19,34	940	13	0,281941	-8,84	2,59	1,8
26,1	0,001043	10,58	0,282326	81,66	684	19	0,282313	-1,42	1,35	1,3
27,1	0,000659	4,45	0,281057	28,84	2586	26	0,281024	-3,51	1,20	3,0
28,1	0,000409	3,15	0,281986	46,76	966	32	0,281979	-6,89	3,67	1,7
29,1	0,000964	7,73	0,282172	25,88	658	20	0,282160	-7,44	2,73	1,5
30,1	0,000541	3,36	0,282188	17,28	652	29	0,282181	-6,81	1,71	1,5
31,1	0,00083	5,44	0,281877	21,70	971	42	0,281862	-10,93	3,44	1,9
32,1	0,001304	9,94	0,281975	22,70	926	13	0,281952	-8,74	2,97	1,8
33,1	0,000601	3,77	0,282035	35,42	1621	31	0,282016	9,36	3,85	1,7
35,1	0,000791	8,53	0,282362	17,74	685	2	0,282352	-0,02	0,01	1,2
36,1	0,000657	5,11	0,281689	19,76	1804	26	0,281666	1,14	0,30	2,1
37,1	0,000703	5,30	0,281484	25,61	2057	43	0,281457	-0,46	0,15	2,4
38,1	0,00075	12,24	0,282029	19,03	988	23	0,282015	-5,12	1,72	1,7
39,1	0,001223	14,80	0,282236	26,54	876	27	0,282216	-0,53	0,23	1,4
41,1	0,000873	5,95	0,281946	25,34	1091	44	0,281928	-5,88	2,08	1,8
42,1	0,00117	14,05	0,282230	24,21	651	18	0,282215	-5,63	2,31	1,4
43,1	0,000898	7,75	0,282204	16,74	638	24	0,282193	-6,70	1,89	1,5
45,1	0,000526	3,43	0,282286	21,07	703	16	0,282279	-2,20	0,59	1,3
46,1	0,00075	5,50	0,282154	16,77	626	20	0,282145	-8,66	2,21	1,5
47,1	0,0014	10,04	0,282151	27,65	609	26	0,282135	-9,41	3,95	1,6

48,1	0,000533	3,42	0,281606	30,35	2004	37	0,281585	2,89	1,03	2,3
49,1	0,001233	8,30	0,282217	25,44	896	21	0,282196	-0,78	0,28	1,5
50,1	0,000657	4,80	0,281804	27,52	849	31	0,281793	-16,13	5,80	2,0
51,1	0,000623	4,87	0,281713	25,47	1018	16	0,281701	-15,57	4,97	2,1
52,1	0,00101	8,05	0,282154	18,76	631	22	0,282142	-8,67	2,63	1,5
53,1	0,00092	5,72	0,281528	15,13	1959	19	0,281494	-1,41	0,31	2,4
54,1	0,000873	5,31	0,282204	16,37	615	37	0,282194	-7,19	1,99	1,5
55,1	0,000655	4,12	0,282359	14,09	713	36	0,282350	0,56	0,13	1,2
56,1	0,001091	6,55	0,281445	19,76	1836	32	0,281407	-7,32	2,05	2,5
57,1	0,001685	10,14	0,282096	23,07	647	44	0,282075	-10,67	4,27	1,6
58,1	0,000563	3,39	0,282046	19,63	701	20	0,282039	-10,76	2,78	1,7
60,1	0,001358	8,18	0,282252	16,18	688	13	0,282235	-4,11	1,08	1,4
61,1	0,001237	7,48	0,281224	14,72	1844	59	0,281180	-15,19	3,86	2,8
63,1	0,000763	4,61	0,282184	24,11	672	38	0,282174	-6,62	2,27	1,5
65,1	0,002222	13,35	0,282483	18,21	668	53	0,282455	3,24	1,28	1,1
66,1	0,001755	12,06	0,282046	16,44	663	46	0,282024	-12,12	4,29	1,7
67,1	0,001435	8,61	0,282155	18,16	948	40	0,282129	-1,98	0,61	1,5
68,1	0,00058	5,42	0,281438	19,64	1966	26	0,281416	-4,01	1,06	2,5
69,1	0,000638	6,21	0,282373	28,58	704	40	0,282365	0,86	0,35	1,2
70,1	0,000479	3,35	0,281622	386,74	1823	45	0,281606	-0,58	2,26	2,2
71,1	0,001629	11,39	0,281995	25,18	836	43	0,281969	-10,18	4,25	1,8
72,1	0,000625	3,99	0,281470	14,89	1884	21	0,281447	-4,79	0,96	2,4
73,1	0,000681	4,17	0,281847	26,03	1180	32	0,281832	-7,26	2,39	1,9
74,1	0,00103	6,49	0,282076	17,87	657	31	0,282063	-10,89	3,17	1,6
75,1	0,000739	6,68	0,282109	408,14	681	54	0,282099	-9,07	38,32	1,6
77,1	0,000864	9,96	0,282403	228,14	657	28	0,282392	0,78	1,89	1,2
78,1	0,001054	8,11	0,282132	18,52	657	31	0,282119	-8,88	2,78	1,6
79,1	0,000569	4,77	0,281486	19,24	1984	47	0,281465	-1,85	0,49	2,4
80,1	0,000855	5,61	0,281673	25,03	1739	37	0,281644	-1,13	0,37	2,2
81,1	0,000627	3,91	0,281214	21,46	2030	20	0,281190	-10,57	2,78	2,8
82,1	0,001037	11,37	0,281384	23,49	1998	44	0,281344	-5,82	2,16	2,6
83,1	0,000562	3,41	0,281440	19,80	2182	31	0,281416	1,01	0,25	2,5
84,1	0,001122	16,40	0,282087	20,94	1420	31	0,282057	6,19	2,45	1,6
85,1	0,001837	15,33	0,282288	23,98	695	31	0,282264	-2,90	1,27	1,4
86,1	0,000833	7,73	0,281691	18,78	1773	51	0,281663	0,32	0,09	2,2
87,1	0,001181	7,76	0,282222	20,60	706	29	0,282206	-4,70	1,53	1,4
88,1	0,001615	10,10	0,282044	24,61	1042	14	0,282012	-4,00	1,44	1,7
89,1	0,000621	3,93	0,282183	19,84	921	24	0,282172	-1,05	0,28	1,5
90,1	0,000666	4,10	0,282143	21,75	1150	39	0,282128	2,57	0,75	1,5
92,1	0,000948	5,69	0,282202	27,31	937	31	0,282185	-0,23	0,08	1,5
93,1	0,00125	7,61	0,282109	22,43	672	32	0,282093	-9,47	3,30	1,6
94,1	0,000543	3,32	0,281407	21,38	1873	53	0,281388	-7,16	1,97	2,5
95,1	0,000897	5,39	0,281528	23,13	1878	54	0,281496	-3,19	1,00	2,4
96,1	0,000519	3,34	0,282139	31,17	647	38	0,282132	-8,66	3,50	1,5
97,1	0,000681	4,46	0,282279	21,78	650	20	0,282270	-3,70	1,09	1,3

98,1	0,000473	2,89	0,281032	17,21	2750	51	0,281007	-0,29	0,06	3,0
99,1	0,001574	9,58	0,282049	20,30	984	23	0,282020	-5,05	1,63	1,7
100,1	0,001476	8,92	0,282532	29,51	855	22	0,282509	9,37	3,84	1,0
101,1	0,000702	4,29	0,282147	30,95	676	24	0,282138	-7,79	3,02	1,5
102,1	0,000767	4,69	0,282105	29,86	992	28	0,282091	-2,35	0,88	1,6
103,1	0,001099	6,63	0,282125	19,24	656	20	0,282111	-9,19	2,66	1,6
104,1	0,000759	3,29	0,281200	18,46	2351	64	0,281166	-3,97	0,97	2,8
105,1	0,000776	4,92	0,281940	30,30	938	27	0,281926	-9,39	3,58	1,8
106,1	0,001578	17,83	0,282147	22,05	717	16	0,282126	-7,32	3,08	1,6
107,1	0,001107	6,71	0,282066	18,39	1042	45	0,282044	-2,86	0,84	1,7
108,1	0,002064	12,81	0,282223	20,35	639	16	0,282198	-6,50	2,32	1,5
109,1	0,001454	9,25	0,282324	25,61	682	26	0,282305	-1,74	0,67	1,3
110,1	0,0016	9,83	0,282088	26,54	649	15	0,282069	-10,86	4,20	1,6
111,1	0,001364	8,38	0,282074	25,44	673	12	0,282057	-10,75	3,83	1,7
112,1	0,00093	5,94	0,282292	29,46	679	20	0,282280	-2,69	1,03	1,3
113,1	0,000839	5,08	0,282182	18,20	646	19	0,282172	-7,28	1,91	1,5
114,1	0,000981	5,89	0,282483	19,35	668	19	0,282471	3,82	1,07	1,1
115,1	0,002445	17,44	0,282142	18,93	927	11	0,282099	-3,53	1,32	1,6
116,1	0,00109	7,48	0,282356	25,99	613	12	0,282343	-1,95	0,69	1,3

SD-4.1a				Isotope ratios[c]							Ages (Ma)								
Spot number		**U**		**^{207}Pb/**	**2 s**	**^{206}Pb/**	**2 s**		**^{207}Pb/**	**2 s**	**^{206}Pb/**	**2 s**	**^{207}Pb/**	**2 s**	**^{207}Pb/**	**2 s**	**%**		
	f_{206}[a]	**ppm**	**Th/U[b]**	**^{235}U**	**[%]**	**^{238}U**	**[%]**	**Rho[d]**	**^{206}Pb[e]**	**[%]**	**^{238}U**	**abs**	**^{235}U**	**abs**	**^{206}Pb**	**abs**	**Conc.**	**Conc.Age**	**Error**
DF4-007	0,124	135	0,78	1,4796	2,83	0,155804	1,81	0,64	0,068874	2,18	933	16	922	17	895	45	101,54	933	16
DF4-008	0,010	275	0,77	1,5305	2,73	0,159364	1,81	0,66	0,069653	2,04	953	16	943	17	918	42	101,43	942	16
DF4-009	0,000	51	0,61	2,1627	2,86	0,200273	1,84	0,64	0,078320	2,20	1177	20	1169	20	1155	44	101,02	1160	40
DF4-010	0,025	70	0,70	3,4317	3,14	0,265864	1,82	0,58	0,093617	2,56	1520	25	1512	25	1500	48	100,95	1549	40
~~DF4-012~~	~~1,000~~	~~144~~	~~0,98~~	~~2,0773~~	~~4,62~~	~~0,194399~~	~~2,10~~	~~0,46~~	~~0,077499~~	~~4,11~~	~~1145~~	~~22~~	~~1141~~	~~32~~	~~1134~~	~~82~~	~~100,69~~	~~1154~~	~~46~~
DF4-013	0,000	334	0,82	1,5777	2,72	0,161025	1,78	0,65	0,071060	2,05	962	16	961	17	959	42	100,42	953	16
DF4-014	0,000	246	0,73	2,0988	2,72	0,195131	1,79	0,66	0,078010	2,05	1149	19	1148	19	1147	41	100,42	1134	82
~~DF4-015~~	~~1,000~~	~~197~~	~~0,79~~	~~3,0237~~	~~3,73~~	~~0,245217~~	~~1,92~~	~~0,52~~	~~0,089430~~	~~3,19~~	~~1414~~	~~25~~	~~1414~~	~~29~~	~~1413~~	~~61~~	~~100,41~~	~~1463~~	~~58~~
DF4-016	0,000	53	0,86	1,4114	3,48	0,148853	1,86	0,54	0,068770	2,94	895	16	894	21	892	61	100,39	895	16
DF4-017	0,017	181	1,84	1,5496	2,76	0,158949	1,80	0,65	0,070708	2,09	951	16	950	17	949	43	100,38	951	16
DF4-018	0,004	489	0,62	1,5926	2,71	0,161935	1,83	0,68	0,071327	1,99	968	17	967	17	967	41	100,34	958	17
DF4-019	0,033	361	0,82	5,1242	2,70	0,329902	1,76	0,65	0,112653	2,04	1838	28	1840	23	1843	37	100,34	1851	49
~~DF4-020~~	~~1,000~~	~~304~~	~~1,72~~	~~0,8299~~	~~4,95~~	~~0,099944~~	~~2,69~~	~~0,54~~	~~0,060226~~	~~4,15~~	~~614~~	~~16~~	~~614~~	~~23~~	~~612~~	~~90~~	~~100,31~~	~~614~~	~~16~~
DF4-027	0,351	80	0,88	6,8416	3,19	0,382272	1,92	0,60	0,129803	2,55	2087	35	2091	29	2095	45	100,28	2095	45
DF4-028	0,000	122	0,76	2,2946	3,53	0,206345	1,81	0,51	0,080650	3,03	1209	20	1211	25	1213	60	100,26	1213	60
~~DF4-029~~	~~1,000~~	~~128~~	~~1,02~~	~~2,1440~~	~~4,08~~	~~0,197514~~	~~2,20~~	~~0,54~~	~~0,078725~~	~~3,43~~	~~1162~~	~~24~~	~~1163~~	~~29~~	~~1165~~	~~68~~	~~100,26~~	~~1155~~	~~44~~
DF4-030	0,032	381	0,58	2,1270	2,70	0,196476	1,77	0,66	0,078515	2,04	1156	19	1158	19	1160	40	100,25	1165	68
DF4-031	0,077	123	0,38	2,9941	2,93	0,243308	1,93	0,66	0,089251	2,20	1404	25	1406	23	1410	42	100,24	1401	41
DF4-032	0,000	101	0,68	5,2359	2,73	0,333284	1,79	0,66	0,113940	2,05	1854	29	1858	24	1863	37	100,23	1863	37
DF4-033	0,098	83	1,04	6,4813	2,73	0,371870	1,78	0,65	0,126406	2,08	2038	31	2043	24	2049	37	100,23	2028	39
DF4-036	0,034	414	0,92	7,0120	2,79	0,386663	1,73	0,62	0,131525	2,19	2107	31	2113	25	2118	38	100,22	2118	38
DF4-037	0,000	51	1,08	5,4144	3,02	0,339079	1,94	0,64	0,115810	2,31	1882	32	1887	26	1893	42	100,20	1900	37
DF4-038	0,070	44	1,56	11,0000	2,86	0,477114	1,75	0,61	0,167214	2,26	2515	37	2523	27	2530	38	100,18	2530	38
DF4-039	0,000	59	1,18	4,3450	2,95	0,301216	1,78	0,60	0,104620	2,35	1697	27	1702	25	1708	43	100,17	1778	38
DF4-040	0,000	92	1,42	2,2646	2,80	0,204357	1,75	0,62	0,080370	2,19	1199	19	1201	20	1206	43	100,15	1206	43
DF4-047	0,041	96	1,23	5,1646	2,75	0,330535	1,80	0,65	0,113323	2,08	1841	29	1847	24	1853	38	100,14	1853	38
DF4-048	0,045	248	0,52	2,7315	2,87	0,229791	1,86	0,65	0,086212	2,18	1333	23	1337	22	1343	42	100,12	1355	40
DF4-049	0,021	328	0,52	6,2129	2,69	0,363553	1,76	0,65	0,123944	2,03	1999	31	2006	24	2014	36	100,11	2033	36
DF4-050	0,000	73	1,84	6,3112	2,81	0,366332	1,73	0,62	0,124950	2,21	2012	30	2020	25	2028	39	100,08	2043	36
DF4-051	0,000	312	0,62	1,6731	2,73	0,167067	1,79	0,65	0,072630	2,07	996	17	998	18	1004	42	100,08	973	16
DF4-052	0,022	286	0,71	25,6411	2,69	0,672967	1,76	0,66	0,276339	2,03	3317	46	3333	27	3342	32	100,08	3342	32
DF4-053	0,000	19	0,95	4,3640	3,08	0,301493	1,86	0,60	0,104980	2,46	1699	28	1706	26	1714	45	100,04	1710	52
~~DF4-054~~	~~1,000~~	~~157~~	~~1,33~~	~~5,7028~~	~~3,26~~	~~0,347662~~	~~1,90~~	~~0,58~~	~~0,118968~~	~~2,65~~	~~1923~~	~~32~~	~~1932~~	~~29~~	~~1941~~	~~47~~	~~100,03~~	~~1943~~	~~39~~
DF4-056	0,072	82	0,55	11,8713	3,06	0,492520	1,79	0,58	0,174813	2,48	2582	39	2594	29	2604	41	100,03	2604	41

DF4-057	0,000	108	0,67	2,9416	2,74	0,240094	1,75	0,64	0,088860	2,12	1387	22	1393	21	1401	41	100,00	1457	39
DF4-059	0,286	83	1,89	1,6224	3,41	0,163419	2,05	0,60	0,072004	2,73	976	19	979	22	986	56	100,00	962	16
DF4-067	0,000	81	0,89	5,4368	2,74	0,338990	1,80	0,66	0,116320	2,06	1882	30	1891	24	1900	37	99,99	1893	42
~~DF4-068~~	~~1,000~~	~~89~~	~~1,25~~	~~5,1276~~	~~3,31~~	~~0,328597~~	~~1,89~~	~~0,57~~	~~0,113176~~	~~2,72~~	~~1832~~	~~30~~	~~1841~~	~~29~~	~~1851~~	~~49~~	~~99,96~~	~~1843~~	~~37~~
DF4-069	0,038	129	1,57	5,1969	2,78	0,330931	1,83	0,66	0,113896	2,09	1843	30	1852	24	1862	38	99,96	1862	38
DF4-072	0,096	75	1,22	6,4494	2,83	0,369684	1,74	0,61	0,126528	2,23	2028	31	2039	25	2050	39	99,93	2050	39
DF4-074	0,051	303	0,60	17,6704	2,80	0,581270	1,76	0,63	0,220479	2,18	2954	42	2972	27	2984	35	99,93	2984	35
DF4-075	0,018	557	0,73	1,1051	2,81	0,123943	1,71	0,61	0,064669	2,23	753	12	756	15	764	47	99,92	753	12
~~DF4-076~~	~~1,000~~	~~50~~	~~1,33~~	~~4,3451~~	~~3,52~~	~~0,300257~~	~~1,88~~	~~0,53~~	~~0,104956~~	~~2,98~~	~~1693~~	~~28~~	~~1702~~	~~30~~	~~1714~~	~~55~~	~~99,89~~	~~1759~~	~~37~~
DF4-077	0,149	69	1,40	4,6558	2,96	0,311737	1,79	0,60	0,108318	2,36	1749	28	1759	25	1771	43	99,87	1714	45
DF4-078	0,000	169	0,65	2,4117	2,84	0,212070	1,93	0,68	0,082480	2,09	1240	22	1246	21	1257	41	99,87	1257	41
DF4-079	0,021	263	0,92	5,6786	2,76	0,345704	1,70	0,62	0,119135	2,17	1914	29	1928	24	1943	39	99,74	1956	41
DF4-080	0,000	441	0,59	1,6230	2,69	0,162924	1,74	0,65	0,072250	2,05	973	16	979	17	993	42	99,69	968	17
DF4-087	0,102	70	1,59	4,6971	2,84	0,312400	1,91	0,67	0,109049	2,10	1753	30	1767	24	1784	38	99,64	1784	38
DF4-088	0,000	101	0,91	5,7969	2,90	0,348730	1,76	0,61	0,120560	2,31	1929	30	1946	25	1965	41	99,57	1965	41
DF4-091	0,000	105	1,47	5,7227	2,89	0,345843	1,74	0,60	0,120010	2,30	1915	29	1935	25	1956	41	99,43	1941	47
DF4-093	0,000	138	0,69	3,5049	2,76	0,264569	1,73	0,63	0,096080	2,14	1513	24	1528	22	1549	40	99,43	1565	40
DF4-094	0,000	244	0,73	6,2435	2,70	0,361447	1,79	0,66	0,125280	2,03	1989	31	2011	24	2033	36	99,40	2053	36
DF4-095	0,000	57	1,65	4,2680	3,40	0,295510	1,92	0,56	0,104750	2,81	1669	29	1687	28	1710	52	99,36	1745	45
DF4-096	0,187	130	1,21	4,9063	2,99	0,318620	2,06	0,69	0,111681	2,17	1783	32	1803	26	1827	39	99,32	1827	39
DF4-098	0,000	119	2,07	6,3015	2,74	0,362663	1,81	0,66	0,126020	2,06	1995	31	2019	24	2043	36	99,29	2014	36
DF4-099	0,000	193	0,35	2,7018	2,72	0,225855	1,73	0,64	0,086760	2,10	1313	21	1329	20	1355	40	99,17	1343	42
DF4-100	0,016	259	0,25	6,3497	2,76	0,363336	1,83	0,66	0,126750	2,07	1998	32	2025	25	2053	36	99,12	2049	37
DF4-107	0,000	302	1,07	2,0342	3,00	0,188446	1,93	0,64	0,078290	2,30	1113	20	1127	21	1154	46	99,10	1147	41
DF4-111	0,115	75	1,14	3,5431	2,78	0,265172	1,80	0,65	0,096908	2,12	1516	25	1537	22	1565	40	99,07	1500	48
~~DF4-112~~	~~1,000~~	~~376~~	~~0,66~~	~~3,0481~~	~~3,60~~	~~0,240866~~	~~1,92~~	~~0,53~~	~~0,091782~~	~~3,05~~	~~1391~~	~~24~~	~~1420~~	~~28~~	~~1463~~	~~58~~	~~98,39~~	~~1413~~	~~61~~
DF4-113	0,045	76	0,53	4,3285	3,03	0,294076	1,77	0,58	0,106752	2,46	1662	26	1699	25	1745	45	98,26	1714	55
DF4-116	0,128	201	0,55	2,9940	2,82	0,237336	1,91	0,68	0,091493	2,07	1373	24	1406	22	1457	39	98,03	1410	42
DF4-119	0,000	248	1,57	4,3734	2,88	0,294758	2,03	0,70	0,107610	2,04	1665	30	1707	24	1759	37	97,97	1708	43
DF4-120	0,261	76	0,59	1,6347	3,04	0,160244	1,93	0,63	0,073986	2,35	958	17	984	19	1041	47	97,72	976	19
~~DF4-131~~	~~1,000~~	~~339~~	~~0,76~~	~~1,7563~~	~~3,97~~	~~0,167947~~	~~2,08~~	~~0,53~~	~~0,075844~~	~~3,38~~	~~1001~~	~~20~~	~~1029~~	~~26~~	~~1091~~	~~68~~	~~97,54~~	~~1091~~	~~68~~
DF4-138	0,000	194	1,44	4,3655	2,71	0,291218	1,72	0,63	0,108720	2,10	1648	25	1706	23	1778	38	97,02	1771	43
DF4-140	0,122	76	1,53	1,6105	2,89	0,157357	1,83	0,63	0,074230	2,23	942	16	974	18	1048	45	97,00	996	17

SD-4.1b				Isotope ratios[c]							Ages (Ma)								
Spot number		**U**		**^{207}Pb/**	**2 s**	**^{206}Pb/**	**2 s**		**^{207}Pb/**	**2 s**	**^{206}Pb/**	**2 s**	**^{207}Pb/**	**2 s**	**^{207}Pb/**	**2 s**	**%**		
	f_{206}[a]	**ppm**	**Th/U[b]**	**^{235}U**	**[%]**	**^{238}U**	**[%]**	**Rho[d]**	**^{206}Pb[e]**	**[%]**	**^{238}U**	**abs**	**^{235}U**	**abs**	**^{206}Pb**	**abs**	**Conc.**	**Conc.Age**	**Error**
DF18-287	0	20,339	2,39469	1,6315	3,335	0,16820	1,996	0,5984	0,07035	2,672	1002	18	982	21	939	54,8	101,860	939	55
DF18-288	0	163,22	0,92009	1,7082	2,912	0,17320	1,961	0,67347	0,07153	2,153	1030	19	1012	19	973	43,9	101,640	973	44
~~DF18-289~~	~~1,31505~~	~~27,353~~	~~1,82966~~	~~12,5270~~	~~3,478~~	~~0,51580~~	~~2,17~~	~~0,62393~~	~~0,17614~~	~~2,718~~	~~2681~~	~~48~~	~~2645~~	~~33~~	~~2617~~	~~45,2~~	~~101,144~~	~~2617~~	~~45~~
DF18-290	0	24,35	1,11520	1,5944	3,522	0,16417	2,045	0,5806	0,07044	2,868	980	19	968	22	941	58,8	101,079	980	19
DF18-291	0	158,45	1,41215	6,9321	2,932	0,39086	1,893	0,64557	0,12863	2,239	2127	34	2103	26	2079	39,4	100,922	2079	39
DF18-292	0,25662	68,197	1,21053	1,5290	3,263	0,15905	2,073	0,63536	0,06972	2,52	951	18	942	20	920	51,8	100,856	951	18
DF18-293	0	95,662	1,06408	12,6385	2,825	0,51557	1,911	0,67628	0,17779	2,081	2680	42	2653	27	2632	34,6	100,789	2632	35
DF18-294	0	48,1	1,02069	5,3575	3,035	0,34207	1,951	0,64295	0,11359	2,324	1897	32	1878	26	1858	42	100,776	1858	42
DF18-295	0	175,61	0,68048	2,8922	2,956	0,24119	1,992	0,67377	0,08697	2,185	1393	25	1380	23	1360	42,1	100,760	1360	42
DF18-296	0,08022	123,2	0,59849	1,6439	3,018	0,16709	1,975	0,65457	0,07135	2,282	996	18	987	19	968	46,6	100,751	996	18
DF18-297	0	61,873	0,69507	3,5806	3,025	0,27338	1,971	0,65147	0,09499	2,295	1558	27	1545	24	1528	43,2	100,630	1528	43
DF18-298	0	94,11	1,50730	1,7037	3,13	0,17088	2,035	0,65012	0,07231	2,379	1017	19	1010	20	995	48,3	100,547	995	48
DF18-299	0	272,19	0,69805	1,6984	3,007	0,17042	2,005	0,66679	0,07228	2,241	1014	19	1008	19	994	45,6	100,495	994	46
DF18-300	0	72,872	1,17329	1,8027	3,113	0,17742	2,028	0,65156	0,07369	2,361	1053	20	1046	20	1033	47,7	100,463	1033	48
DF18-307	0,03538	118,63	1,07424	12,6629	2,798	0,51383	1,964	0,70206	0,17874	1,992	2673	43	2655	27	2641	33,1	100,441	2641	33
~~DF18-308~~	~~1~~	~~425,42~~	~~1,14955~~	~~1,6822~~	~~4,159~~	~~0,16920~~	~~2,272~~	~~0,54624~~	~~0,07211~~	~~3,484~~	~~1008~~	~~21~~	~~1002~~	~~27~~	~~989~~	~~70,9~~	~~100,441~~	~~989~~	~~71~~
DF18-309	0,07243	326,29	0,33240	3,6599	2,837	0,27624	1,922	0,67744	0,09609	2,087	1572	27	1563	23	1550	39,2	100,429	1550	39
DF18-310	0,07537	206,01	0,67324	1,7605	2,888	0,17452	1,937	0,67072	0,07316	2,142	1037	19	1031	19	1019	43,4	100,422	1019	43
DF18-311	0,03939	469,16	0,27316	1,8221	3,038	0,17863	2,015	0,66328	0,07398	2,273	1059	20	1053	20	1041	45,9	100,420	1041	46
DF18-312	0	77,708	0,69558	1,6594	2,988	0,16745	1,993	0,66696	0,07187	2,226	998	18	993	19	982	45,3	100,349	998	18
DF18-313	0	145,52	1,17480	5,3768	2,834	0,34097	1,904	0,67202	0,11437	2,098	1891	31	1881	25	1870	37,9	100,329	1870	38
DF18-314	0	132,87	1,04963	6,6590	3,154	0,38046	2,071	0,65662	0,12694	2,379	2078	37	2067	28	2056	42	100,324	2056	42
DF18-315	0,15024	51,823	0,42994	3,5222	3,233	0,26981	2,059	0,63705	0,09468	2,492	1540	28	1532	26	1522	47	100,308	1522	47
DF18-316	0	113,38	0,77451	1,6717	3,04	0,16821	1,984	0,65266	0,07208	2,303	1002	18	998	19	988	46,9	100,292	988	47
DF18-317	0,04585	148,22	2,03481	6,9662	3,008	0,38894	2,031	0,67536	0,12990	2,218	2118	37	2107	27	2097	39	100,291	2097	39
DF18-318	0,04442	163,86	1,82418	6,4905	2,831	0,37543	1,976	0,69803	0,12538	2,027	2055	35	2045	25	2034	35,9	100,286	2034	36
DF18-319	0,02227	181,17	0,93150	12,6180	2,945	0,51191	2,026	0,68807	0,17877	2,137	2665	44	2652	28	2641	35,5	100,260	2641	35
DF18-320	0,07247	62,205	0,53125	1,5493	3,097	0,15950	1,93	0,62331	0,07045	2,422	954	17	950	19	941	49,6	100,255	954	17
DF18-327	0,14571	54,104	0,38655	2,2640	3,123	0,20576	2,047	0,65534	0,07980	2,359	1206	22	1201	22	1192	46,6	100,251	1192	47
DF18-328	0,02025	442,09	0,57502	1,7286	2,937	0,17204	2,01	0,68438	0,07288	2,141	1023	19	1019	19	1010	43,4	100,250	1010	43
DF18-329	0,08161	130,07	1,46028	6,4386	2,898	0,37373	2,012	0,69443	0,12495	2,085	2047	35	2038	26	2028	36,9	100,243	2028	37
DF18-330	0,15275	157,71	0,99131	5,3209	2,827	0,33868	1,979	0,69996	0,11395	2,019	1880	32	1872	24	1863	36,4	100,221	1863	36
DF18-331	0	90,787	0,55838	11,8060	2,942	0,49675	1,975	0,67114	0,17237	2,181	2600	42	2589	28	2581	36,4	100,176	2581	36
DF18-332	0	98,902	0,82772	12,8218	2,913	0,51479	1,992	0,68369	0,18064	2,126	2677	44	2667	28	2659	35,2	100,152	2659	35

DF18-333	0	126,65	1,19493	6,6338	2,818	0,37896	1,968	0,69847	0,12696	2,016	2071	35	2064	25	2056	35,6	100,148	2056	36
DF18-334	0,06425	63,093	1,88419	7,2312	3,029	0,39548	2,028	0,66972	0,13261	2,249	2148	37	2140	27	2133	39,4	100,143	2133	39
DF18-335	0	163,43	2,30671	6,8265	2,955	0,38437	2,019	0,68312	0,12881	2,158	2097	36	2089	26	2082	38	100,138	2082	38
DF18-336	0	63,226	0,84670	2,3830	3,597	0,21232	1,988	0,55275	0,08140	2,998	1241	22	1238	26	1231	58,8	100,127	1231	59
~~DF18-337~~	~~1~~	~~119,96~~	~~0,70171~~	~~6,6432~~	~~3,357~~	~~0,37911~~	~~2,053~~	~~0,61145~~	~~0,12709~~	~~2,657~~	~~2072~~	~~36~~	~~2065~~	~~30~~	~~2058~~	~~46,9~~	~~100,121~~	~~2058~~	~~47~~
DF18-338	0	209,1	0,20507	2,9520	2,875	0,24242	1,982	0,68925	0,08832	2,083	1399	25	1395	22	1389	40	100,096	1389	40
DF18-339	0,07909	190,4	0,72030	5,3390	2,812	0,33878	1,977	0,703	0,11430	2	1881	32	1875	24	1869	36,1	100,091	1869	36
DF18-340	0	79,216	1,62821	5,8387	3,027	0,35493	1,892	0,62486	0,11931	2,364	1958	32	1952	27	1946	42,3	100,089	1946	42
DF18-347	0,01583	73,925	1,32795	7,8048	3,052	0,41013	1,985	0,65036	0,13802	2,319	2216	37	2209	28	2202	40,3	100,082	2202	40
DF18-348	0,09601	185,56	0,41770	3,1678	2,996	0,25283	1,997	0,66666	0,09087	2,233	1453	26	1449	23	1444	42,5	100,069	1444	43
DF18-349	0	8,6763	0,00000	1,8459	4,828	0,17950	2,363	0,48943	0,07458	4,21	1064	23	1062	32	1057	84,8	100,064	1057	85
DF18-350	0,04797	226,32	0,83783	6,7642	2,795	0,38223	1,972	0,70567	0,12835	1,98	2087	35	2081	25	2075	34,9	100,051	2075	35
~~DF18-351~~	~~1~~	~~360,9~~	~~1,15979~~	~~1,8560~~	~~4,08~~	~~0,18014~~	~~2,24~~	~~0,54887~~	~~0,07473~~	~~3,411~~	~~1068~~	~~22~~	~~1066~~	~~27~~	~~1061~~	~~68,6~~	~~100,048~~	~~1061~~	~~69~~
DF18-352	0	40,579	1,46520	7,0077	3,148	0,38892	2,052	0,65181	0,13068	2,388	2118	37	2112	28	2107	41,9	100,036	2107	42
DF18-353	0	249,19	0,93403	3,6992	2,937	0,27670	1,983	0,67536	0,09696	2,166	1575	28	1571	24	1566	40,6	100,031	1566	41
DF18-354	0,08115	366,7	1,84897	1,7134	2,923	0,17056	1,947	0,66615	0,07286	2,18	1015	18	1014	19	1010	44,2	100,010	1010	44
DF18-355	0	123,51	0,80272	12,8000	3,021	0,51344	2,02	0,66885	0,18081	2,245	2671	44	2665	29	2660	37,2	99,996	2660	37
DF18-356	0,01235	263,17	0,26206	10,7974	2,799	0,47640	1,975	0,70559	0,16438	1,983	2512	41	2506	26	2501	33,4	99,994	2501	33
~~DF18-357~~	~~1~~	~~87,714~~	~~0,64279~~	~~1,7031~~	~~4,402~~	~~0,16982~~	~~2,386~~	~~0,54203~~	~~0,07274~~	~~3,699~~	~~1011~~	~~22~~	~~1010~~	~~29~~	~~1007~~	~~75~~	~~99,990~~	~~1007~~	~~75~~
DF18-358	0,32456	55,285	0,75447	2,2970	3,838	0,20706	2,14	0,55753	0,08046	3,186	1213	24	1211	27	1208	62,7	99,977	1208	63
DF18-359	0	87,131	1,66986	1,7986	2,955	0,17621	1,985	0,67187	0,07403	2,188	1046	19	1045	19	1042	44,2	99,970	1042	44
DF18-360	0,05367	320,75	0,63284	5,3008	2,886	0,33689	1,993	0,69057	0,11412	2,088	1872	32	1869	25	1866	37,7	99,934	1866	38
DF18-367	0	143,78	0,91164	5,1337	2,855	0,33102	1,955	0,6849	0,11248	2,08	1843	31	1842	25	1840	37,7	99,879	1840	38
~~DF18-368~~	~~1~~	~~105,42~~	~~1,02679~~	~~18,4371~~	~~3,061~~	~~0,59665~~	~~1,897~~	~~0,61959~~	~~0,22412~~	~~2,403~~	~~3016~~	~~46~~	~~3013~~	~~30~~	~~3010~~	~~38,6~~	~~99,871~~	~~3010~~	~~39~~
DF18-369	0	56,304	0,93302	1,5248	3	0,15706	1,958	0,65281	0,07041	2,272	940	17	940	19	940	46,6	99,861	940	17
DF18-370	0	79,102	0,76575	10,8672	2,912	0,47632	1,908	0,65515	0,16547	2,2	2511	40	2512	27	2512	37	99,741	2512	37
DF18-371	0,00832	196,65	1,65728	1,9221	2,871	0,18376	1,947	0,67835	0,07586	2,109	1087	19	1089	19	1091	42,2	99,721	1091	42
DF18-372	0	58,366	0,93496	9,3523	3,18	0,44431	1,945	0,6118	0,15266	2,515	2370	39	2373	30	2376	42,9	99,634	2376	43
DF18-373	0	235,11	1,04796	10,8173	2,886	0,47462	1,961	0,6795	0,16530	2,117	2504	41	2508	27	2511	35,6	99,616	2511	36
DF18-374	0,06094	130,85	0,62765	5,9291	2,915	0,35531	2,02	0,69307	0,12103	2,101	1960	34	1966	26	1971	37,4	99,501	1971	37
DF18-375	0	110,61	0,94620	1,5652	3,198	0,15930	2,032	0,63528	0,07126	2,47	953	18	957	20	965	50,4	99,477	953	18
DF18-376	0,13273	163,87	0,92742	10,6519	3,242	0,46998	2,05	0,63226	0,16438	2,512	2483	42	2493	31	2501	42,3	99,375	2501	42
DF18-377	0	53,718	0,90833	5,9488	2,945	0,35510	1,913	0,64973	0,12150	2,239	1959	32	1968	26	1978	39,9	99,305	1978	40
DF18-378	0,00856	225,9	0,40588	9,3902	2,952	0,44291	1,911	0,64729	0,15377	2,25	2364	38	2377	27	2388	38,3	99,214	2388	38
DF18-379	0,04673	183,81	1,55025	5,8965	3,244	0,35113	2,01	0,61952	0,12179	2,546	1940	34	1961	29	1983	45,3	98,731	1983	45
DF18-380	0	267,96	1,01818	1,2237	3,088	0,13238	1,959	0,63443	0,06704	2,387	801	15	811	17	839	49,7	98,640	801	15
DF18-387	0,03073	429,73	1,26930	1,6190	2,924	0,15822	1,881	0,64334	0,07422	2,238	947	17	978	18	1047	45,1	96,711	947	17
DF18-388	0,05864	262,55	1,00628	11,6141	2,831	0,46756	1,935	0,68358	0,18015	2,066	2473	40	2574	27	2654	34,3	95,849	2654	34
~~DF18-389~~	~~1~~	~~120,05~~	~~1,00259~~	~~5,6078~~	~~3,344~~	~~0,32757~~	~~2,034~~	~~0,6082~~	~~0,12416~~	~~2,655~~	~~1827~~	~~32~~	~~1917~~	~~29~~	~~2017~~	~~47,1~~	~~95,064~~	~~2017~~	~~47~~

DF18-390	0,02665	301,25	1,14360	4,6130	2,838	0,29263	1,91	0,67286	0,11433	2,1	1655	28	1752	24	1869	37,9	94,270	1869	38
DF18-391	0,047	265,42	0,52583	14,4906	2,799	0,48741	1,906	0,68076	0,21562	2,05	2559	40	2782	27	2948	33,1	91,761	2948	33
DF18-392	0,02232	230,15	1,17921	5,1632	2,816	0,30027	1,875	0,66573	0,12471	2,101	1693	28	1847	24	2025	37,2	91,468	2025	37

SD-4.1c	Ratios[c]							Age (Ma)						% Disc.[f]		
Spot number	$^{207}Pb^*/^{235}U$	±	$^{206}Pb^*/^{238}U$	±	Rho 1[d]	$^{207}Pb^*/^{206}Pb^*$	±	$^{206}Pb/^{238}U$	±	$^{207}Pb/^{235}U$	±	$^{207}Pb/^{206}Pb$	±		*f*-206[a]	$^{232}Th/^{238}U$[b]
~~**DF10-27**~~	~~**7,532760205**~~	~~**2,7740844 7**~~	~~**0,34365**~~	~~**1,3431686 18**~~	~~**0,4841844 7**~~	~~**0,158977813**~~	~~**2,4272294 3**~~	~~**1904**~~	~~**22**~~	~~**2177**~~	~~**25**~~	~~**2445**~~	~~**41**~~	~~**114**~~	~~**1,000000**~~	~~**0,393013308**~~
DF10-28	1,557638771	2,6366143 82	0,1571	1,2221514 96	0,4635306 19	0,07191	2,3362536 5	941	11	954	16	983	48	101	0,000000	0,377539436
~~**DF10-29**~~	~~**2,976790608**~~	~~**3,3771476 16**~~	~~**0,24055**~~	~~**1,4644701 69**~~	~~**0,4336411 48**~~	~~**0,089751487**~~	~~**3,0430992 67**~~	~~**1390**~~	~~**18**~~	~~**1402**~~	~~**26**~~	~~**1420**~~	~~**58**~~	~~**101**~~	~~**1,000000**~~	~~**0,232752116**~~
DF10-30	1,582695491	3,4754309 18	0,15724	1,5762893 21	0,4535521 95	0,073001714	3,0974073 1	941	14	963	22	1014	63	102	0,745461	1,060023043
~~**DF10-31**~~	~~2,254290166~~	~~2,4399606 88~~	~~0,20023~~	~~1,2289870 72~~	~~0,5036913 41~~	~~0,081654363~~	~~2,1078422 47~~	~~1177~~	~~13~~	~~1198~~	~~17~~	~~1237~~	~~41~~	~~102~~	~~0,031387~~	~~0,468268064~~
~~**DF10-32**~~	~~**5,356384177**~~	~~**2,9625969 59**~~	~~**0,31762**~~	~~**1,3631442 98**~~	~~**0,4601180 38**~~	~~**0,122310179**~~	~~**2,6303646 82**~~	~~**1778**~~	~~**21**~~	~~**1878**~~	~~**26**~~	~~**1990**~~	~~**47**~~	~~**106**~~	~~**1,000000**~~	~~**0,195388127**~~
DF10-33	1,524234514	2,6764226 22	0,15665	1,2767315 67	0,4770291 35	0,07057	2,3522743 38	938	11	940	17	945	48	100	0,000000	0,607184093
~~**DF10-34**~~	~~**12,78181221**~~	~~**5,6596213 58**~~	~~**0,19136**~~	~~**3,4698996 66**~~	~~**0,6130974 93**~~	~~**0,48444**~~	~~**4,4711419 37**~~	~~**1129**~~	~~**36**~~	~~**2664**~~	~~**55**~~	~~**4195**~~	~~**66**~~	~~**236**~~	~~**0,000000**~~	~~**0,049642804**~~
DF10-35	1,542773945	2,4862578 67	0,15582	1,2578633 88	0,5059263 58	0,071808825	2,1445880 44	934	11	948	15	981	44	102	0,001636	0,347161051
DF10-36	4,177163726	2,4941130 36	0,28114	1,2591591 38	0,5048524 74	0,10776	2,1529324 42	1597	18	1670	21	1762	39	105	0,000000	0,703505713
~~**DF10-37**~~	~~**2,356449415**~~	~~**2,4803739 93**~~	~~**0,15762**~~	~~**1,2195783 3**~~	~~**0,4916913 07**~~	~~**0,108429018**~~	~~**2,1598342 17**~~	~~**944**~~	~~**11**~~	~~**1230**~~	~~**18**~~	~~**1773**~~	~~**39**~~	~~**130**~~	~~**0,046997**~~	~~**0,184878652**~~
~~**DF10-38**~~	~~**4,975386491**~~	~~**2,4340280 88**~~	~~**0,28473**~~	~~**1,2297822 77**~~	~~**0,5052457 21**~~	~~**0,12673376**~~	~~**2,1005066 73**~~	~~**1615**~~	~~**18**~~	~~**1815**~~	~~**21**~~	~~**2053**~~	~~**37**~~	~~**112**~~	~~**0,052240**~~	~~**0,301806744**~~
~~**DF10-39**~~	~~**18,44621862**~~	~~**6,3830396 49**~~	~~**0,25539**~~	~~**5,2186758 93**~~	~~**0,8175847 53**~~	~~**0,523844259**~~	~~**3,6754070 63**~~	~~**1466**~~	~~**69**~~	~~**3013**~~	~~**63**~~	~~**4310**~~	~~**54**~~	~~**206**~~	~~**6,205146**~~	~~**0,040341123**~~
~~**DF10-40**~~	~~**2,05324608**~~	~~**2,6777762 2**~~	~~**0,158**~~	~~**1,3362063 83**~~	~~**0,4989985 25**~~	~~**0,094250278**~~	~~**2,3205684 62**~~	~~**946**~~	~~**12**~~	~~**1133**~~	~~**18**~~	~~**1513**~~	~~**44**~~	~~**120**~~	~~**0,338080**~~	~~**0,27663114**~~
DF10-47	3,97154026	2,5770433 78	0,26828	1,2995326 99	0,5042727 3	0,107366649	2,2253915 02	1532	18	1628	21	1755	41	106	0,105463	0,346987441
DF10-48	1,570185837	3,1608566 03	0,15672	1,4723961 69	0,4658218 81	0,072665013	2,7969740 76	939	13	958	20	1005	57	102	0,431607	0,572205803
~~**DF10-49**~~	~~**12,96802726**~~	~~**11,938989 96**~~	~~**0,19764**~~	~~**10,730179 89**~~	~~**0,8987510 6**~~	~~**0,475880375**~~	~~**5,2347608 31**~~	~~**1163**~~	~~**11 5**~~	~~**2677**~~	~~**11 9**~~	~~**4168**~~	~~**77**~~	~~**230**~~	~~**10,468021**~~	~~**0,266267335**~~
~~**DF10-51**~~	~~**7,368699399**~~	~~**2,5905668 69**~~	~~**0,33745**~~	~~**1,3049081 28**~~	~~**0,5037152 85**~~	~~**0,158372631**~~	~~**2,2379123 03**~~	~~**1874**~~	~~**21**~~	~~**2157**~~	~~**23**~~	~~**2438**~~	~~**38**~~	~~**115**~~	~~**0,086662**~~	~~**0,378225339**~~
~~**DF10-52**~~	~~**0,880038538**~~	~~**4,6407490 17**~~	~~**0,10094**~~	~~**2,4299931 59**~~	~~**0,5236208 96**~~	~~**0,063232029**~~	~~**3,9536925 38**~~	~~**620**~~	~~**14**~~	~~**641**~~	~~**22**~~	~~**716**~~	~~**84**~~	~~**103**~~	~~**1,000000**~~	~~**0,354954322**~~
~~**DF10-53**~~	~~**12,92208433**~~	~~**6,8200373 73**~~	~~**0,19306**~~	~~**4,4390121 68**~~	~~**0,6508779 83**~~	~~**0,48544384**~~	~~**5,1776520 49**~~	~~**1138**~~	~~**46**~~	~~**2674**~~	~~**66**~~	~~**4198**~~	~~**77**~~	~~**235**~~	~~**2,671805**~~	~~**0,057832725**~~

DF10-54	37,84005034	44,57751007	0,37674	17,03406619	0,382122424	0,728465012	41,19459908	2061	308	3716	578	4788	590	180	10,729515	0,043724507
DF10-55	2,429356139	2,846302163	0,18181	1,395068975	0,490133828	0,096910792	2,480971293	1077	14	1251	21	1565	47	116	0,410243	0,100356008
DF10-56	1,938308177	3,446681434	0,15661	1,636573663	0,474825914	0,089763972	3,033354504	938	14	1094	23	1421	58	117	0,062378	0,234112572
DF10-57	11,93816806	3,951015734	0,18986	2,148951859	0,543898583	0,45604	3,315498664	1121	22	2600	38	4105	49	232	0,000000	0,120408506
DF10-58	19,57617665	7,625688845	0,2753	6,256544139	0,820456259	0,515727618	4,359677258	1568	88	3071	76	4287	64	196	8,191046	0,067430214
DF10-59	10,04114009	7,823940983	0,18537	5,774011845	0,737992766	0,392864061	5,279662841	1096	58	2439	75	3882	80	222	4,445186	0,066721354
DF10-60	13,83141313	6,889746751	0,19533	4,122423005	0,598341732	0,513566076	5,520347712	1150	44	2738	67	4281	81	238	1,000000	0,050161921
SD 4.1 c	-	-	Ratiose	-	-	-	-	-	-	Age (Ma)	-	-	-	%	-	-
Spot number	207Pb*/235U	±	206Pb*/238U	±	Rho 1d	207Pb*/206Pb*	±	206Pb/238U	±	207Pb/235U	±	207Pb/206Pb	±	Disc. f	f-206a	232Th/238Ub
DF26-67	0,6193582	4,5802753	0,07683	3,1917569	1,4350327	0,05852	4,5796309	477	15	489	18	549	100	115	0,0908069	37,375258
DF26-68	0,6185732	4,1315303	0,0772	3,172871	1,3021425	0,0581	4,130809	479	15	489	16	534	90	111	1	25,9862
DF26-69	8,651051944	4,038648993	0,41736	3,175269197	1,271907509	0,15036	4,017025805	2248	61	2302	37	2350	69	105	0,017382046	0,262657814
DF26-70	0,6177435	4,1809352	0,07681	3,1267562	1,3371478	0,05837	4,1802296	477	14	488	16	544	91	114	0,0691786	2,9234957
DF26-71	2,7196317	4,1084954	0,15991	3,2307884	1,2716696	0,12374	4,1053823	956	29	1334	31	2011	73	210	0,3165434	0,5084682
DF26-72	0,8308609	4,6043945	0,07914	3,1721029	1,4515275	0,07646	4,6037144	491	15	614	21	1107	92	224	0,4143637	27,566567
DF26-73	0,9535871	5,7320156	0,08026	4,1918199	1,3674289	0,08654	5,7314537	498	20	680	29	1350	111	270	0,4266692	0,6013903
DF26-74	0,9170504	4,553389419	0,10813	3,283085175	1,386923938	0,06151	4,552105349	662	21	661	22	657	98	99	0	0,003086803
DF26-75	0,898893713	4,518082706	0,10521	3,232909038	1,397528558	0,06199	4,516857558	645	20	651	22	674	97	104	0,039501992	0,001053079
DF26-76	0,5861974	4,1364544	0,0364	3,1912705	1,2961779	0,11798	4,1362943	230	7	468	16	1926	74	828	1,0005368	0,1805106
DF26-77	0,92095166	5,593640706	0,10859	3,453356663	1,619769185	0,06151	5,592586571	665	22	663	28	657	120	99	0	0,003303183
DF26-78	0,6176677	4,0592002	0,07702	3,1802566	1,2763751	0,05815	4,0584695	478	15	488	16	535	89	112	1	22,85738
DF26-79	0,6185981	4,2538275	0,07704	3,3141788	1,2835238	0,05831	4,2531298	478	15	489	17	541	93	113	0,1270287	27,94297
DF26-80	1,1606692	4,2997706	0,08177	3,189939	1,3479162	0,10328	4,298993	507	16	782	24	1684	79	331	0,3225381	0,3487603
DF26-87	6,380742889	5,038334208	0,36133	3,419917249	0,678779356	0,12815	5,025360905	1988	59	2030	45	2073	89	104	0,058160461	0,596319249

DF26-88	1,42056	4,2748919	0,08423	1,3327546	0,3117633	0,1226	4,274062	521	7	898	26	1994	76	382	0,2297572	0,4204204
DF26-89	0,7534741	4,3962982	0,0781	1,3848057	0,3149936	0,07007	4,3956044	485	6	570	19	930	90	191	0,141764	0,2331561
DF26-90	0,6396563	4,2752065	0,07754	1,3167674	0,3080009	0,05989	4,2745033	481	6	502	17	600	93	124	0,1000414	36,403249
DF26-91	0,6126119	4,1616006	0,07703	1,2981986	0,3119469	0,05768	4,1608877	478	6	485	16	518	91	108	0,0002346	3,3261596
DF26-92	0,888022222	6,063496755	0,10535	1,676777585	0,276536403	0,06136	6,062581486	646	10	645	29	652	130	100	0,367123677	0,550689599
DF26-93	3,0448853	4,564447	0,16811	1,4057244	0,3079725	0,13154	4,5613502	1002	13	1419	36	2119	80	211	0,1338555	0,5201954
DF26-94	1,301654	4,9853319	0,08291	1,4243019	0,2856985	0,11395	4,9846424	513	7	846	29	1863	90	363	0,0752606	0,0818115
DF26-95	5,4576933	4,1890901	0,29997	1,2949696	0,3091291	0,13211	4,1783362	1691	19	1894	37	2126	73	126	0,116365	0,5037347
DF26-96	0,617026	4,3017756	0,07762	1,3400031	0,3115	0,05766	4,3010753	482	6	488	17	517	94	107	0,010612	26,603324
DF26-97	3,517121	4,6090601	0,20699	1,2960541	0,281197	0,12336	4,6044099	1213	14	1531	37	2005	82	165	0,1007309	0,5741651
DF26-98	0,6189253	4,7658227	0,07745	1,3677209	0,2869853	0,05792	4,7651934	481	6	489	19	527	104	110	1	41,402966
DF26-99	0,922014825	4,763930195	0,10907	1,338589896	0,280984364	0,06131	4,762681455	667	8	663	23	650	102	97	0	0
DF26-100	0,9259037	5,4248092	0,10826	1,4944858	0,2754909	0,06195	5,4237288	663	9	665	27	672	116	102	1	0,0007658